Ionic Liquids for Carbon Dioxide Separation on Membranes

Sandra D. HOJNIAK

Supervisor:
Prof. K. Binnemans

Members of the
Examination Committee:
Prof. W. Dehaen
Prof. E. Nies
Prof. I. Vankelecom
Prof. W. De Borggraeve
Prof. M. Smet
Prof. Ch. Stevens

Dissertation presented in partial fulfilment of the requirements for the degree of Doctor in Science

October 2014

Uitgegeven in eigen beheer, Sandra D. Hojniak, te Heverlee

ISBN 978-90-8649-761-4
D/2014/10705/69

To my parents

Acknowledgements

Four PhD years have passed like a year, but then, a very busy and eventful year!

A PhD counts for more than the precious experience in solving the scientific problems. Equally important is the way we shape our characters. We learn how not to give up, and if we maybe gave up on something for a while, we learn how to get back on track. We learn how to improve our management skills, prioritising, multi-tasking etc. We learn how to be patient and persistent – no results, bad results, technical problems, all of these are common as common cold. And we learn how to work in a group, first a group of colleagues, then a group of friends. And I am very grateful for all these experiences!

I would like to express my thanks to many people who contributed to the course of this PhD.

First of all, I would like to thank my promoters, Prof. Koen Binnemans and Prof. Wim Dehaen, for enabling me to begin my PhD. Thank you for all our meetings, your time and concern!

I would like to thank my assessors, Prof. Ivo Vankelecom and Prof. Wim DeBorggraeve for helping me out with questions and problems and for being always so student-friendly!

I would also like to express my gratitude to the remaining members of my PhD jury: Prof. Eric Nies, Prof. Mario Smet and Prof. Christian Stevens, for their valuable comments and suggestions and a very nice atmosphere during my preliminary defense! I really appreciate it!

I also wish to acknowledge KU Leuven (IOF Platform) for funding my PhD scholarship.

Since science is (among other) about cooperation, my PhD would not be possible, without several great co-authors and friends:

I would like to express my gratitude to Prof. Sergei Kazarian, from Imperial College, London, not only for giving me a credit of trust that I could learn some FTIR in just two weeks, but also for the kind help, patience and countless advices!

Dr Asim Khan: Asim, thank you for introducing me to the world of gas separations, for all the measurements you performed, your "easy-goingness" and nice chats!

Lu Soon Chien: Lu, thank you for all your hard work, your model persistence in fighting obstacles, and nice chats as well!

Dr Oldamur Hollóczki: Oldamur, thank you for your expertise in quantum chemical calculations and all the interesting e-mails we exchanged!

Dr Ian Silverwood: Ian, thank you for your expertise in IR spectroscopy and for all your patience (with me)! And for answering my e-mails the fastest in the world!

Roman Matthesen: Roman, thank you for all these hours we spent doing TGA that never worked out but at least we trained in some of the abovementioned virtues, such as patience, and we certainly had fun!

Thank you, Sven Dewilde and Katrien Verachtert, my master students for your nice work and no explosions that I would have been responsible for ;)

Thank you Karel for your NMR expertise and Congo stories, Dirk and Paul for your help with all the practical stuff from solvent delivery to disposal of suspiciously beeping packages. Rita, thank you very much for all your help in fixing things "for yesterday" and your willingness to help!

The PhD also would not be the same without the people with whom I worked every day. Although being scientifically a bit of a lonelier island with my CO_2 separations in the extraction group, I certainly had enough interaction in the lab and in the office! Thanks:

To my officemates from earlier and now! Evert, Noboru, Sil, Sven, Daphne, Nilay, Senol, for all the good times we had in our too cold/too hot office (delete where inapplicable). For many, many nice memories, quite stupid games (see: the serious chocolate game), for our Apple Hour (4 p.m.!) and other strange but our own customs! and for listening to my more or less funny stories…

To the lovely floormates: Tom, Jeroen, Lethesh, Kathleen, Gijs, Sophia, Alok, Mercedes for all the funny chats!

To Neil and Kristian, for the motivation to run and discussions about the world, politics, sociology, you name it!

For the 3rd floor team: Elke, Sophie, Gregory, Karen, Kim Nga, Giang, Matthias, Stef, Annelies, Michael and Vincent, for their constant laughter and optimism.

There are also many people not necessarily related to Celestijnenlaan 200F, who where around during these 4 years, to laugh, to talk, to share:

To my dear friends: especially to Kamka and Michał, Pati and Muamar, Sil and Gitte, Brecht, Gosia and Bartek, Nigam, and many many more wonderful people!

To my dear friends in Poland: Madzia, Aneta, Martuś, Natka for making me feel, on my returns, like I have never left…:*

To Miriam, Ivo, Jochem, Charlotte, Margot and the rest of the big big Family, for being my "expat family" for the last couple of years! And for the possibility to blend in a little, by getting to know the customs and traditions, the language and the cuisine of exotic Belgium!

To Louisa, Hugo (†) en Familie, dank u wel voor een haven in Denderbelle waar iedereen zich onmidelijk thuis en welkom voelt en voor de echt warme sfeer!

To Ciocia Mary, Ciocia Regina and Babcia for being great examples of strong women!

Finally, to my dearest and closest Family in Wrocław! Mamusia, Tatuś, Daniłło and Nori! Thank you so much for always believing in me, and for the loads of support, I have been always receiving from you, even if your own decisions would have been different. Mamusiu (strong woman and unbeatable explorer), Tatko, (thorough and creative discoverer), you are my biggest role models! My dear Braciszku, thank you for all your technological support, without you I would still be using Nokia 3510 and for your nice persistence in climbing up not forgetting about Wrocław☺

And last, but you all know that not least, I would like to thank my Pieterke, my companion for good and for bad during this PhD and beyond, my support, my rock and my coach in optimism! For always but always believing in me, for dealing with small and big things and for the re-introduction to stargazing! Thank you, my Love!

Abstract

Reducing carbon dioxide (CO_2) emissions is not only ecologist's dream. Re-use of this gas can be beneficial for many industries where it is an important substrate. Since in the majority of the cases CO_2 leaves the industrial site mixed with other gases, it has to be purified before it is captured. One promising method involves the use of membranes incorporating *ionic liquids* (ILs) that readily absorb CO_2. Although several well-performing ILs have been tested for this application, the search for an industrially relevant one is still ongoing. More importantly, the structure-performance relationship of the ILs as well as the dissolution mechanism of CO_2 in ILs is not yet fully understood.

This PhD thesis focuses on the design and synthesis of ILs for the separation of CO_2 from N_2 or CH_4 on Supported Ionic Liquid Membranes (SILMs) and IL-polymer blend membranes, as well as on establishing the structure-performance relation-ship of the novel compounds in CO_2 separation.

A study of a series of tri(ethylene glycol)-functionalized ILs based on different cationic cores showed that cations influence CO_2 separation to a similar extent as anions. Gas separation selectivities of these monocationic compounds were on average two times lower than those of their dicationic analogues, due to the lower permeances of N_2 and CH_4 through the IL layer and more interaction sites for CO_2 in the latter.

Similarly to the tri(ethylene glycol), the nitrile group was repeatedly reported to be very efficient in improving CO_2 separations. Therefore, both moieties were combined into the pyrrolidinium and imidazolium ILs and used to prepare membranes. These ILs exhibited *ca*. 2.3 times higher CO_2/N_2 and CO_2/CH_4 gas separation selectivities than analogous ILs functionalized only with a glycol chain. In-situ

FTIR-ATR spectroscopy was used to study the solubility of CO_2, IL swelling and the interactions of CO_2 with the nitrile group. The difunctionalized ILs were found to interact stronger with CO_2 than the glycol-functionalized ILs.

The widespread use of such highly functionalized ILs is restricted by the elaborate synthesis and the difficulties in purification, which lead to low yields. To overcome these problems and to propose a new approach to CO_2 separation, metal-containing ILs were designed and evaluated for membrane performance. The compounds were composed of complex cations and bis(trifluoromethylsulfonyl)imide anions. In each cation, six imidazole ligands functionalized with a nitrile or an oligo(ethylene oxide) group were coordinated to a d-block central metal ion. Crystal structures of the nitrile-containing ILs were obtained. In order to explore the potential of the direct CO_2-metal chemical binding, analogous ILs but with four or five ligands were examined for gas separation performance and showed selectivities similar to the hexacoordinate ILs. The membranes prepared from blends of these ILs and polymers, provided moderate selectivities.

Nederlandstalige Abstract

Het verlagen van de CO_2 emissie is niet alleen een droom van de ecologist, maar het hergebruik van dit gas kan ook voordelig zijn voor de industrie waar CO_2 een belangrijke grondstof is. Sinds in de meeste gevallen, CO_2 met andere gassen vermengd is, moet het eerst gezuiverd worden alvorens men het kan vangen. Een beloftevolle methode maakt gebruik van membranen die ionische vloeistoffen (ILs) bevatten die CO_2 absorberen. Hoewel verschillende ionische vloeistoffen in het verleden getest zijn geweest, is de zoektocht naar een industrieel relevante ionische vloeistof nog steeds lopende. Meer nog, de verbanden tussen de structuur en de performanties van de ionische vloeistoffen, alsook het oplossingsmechanisme van CO_2 in ionische vloeistoffen is nog steeds niet volledig opgehelderd.

Deze doctoraatsverhandeling is gericht op de ontwikkeling en synthese van ionische vloeistoffen voor de scheiding van CO_2 van N_2 en CH_4 in Supported Ionic Liquid Membranes (SILMs) en IL-polymeer blend membranen. Ook de verbanden tussen de structuur en de performantie van deze nieuwe verbindingen worden onderzocht.

De studie van een reeks tri(ethyleen glycol)-gefunctionaliseerde ionische vloeistoffen met verschillende kationische kernen heeft aangetoond dat kationen de scheiding van CO_2 in gelijke mate beïnvloeden als de anionen. De selectiviteiten van deze monokationische verbindingen waren gemiddeld twee keer lager dan deze van de dikationische analogen. Dit kan verklaard worden door de lagere permeantie van stikstof en methaan door de ionische vloeistof laag en de grotere hoeveelheid aan interactie sites voor CO_2.

Naast de tri(ethyleen glycol)groep, is ook vaak gerapporteerd dat de nitrilgroep de CO_2 scheiding sterk verbetert. Omwille van deze reden werden vervolgens beide groepen ingebouwd in pyrrolidinium en imidazolium ionische vloeistoffen. Deze ionische vloeistoffen

vertoonden een 2.3 keer hogere selectiviteit voor CO_2/N_2 en CO_2/CH_4 scheidingen in vergelijking met de analoge ionische vloeistoffen die enkel met de glycolketen gefunctionaliseerd waren. In situ FTIR-ATR spectroscopische methoden werden gebruikt om de oplosbaarheid van CO_2, de opzwelling van ionische vloeistoffen en de interacties van CO_2 met de nitrilgroep te bestuderen. De digefunctionaliseerde ionische vloeistoffen interageerden sterker met CO_2 dan de glycol-gefunctionaliseerde ionische vloeistoffen.

Een nadeel van het gebruik van dergelijke sterk gefunctionaliseerde ionische vloeistoffen is echter de complexe synthese en de opzuiveringsmoeilijkheden die leiden tot lage synthese rendementen. Om deze problemen te vermijden, werden metaalhoudende ionische vloeistoffen ontwikkeld en geëvalueerd op hun membraanperformanties. De verbindingen bestonden uit complexe kationen en bis(trifluoromethylsulfonyl) imide anionen. In elk kation werden zes imidazoolliganden met een nitril of oligo(ethyleen oxide) groep gecoördineerd aan het centrale d-blok metaalion. Kristalstructuren van de nitril-gebaseerde ionische vloeistoffen werden bepaald. Analoge ionische vloeistoffen met vier of vijf liganden werden eveneens bestudeerd en vertoonden een gelijkaardige selectiviteit als de zes-gecoördineerde ionische vloeistoffen. Matige selectiviteiten werden bekomen voor membranen bestaande uit een 'blend' van deze ionische vloeistoffen met polymeren.

Table of Contents

Acknowledgements .....
Abstract i
Nederlandstalige Abstract iii
List of Abbreviations ix
Scope and Outline xiii

Scope xiii
Thesis objectives xiii
Thesis Outline xiv

1. Carbon dioxide 1

1.1. The carbon dioxide issue 1

1.1.1. Carbon dioxide sources 2
1.1.2. Applications of carbon dioxide 3
1.1.3. Electronic properties of CO_2 and its reactivity 4

1.2. Carbon dioxide separation and capture 5

1.2.1. Cryogenic distillation 6
1.2.2. CO_2 adsorption 6
1.2.3. CO_2 absorption 9
1.2.4. Membrane gas separation 12

1.3. References 14

2. Ionic liquids 19

2.1. Introduction 19
2.2. Properties of ILs 21

2.2.1. Melting point 21
2.2.2. Viscosity 22

2.3. "Green" aspects of ILs 22
2.4. Applications of ILs 23
2.5. References 25

3. Supported Ionic Liquid Membranes (SILMs) 27
3.1. Solution-diffusion mechanism 27
3.1.1. Robeson plot 29
3.2. Designing ILs for SILMs 30
3.2.1. Influencing the diffusion coefficient 30
3.2.2. Influencing the solubility coefficient 30
3.2.3. Physical vs. chemical absorption 31
3.2.4. Mechanism of physical gas dissolution in ILs 31
3.2.5. Designing a CO_2-phile 33
3.2.6. Challenges in the synthesis of ILs for SILMs 36
3.3. References 37
4. Influence of Cation Type and Charge on the Performance of SILMs 43
4.1. Introduction 43
4.2. Results and Discussion 45
4.2.1. Monocationic ionic liquids 45
4.2.2. The influence of the cationic core on selectivity 47
4.2.3. Dicationic ILs – membrane performance 49
4.2.4. Quantum chemical calculations 55
4.3. Conclusions 58
4.4. Experimental section 59
4.4.1. Syntheses 59
4.4.2. Membrane preparation and measurements 63
4.4.3. DFT calculations 64
4.5. References 65
5. Separation of CO_2 from N_2 and CH_4 by Nitrile/Glycol-Difunctionalized Ionic Liquids 69
5.1. Introduction 70

5.1.1. Attenuated Total Reflection Spectroscopy 70
5.1.2. Infrared spectroscopy of carbon dioxide 72
5.1.3. Infrared study of CO_2-IL systems 74
5.2. Results and discussion 75
5.2.1. SILM performance of monocationic ILs 75
5.2.2. SILM performance of dicationic ILs 81
5.2.3. In situ FTIR-ATR study of the IL-CO_2 system 82
5.3. Conclusions 89
5.4. Experimental part 91
5.4.1. Syntheses 91
5.4.2. Instruments and methods 95
5.5. References 100
6. Metal-containing ILs 105
for separation of CO_2 from N_2 105
6.1. Introduction 105
6.1.1. Polymer-IL blend membranes 105
6.1.2. Metal-based CO_2 absorption and separation 106
6.2. Results and discussion 107
6.2.1. Approach 1: Hexacoordinated ILs – physical CO_2 binding 108
6.2.2. Approach 2: Tetra- and pentacoordinate ILs – a possibility for chemical CO_2 binding 113
6.2.3. Crystal structures 120
6.3. Conclusions 125
6.4. Experimental 126
6.4.1. Materials and instruments 126
6.4.2. Syntheses 126
6.4.3. Membrane preparation and measurements 130

6.4.4. XRD measurements 131
6.5. References 135
General Conclusions and Future Perspectives 141
Future perspectives 143
Health, Safety and Environment Aspects 147
Publications 149
Attended Conferences 151

List of Abbreviations

Symbol	Name
α	Selectivity
a.u.	Arbitrary units
ATR	Attenuated Total Reflectance
[$BrC_{10}BrC_{10}Im$][Br]	[1-(Bromodecyl)-3-(bromodecyl)imidazolium][Br]
[BzMIM][TfO]	1-Benzyl-3-methylimidazolium triflate
[C_2MIM][TFA]	1-Ethyl-3-methyl-imidazolium trifluoroacetate
[C_4MIM]Cl	1-butyl-3-methylimidazolium chloride
[C_4mim][Tf_2N]	1-butyl-3-methylimidazolium bis(trifluoromethanesulfonyl)imide
CCS	Carbon Capture and Storage
CHN	Elemental analysis of carbon, hydrogen and nitrogen
CSD	Cambridge Structural Database
cP	Centipoises, a unit of dynamic viscosity
Cyphos® 101	Tri(hexyl)tetradecylphosphonium chloride
D	Diffusivity coefficient
DBS	Dodecylbenzenesulfonate anion
DCA	Dicyanoamide anion
DCM	Dichloromethane
DFT	Density Functional Theory
DMSO	Dimethylsulfoxide

Symbol	Name
DSC	Differential Scanning Calorimetry
FFV	Fractional Free Volume
FWHM	Full Width at Half Maximum
FTIR	Fourier Transform Infrared spectroscopy
GPU	Gas Permeance Unit (1 GPU = 10^{-6} cm^3 (STP) / cm^2 (s cm Hg)
ILs	Ionic Liquids
MGS	Membrane Gas Separation
MOF	Metal-Organic Framework
m.p.	Melting point
n.d.	Not determined
NMR	Nuclear Magnetic Resonance spectroscopy
$[P_{4444}]$[TF-Leu]	Tetrabutylphosphonium *N*-trifluoromethanesulfonyl leucine
PEG	Poly(ethylene glycol)
P_i	Permeability (permeance) of component i through the membrane
Poly(IL)	Polymeric (polymerized) IL
$RCOO^-$	Carboxylate anion
S	Solubility coefficient
SCN	Thiocyanate anion
S-D	Solution-Diffusion mechanism
SLM	Supported Liquid Membrane
SILM	Supported Ionic Liquid Membrane
STP	Standard Temperature and Pressure

Symbol	Name
TCM	Tricyanomethanide anion
TEG	Tri(ethylene glycol)
TFA	Trifluoroacetate anion
T_g	Glass transition temperature
TIR	Total Internal Reflection
TsO^-	*p*-toluene sulfonate anion
ν_n	A vibration mode of a molecule in IR
UV-VIS	Ultraviolet-visible region of the electromagnetic spectrum

Scope and Outline

Scope

Human activity contributes to the steady increase of the carbon dioxide (CO_2) concentration in the atmosphere. Although the impact of this increase on the climate is controversial, there is a general consensus that one should limit the release of this gas into the atmosphere. Since in the majority of cases, CO_2 leaves the industrial site in a mixture of other gases, it has to be purified before it can be captured or re-used as a chemical feedstock.

One promising method involves the use of membranes that incorporate non-molecular solvents, namely, *ionic liquids* (ILs) that readily absorb CO_2. The parameters of the gas transport through an IL-containing membrane can be tuned by adjusting the molecular structures of these solvents. Although several well-performing ILs have already been incorporated into membranes, the search for an industrially suitable solvent is still in progress. More importantly, the structure-performance relationships of the ILs as well as the dissolution mechanism of CO_2 in ILs are not yet fully understood.

Thesis objectives

The aim of this PhD thesis was to design and synthesize new ionic liquids (ILs) for the purpose of CO_2 separation from N_2 and CH_4 on membranes.

First of all, the ILs in question were required to readily solubilise CO_2. Moreover, in order to provide efficient membrane gas separation (fast and facile desorption of the gas) the IL-CO_2 interactions responsible for the solubilisation could not be too strong. The emphasis was thus placed on preparing ILs that physically interact with CO_2, without a formation of chemical bonds.

Apart from the quest for the most effective IL, it was equally important to deepen the understanding about the structure-properties relationship for ILs in gas separations. The interpretation of the membrane experiment results was therefore to be supported by infrared spectroscopy of IL-CO_2 systems.

As in the literature published prior to this thesis, the use of cation was somewhat neglected, efforts were to be directed into obtaining new cations and study the influence of their functionalization on the performance of the resulting ILs.

Thesis Outline

The literature study consists of three chapters and describes the current status of CO_2 research. *Chapter 1* gives an introduction to the CO_2 problem and discusses the currently used solutions. *Chapter 2* presents the properties and applications of ILs. In *Chapter 3* the mechanism of gas separation on Supported Ionic Liquids Membranes (SILMs) is shown, and the design of ILs for CO_2 separation is presented.

Chapters 4–6 present the results of the original research. In *Chapter 4*, the influence of IL cations on CO_2 separation on SILMs is investigated with the example of novel ILs with a tri(ethylene glycol) chain, appended to imidazolium, pyrrolidinium, piperidinium, and morpholinium cations. Subsequently, the influence of the double charge is investigated, by testing the performance of SILMs containing novel symmetrical dicationic ILs, analogous to the monocationic ILs from the first part of the study. Quantum chemical calculations are employed to investigate the differences in interaction of CO_2 with the two types of ILs.

Similarly to the oligo(ethylene glycol), the nitrile group was repeatedly reported to be very efficient in improving CO_2 separations. Therefore, in *Chapter 5*, both moieties are incorporated into the pyrrolidinium and imidazolium ILs and are used to prepare SILMs

and evaluated for CO_2 separation from N_2 and CH_4. The performance of the IL-CO_2 system is explored with the help of *in-situ* FTIR-ATR spectroscopy.

Chapter 6 describes the design, synthesis and performance of novel metal-containing ILs of two types. The first type is composed of complex cations and Tf_2N anions. In each cation, six imidazole ligands functionalised with a nitrile or an ether group are coordinated to the central metal ion: Ni^{2+}, Zn^{2+} or Mn^{2+}. Hexacoordination prevents any direct metal-CO_2 bonding, resulting in physisorption. In the second type of ILs, chemical absorption was involved, as the complex cations were tetracoordinate, thus leaving the possibility for a CO_2-metal bond formation.

Finally, the last section provides future perspectives for this research topic.

1.
Carbon dioxide

1.1. The carbon dioxide issue

70 years ago there were 24 000 motor vehicles in Belgium;
in 2013- over six million.[1]

This comparison pictures the rapid industrialisation happening around us which is inseparably bound with an increased energy demand. Since the industrial revolution in the 19th century, the global energy production is mainly based on the combustion of fossil fuels.[2] Burning coal or natural gas in air to produce energy, releases vast amounts of carbon dioxide (CO_2) into the atmosphere:

$$\text{Fossil fuels} + \text{air } (O_2 + N_2) \rightarrow CO_2 + N_2 + H_2O + \text{various impurities} \qquad 1.1$$

It is estimated that about 400 ppm (0.04%) of CO_2 are currently present in the atmosphere.[3] Although this value is not alarming, the monotonic increase of the CO_2 concentration is of concern. Since the 1980s, the CO_2 concentration has increased by 15%, rising between 0.5 and 2.2 ppm per year.[4] Whereas CO_2 is acutely toxic to humans only in high concentrations, it can be partly responsible for certain undesired atmospheric changes such as global warming or acid rains.[5]

It is estimated that 26% of the global CO_2 emission from anthropogenic sources comes from power plants burning fossil fuels.[6] Apart from the *flue gas* generated in fossil fuel combustion, CO_2 is also released as a by-product of various industrial processes, some of which

are briefly described below, and as a metabolite of animals and plants. It is important to note that in nearly every process, CO_2 is released along with other volatile components – organic vapours or gases.

1.1.1. Carbon dioxide sources

Natural gas processing. Natural gas consists of 80-95% methane and, depending on the source, contains a variable amount of CO_2 (typically 5-20 vol. %) as well as other impurities, such as higher hydrocarbons and sulphur compounds.[7] Removal of CO_2 and H_2S from natural gas is termed "*natural gas sweetening*", referring to the acidic and corrosive nature of these two compounds in the presence of water. To minimize the corrosion of pipelines only 2-4% of CO_2 can remain in natural gas.[8]

Ammonia and hydrogen plants. The production of hydrogen in ammonia plants and hydrogen plants generates CO_2 from synthesis gas (syngas) in the water-gas shift reaction:

$$CH_4 + H_2O \leftrightarrows CO + H_2 \qquad 1.2a$$

$$CO + H_2O \leftrightarrows CO_2 + H_2 \qquad 1.2b$$

The production of each ton of ammonia gas releases one ton of CO_2 as a by-product.[9]

Biogas production. Anaerobic digestion of organic matter by microorganisms in biogas production generates CO_2 along with CH_4:[10]

$$C_6H_{12}O_6 \text{ (glucose)} \rightarrow 3\ CO_2 + 3\ CH_4 \qquad 1.3$$

Ethanol fermentation. Production of industrial alcohol and alcoholic beverages (e.g. beer) by fermentation of cereals, generates large quantities of CO_2 and a variety of acids, aldehydes and H_2S, according to the schematic reaction:[9]

$$C_6H_{12}O_6 \rightarrow 2\ C_2H_5OH + 2\ CO_2 \qquad 1.4$$

Hall-Héroult process. Vast amounts of CO_2 are also produced in the Hall-Héroult process for aluminium production, by oxidation of the carbon anodes:[11]

$$2\ Al_2O_3 + 3\ C \rightarrow 4\ Al + 3\ CO_2 \qquad 1.5$$

1.1.2. Applications of carbon dioxide

Contrary to popular belief, carbon dioxide has multiple industrial applications. As an abundant, inexpensive and non-flammable gas of low reactivity and interesting physical properties, it is irreplaceable in many branches of industry, from food processing to welding, some of which are pictured in Figure 1.1.

Figure 1.1: Selected applications of solid (sCO_2), liquid (lCO_2), gaseous (gCO_2) and supercritical ($scCO_2$) carbon dioxide.

In food industry, gaseous, liquid and solid CO_2 is used in beverages carbonation, in the stimulation of plant growth in greenhouses, in suppression of microbial growth in food, and as a refrigerant.[9]

Supercritical CO_2 ($scCO_2$) is used as a green solvent in extractions, for example in the production of decaffeinated coffee or in the removal of various impurities from textiles in dry cleaning, owning to its tuneable

physical properties. Depending on temperature and pressure, density, viscosity and solvent strength of $scCO_2$ can be adjusted to resemble those of common organic solvents such as chloroform or hexane and perform similarly in extractions.[12-13]

Many resources are now focused on finding an efficient way of incorporating of CO_2 into chemicals, for example methanol.[14] Liquid and supercritical CO_2 is used in material chemistry for synthesis and processing of polymers, particularly in production of biodegradable polycarbonates from cyclic ethers.[15, 16] Whilst CO_2 is a desirable industrial substrate, tons of this gas are being uncontrollably released every day, that may cause the environmental changes. It is thus wise and economical to find an efficient way for CO_2 recycling.

1.1.3. Electronic properties of CO_2 and its reactivity

To understand CO_2 separation processes on the molecular level, electronic properties of the gas molecule have to be addressed first. Carbon dioxide is a linear and symmetrical molecule. Therefore, despite the large difference in Pauling electronega-tivity between the carbon (2.5) and the oxygen atoms (3.5), it has no dipole moment.

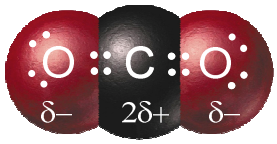

Figure 1.2: Carbon dioxide molecule with indicated partial charges on carbon and oxygen atoms

Nevertheless, there is a charge separation present: a partial positive charge is localized on the carbon atom and two partial negative charges of a twice smaller value are located on the oxygen atoms (Fig 1.2). Such arrangement of four unit charges is termed a *quadrupole*. The electron-deficient carbon atoms are Lewis-acidic while the electron-rich oxygen atoms, with their lone electron pairs are Lewis-basic. As a consequence, CO_2 molecules readily participate in various types of non-covalent

interactions such as Lewis acid-base interactions (importantly, both as a Lewis acid and as a Lewis base), hydrogen bonding (as an acceptor), π-π interactions, quadrupole-dipole, quadrupole-quadrupole or quadrupole-ion interactions.[17,18] Physical absorption or adsorption (*physisorption*) occurs thanks to these non-covalent interactions between the absorbent and the gas without occurrence of a chemical reaction. *Chemisorption*, on the other hand, is based on the formation of a covalent bond between the absorbent and CO_2. Carbon dioxide is a weak electrophile and it reacts with nucleophiles such as amines or hydroxides. It can also coordinate to transition metals (Chapter 6).

1.2. Carbon dioxide separation and capture

Carbon capture and storage (CCS) is a collective name describing a broad range of processes involved in the capture, separation and storage of CO_2 from fossil fuel combustion and large anthropogenic sources.[19] CCS is also called *carbon sequestration*. As shown in section 1.1.1, in the vast majority of cases, CO_2 is generated together with other gases, vapours and solid particles, such as methane and unreacted nitrogen from air (comprising the majority of the flue gas), with various (oxidized) impurities from the fuel, such as nitrous oxides (NO_x = NO, NO_2), sulfur oxides (SO_x = SO_2, SO_3), hydrogen sulfide (H_2S) and carbon monoxide (CO) and with organic vapours (e.g. volatile alcohols) or heavy metals.[20-23] In the rare cases when the flue gas is virtually made of CO_2, it can be captured directly, but in the majority of the situations, a separation step has to be included. Currently, CO_2 removal from gas streams of various origins is achieved by the following methods:[24]

a) Cryogenic distillation (1.2.1)
b) Adsorption processes (1.2.2)
c) Absorption processes (1.2.3)
d) Membrane gas separation (1.2.4)

The processes b–d operate in a *pressure* or *temperature swing* mode, that is, CO_2 is released by means of decreased pressure or increased temperature.[24] The suitability of each process for different conditions is summarized in Table 1. In order to make the process cost effective, the method has to be adjusted to the gas composition, pressure and temperature. Additionally, potential drawbacks such as corrosion, high exploitation costs and low efficiency have to be economized.

1.2.1. Cryogenic distillation

Cryogenic distillation is a physical gas separation method which provides high purity CO_2 especially from CO_2/N_2 and CO_2/CH_4 streams. It is based on the difference in boiling points between CO_2 (b.p. = -57 °C) and N_2 (-196 °C) or CH_4 (-164 °C). In the process, the gas mixture (flue gas) is expanded under conditions which are adjusted to provide liquid CO_2 which remains in the system, while maintaining N_2 or CH_4 in the gaseous state necessary for these gasses to leave the installation. The low temperature demand and the occurrence of a phase change (gaseous to liquid CO_2) makes this very efficient separation process particularly energy intensive.[23]

1.2.2. CO_2 adsorption

Adsorption processes are widely used in industry, especially in CO_2/CH_4 separations.[8] A broad range of adsorption materials includes zeolites, activated carbons, simple inorganic chemicals (e.g. calcium oxide) and more complicated systems such as supported organic molecules, which are all highly porous and have a very high surface area. These materials can bind CO_2 via physisorption or chemisorption.[24]

Activated carbons have been widely used as adsorbents, due to their high availability, low cost, high thermal stability, low sensitivity to moisture and easy regeneration.[25] Their drawback is the inability to capture CO_2 at low pressures.[26] Zeolites are natural or synthetic porous

aluminosilicates, very promising in gas separation, that usually adsorb CO_2 on a physical basis.[24] The regeneration is, however, not always facile and the initial capacity is often not recovered after the first cycle.[24]

Metal-organic frameworks (MOFs) are also porous solids, but, in contrast with zeolites, they consist of metal-organic ligand connections.[24] MOFs possess the highest surface area of all known materials and high free volumes.[27] These properties make them good candidates for storage and separation of gases, especially that MOFs can be tuned for the capture of a particular gas to a higher extent than zeolites, by choosing the metal ions, ligands and adjusting the pore size. Currently, MOFs are not yet able to perform better than amine scrubbers (Section 1.2.3).[28]

Table 1.1 Comparison of currently used worldwide CO_2 separation processes.[24,29-32]

Process	Most suitable application	Main advantages	Main disadvantages
Cryogenic distillation	Gas streams with >75% CO_2	Very high purity CO_2	Very high energy cost
Adsorption	Various CO_2 streams at high pressure	High energy efficiency Low capital cost Good CO_2 separation	Severely lowered CO_2 capacity in the presence of other gases or water
Physical absorption	High pressure streams with high CO_2 content	No corrosion problems	Low efficiency Relatively high cost
Chemical absorption	Various CO_2 streams	High selectivity Up to 100% capture efficiency	Very high energy cost Low CO_2 loading Use of volatile solvents Corrosion problems
Membranes	Streams with high CO_2 concentrations	Small and uncomplicated installations Energy efficient Inexpensive in exploitation	Selectivity vs. permeability trade-off (either high selectivity *or* high permeability feasible)

1.2.3. CO_2 absorption

Absorption of CO_2 occurs in solvents which also can be divided into chemical and physical absorbers. *Physical CO_2 absorbers* are typically ethers, alcohols or carbonyl compounds that form hydrogen bonds with CO_2 molecules or interact with it via Lewis acid-base interactions. Low operating temperature and high pressure are favoured for all physical absorption processes as they increase dissolution of the gas.[33]

The *Selexol* absorption process employs a mixture of dimethylethers of poly(ethylene glycol) and it is preferred for purification of CO_2 streams from H_2S.[31] The *Rectisol* process is based on CO_2 absorption in methanol chilled to temperatures far below 0 °C (-20 °C or even -70 °C) and allows a simultaneous removal of other corrosive components, such as H_2S, carbonyl sulfide, HCN or NH_3.[33,34] The installation for this process requires an additional refrigerating system in comparison with Selexol. Another physical solvent, N-methyl-2-pyrrolidinone, is used in the *Purisol* process, while propylene carbonate is used in the *Fluor* process.[9] Propylene carbonate selectively dissolves large quantities of CO_2 and is non-corrosive and most suitable for gas streams with little or no H_2S.

Physical absorbers tend to be less efficient and less selective in CO_2 capture than chemical absorbers, because physical absorption is less specific. On the other hand, it is much easier to release the physically bonded gas by means of lowered pressure and/or increased temperature.

Natural gas purification (gas sweetening) is currently the largest industrial gas separation process.[20] It is typically achieved via the *chemical absorption*. In the process, the feed gas is pumped into an absorption tower, counter current to the flow of an absorbent liquid. The liquid is then heated up and sent to the stripping tower operating under reduced pressure, where CO_2 is released and the liquid regenerated.[20]

Aqueous solutions of amines and more precisely alkanolamines (alkylamines functionalized with an –OH group) are most commonly used. They are inexpensive in bulk quantities and efficient in gas removal. The amine functionality reacts chemically with CO_2 (vide infra) while the hydroxyl group reduces vapour pressure of the absorbent preventing its loss and helping with its solubilisation in water.[35] Typically, aqueous solutions of primary amines (e.g. monoethanolamine), secondary amines (diethanolamine or diisopropanolamine) and tertiary amines (N-methyldiethanolamine) are used in the industry (Figure 1.3).[36]

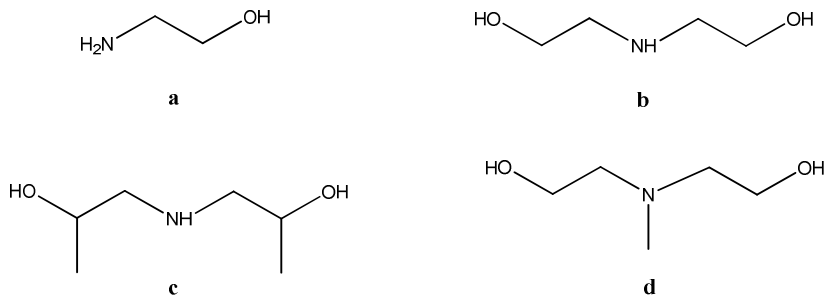

Figure 1.3: Structures of alkanolamines used in gas sweetening: a) monoethanolamine, b) diethanolamine, c) diisopropanolamine, d) N-methyldiethanolamine.

Due to their basic nature, all alkanolamines are able to react both with CO_2 and H_2S, and therefore can be used for a total acid gas removal process (gas sweetening). Depending on the amine and the application, 20–50 wt. % of aqueous solutions are used.[30] CO_2 capacity of an amine and the absorption mechanism depend especially on the structure of the amine and are strongly influenced by the pH and concentration of the solution.[37,38] Several reversible reactions occur when CO_2 dissolves in an aqueous alkanolamine solution but the dissolution mechanism is still debated.[39,40] The most important reaction is shown in Eqs. 1.6[36] Primary (1°) and secondary (2°) alkanolamines react with CO_2 to form ammonium carbamate (Eq. 1.6).[41-42]

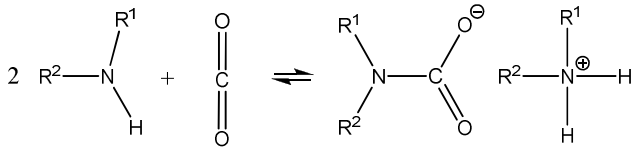

1.6

Thus, two moles of amine are required to capture one mole of CO_2, or in other words, 1 mole of absorbent can bind only 0.5 mole of CO_2. The captured gas is released by thermal decomposition of the carbamate, via the reversed reaction 1.6, and occurs at around 100-150 °C.[25] The relative stability of the carbamates makes the amine solvent regeneration very energy intensive.

Tertiary amines react with CO_2 more slowly than primary or secondary amines, because the lack of the N-H hydrogen prevents them from forming carbamates.[43] Multiple reactions occur in an aqueous solution of tertiary alkanolamine saturated with CO_2, with the major product being a bicarbonate ion (Eq. 1.7):

$$R_1R_2R_3N + CO_2 + H_2O \leftrightarrows R_1R_2R_3HN^+ + HCO_3^- \qquad 1.7$$

Thus, tertiary amines absorb CO_2 in a 1:1 ratio, that is, twice more than 1° and 2° amines, but the absorption process is much slower.[37,38] The high efficiency of CO_2 capture by alkanolamines and low cost of these solvents are responsible for the widespread use of the amine systems worldwide. Nevertheless, there are several serious drawbacks of the systems.

First of all, strong covalent bonds formed between the absorbent and CO_2, require a lot of energy to release the gas, making the amine processes often comparably energy intensive to cryogenic distillation.[32] Secondly, high temperatures used in the process promote the thermal degradation of amines (oxidation, demethylation and dealkylation) to corrosive products such as ammonia or methylamine.[44] What is more, aqueous CO_2 is itself corrosive to carbon steel, therefore corrosion inhibitors are necessary.[30] Even then, constant monitoring is required as corrosion can damage an installation within a few days.[20] Thirdly, amine

solvents are volatile and some absorbent is always lost on gas recovery by heating. The last drawback of these systems is their size: a typical absorption tower has a diameter of 5 m and it is 20 m high, thus, it requires hundreds of litres of the absorbent.[45]

1.2.4. Membrane gas separation

Industrial membrane gas separation (MGS) of CO_2, has become a promising alternative to the previously listed gas removal methods (1.2.1-1.2.3) since the 1980s, especially due to its competitive energy efficiency.[46,47] Gas separation membranes are semi-permeable materials that allow the passage of certain gases while retaining the others (Fig. 1.4).

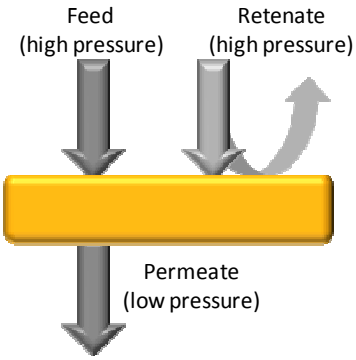

Figure 1.4: A schematic representation of the membrane gas separation process.

In the process, a gas mixture (feed) is directed towards one side of a membrane at elevated pressure. One of the components (permeate) reaches the opposite side while the other component (retenate) is withheld.[48] Membranes can be made of a variety of porous or non-porous materials including ceramics and polymers. Porous membranes, depending on the size of the pores, sieve gases of certain molecular weight or size, and exhibit higher throughput but lower selectivity.[32,48] Non-porous (dense) membranes are less permeable but offer higher selectivity, as they permeate one of the gases from the mixture on the

basis of physical or chemical interactions between the support and the gas.[32,48] Large gas volumes can be dealt with by the use of high surface-to-volume membrane module designs, such as spiral-wound and hollow-fibre modules.[46]

MGS is a continuous process where the extraction and stripping process are combined.[49] Moreover, MGS plants are mechanically uncomplicated and are smaller than alkanolamine plants. They can therefore be used in small-scale and remote production sites, e.g. at farms or at restaurants for beverage dispensers, without the need for highly trained staff to be present.[50]

All these factors contribute to considering MGS a "green" technology. The current natural gas processing market is between 2-5 billion USD/year. Membranes are now the preferred techniques for separating CO_2 from CH_4, even in huge installations, e.g. a 23 million USD investment in Pakistan or smaller ones in Egypt and Thailand.[51] Currently, membrane CO_2 separation is operating mainly for natural gas sweetening.[20] Other, much more novel markets where MGS is involved are flue gas treatment and biogas valorisation.[52,53]

Supported (Ionic) Liquid Membranes

One type of membranes is receiving a growing attention, namely, *Supported Liquid Membranes* (SLMs). A SLM is made of a porous solid support impregnated with a liquid, which is held by capillary forces within the pores.[48] The support can be made of an organic polymer or an inorganic material, for instance ceramics, whereas the liquid can be an organic compound, such as poly(ethylene glycol) or a solution of various organic or inorganic compounds.[48,49] A major drawback of a classical SLM is the instability of the liquid phase in the pores, due to evaporation of the liquid, its deterioration from the support due to the high pressure applied in the separation process or due to its partial solubility in the gas.[54]

In 1995, Supported Ionic Liquid Membranes (SILMs) were introduced, which are SLMs that utilize a novel type of solvents, *Ionic Liquids* (ILs), instead of molecular solvents.[55] SILMs make use of the special properties of ILs such as, for example, thermal stability or negligible volatility and are therefore often able to circumvent the instability problems inherent to SLMs.[56,57] Before the properties of SILMs can be described, the nature of ILs has to be addressed in more detail.

1.3. References

1. Weber, D., *Automobilisering en de overheid in België vóór 1940: besluitvormingsprocessen bij de ontwikkeling van een conflictbeheersingssysteem*. Universiteit Gent. Faculteit Letteren en Wijsbegeerte: Gent, 2008.
2. Liu, Y.; Wang, Z. U.; Zhou, H.-C., Recent advances in carbon dioxide capture with metal-organic frameworks. *Greenhouse Gas Sci Technol.* **2012,** *2*, 239-259.
3. *Climate change 2007-the physical science basis: Working group I contribution to the fourth assessment report of the IPCC*. Cambridge University Press: Cambridge, 2007.
4. Dlugokencky, E., Tans, P. , NOAA/ESRL ftp://aftp.cmdl.noaa.gov/products/trends/co2/co2_annmean_gl.txt.
5. SIGMA-ALDRICH Material Safety Data Sheet for Carbon Dioxide. www.sigma-aldrich.com (accessed 14.03.2014).
6. *Climate Change 2007: Synthesis Report; http://www.ipcc.ch/publications_and_data/ar4/syr/en/spm.html*; IPCC, Geneva, Switzerland: 2007; p 104.
7. Tan, L. S.; Lau, K. K.; Bustam, M. A.; Shariff, A. M., Removal of high concentration CO_2 from natural gas at elevated pressure via absorption process in packed column. *J. Nat. Gas Chem.* **2012,** *21*, 7-10.
8. Cavenati, S.; Grande, C. A.; Rodrigues, A. E., Adsorption Equilibrium of Methane, Carbon Dioxide, and Nitrogen on Zeolite 13X at High Pressures. *J. Chem. Eng. Data* **2004,** *49*, 1095-1101.
9. Pierantozzi, R., Carbon Dioxide. In *Kirk-Othmer Encyclopedia of Chemical Technology*, John Wiley & Sons, Inc.: 2000.
10. Buswell, A. M.; Mueller, H. F., Mechanism of Methane Fermentation. *Ind. Eng. Chem.* **1952,** *44*, 550-552.
11. Kvande, H.; Haupin, W., Inert anodes for Al smelters: Energy balances and environmental impact. *JOM* **2001,** *53*, 29-33.
12. Blanchard, L. A.; Brennecke, J. F., Recovery of Organic Products from Ionic Liquids Using Supercritical Carbon Dioxide. *Ind. Eng. Chem. Res.* **2000,** *40*, 287-292.

13. Eckert, C. A.; Bush, D.; Brown, J. S.; Liotta, C. L., Tuning Solvents for Sustainable Technology. *Ind. Eng. Chem. Res.* **2000,** *39*, 4615-4621.
14. Shi, L.; Yang, G.; Tao, K.; Yoneyama, Y.; Tan, Y.; Tsubaki, N., An Introduction of CO_2 Conversion by Dry Reforming with Methane and New Route of Low-Temperature Methanol Synthesis. *Acc. Chem. Res.* **2013,** *46*, 1838-1847.
15. Cooper, A. I., Polymer synthesis and processing using supercritical carbon dioxide. *J. Mater. Chem.* **2000,** *10*, 207-234.
16. Darensbourg, D. J., Making Plastics from Carbon Dioxide: Salen Metal Complexes as Catalysts for the Production of Polycarbonates from Epoxides and CO_2. *Chem. Rev. (Washington, DC, U. S.)* **2007,** *107*, 2388-2410.
17. Bhargava, B. L.; Balasubramanian, S., Probing anion–carbon dioxide interactions in room temperature ionic liquids: Gas phase cluster calculations. *Chem. Phys. Lett.* **2007,** *444*, 242-246.
18. Galand, N.; Wipff, G., Solvation of benzene derivatives in sc-CO_2: a molecular dynamics study of fluorination effects. *New J. Chem.* **2003,** *27*, 1319-1325.
19. Gibbins, J.; Chalmers, H., Carbon capture and storage. *Energy Policy* **2008,** *36*, 4317-4322.
20. Baker, R. W.; Lokhandwala, K., Natural Gas Processing with Membranes: An Overview. *Ind. Eng. Chem. Res.* **2008,** *47*, 2109-2121.
21. Granite, E. J.; Pennline, H. W., Photochemical Removal of Mercury from Flue Gas. *Ind. Eng. Chem. Res.* **2002,** *41*, 5470-5476.
22. Merkel, T. C.; Lin, H.; Wei, X.; Baker, R., Power plant post-combustion carbon dioxide capture: An opportunity for membranes. *J. Membr. Sci.* **2010,** *359*, 126-139.
23. Aaron, D.; Tsouris, C., Separation of CO_2 from Flue Gas: A Review. *Separ. Sci. Technol.* **2005,** *40*, 321-348.
24. Choi, S.; Drese, J. H.; Jones, C. W., Adsorbent Materials for Carbon Dioxide Capture from Large Anthropogenic Point Sources. *ChemSusChem* **2009,** *2*, 796-854.
25. Yu, C.-H.; Huang, C.-H.; Tan, C.-S., A review of CO_2 capture by absorption and adsorption. *Aerosol Air Qual. Res* **2012,** *12*, 745-769.
26. Plaza, M. G.; García, S.; Rubiera, F.; Pis, J. J.; Pevida, C., Post-combustion CO_2 capture with a commercial activated carbon: Comparison of different regeneration strategies. *Chem. Eng. J.* **2010,** *163*, 41-47.
27. Grünker, R.; Bon, V.; Müller, P.; Stoeck, U.; Krause, S.; Mueller, U.; Senkovska, I.; Kaskel, S., A new metal–organic framework with ultra-high surface area. *Chem. Comm.* **2014,** *50*, 3450-3452.
28. Czaja, A. U.; Trukhan, N.; Muller, U., Industrial applications of metal-organic frameworks. *Chem. Soc. Rev.* **2009,** *38*, 1284-1293.
29. Bara, J. E.; Carlisle, T. K.; Gabriel, C. J.; Camper, D.; Finotello, A.; Gin, D. L.; Noble, R. D., Guide to CO_2 Separations in Imidazolium-Based Room-Temperature Ionic Liquids. *Ind. Eng. Chem. Res.* **2009,** *48*, 2739-2751.

30. Kohl, A., Nielsen, R., *Gas purification*. 5th ed.; Houston, 1997.
31. D'Alessandro, D. M.; Smit, B.; Long, J. R., Carbon Dioxide Capture: Prospects for New Materials. *Angew. Chem. Int. Ed.* **2010,** *49*, 6058-6082.
32. Mahurin, S. M.; Lee, J. S.; Baker, G. A.; Luo, H.; Dai, S., Performance of nitrile-containing anions in task-specific ionic liquids for improved CO_2/N_2 separation. *J. Membr. Sci.* **2010,** *353*, 177-183.
33. Sun, L.; Smith, R., Rectisol wash process simulation and analysis. *J. Clean. Prod.* **2013,** *39*, 321-328.
34. Weiss, H., Rectisol wash for purification of partial oxidation gases. *Gas Sep. Purif.* **1988,** *2*, 171-176.
35. You, J. K.; Park, H.; Yang, S. H.; Hong, W. H.; Shin, W.; Kang, J. K.; Yi, K. B.; Kim, J.-N., Influence of Additives Including Amine and Hydroxyl Groups on Aqueous Ammonia Absorbent for CO_2 Capture. *J. Chem. Phys. B* **2008,** *112*, 4323-4328.
36. Mandal, B. P.; Bandyopadhyay, S. S., Simultaneous absorption of carbon dioxide and hydrogen sulfide into aqueous blends of 2-amino-2-methyl-1-propanol and diethanolamine. *Chem. Eng. Sci.* **2005,** *60*, 6438-6451.
37. Bougie, F.; Iliuta, M. C., Sterically Hindered Amine-Based Absorbents for the Removal of CO_2 from Gas Streams. *J. Chem. Eng. Data* **2012,** *57*, 635-669.
38. Sartori, G.; Savage, D. W., Sterically hindered amines for carbon dioxide removal from gases. *Ind. Eng. Chem. Fundam.* **1983,** *22*, 239-249.
39. Yamada, H.; Matsuzaki, Y.; Higashii, T.; Kazama, S., Density Functional Theory Study on Carbon Dioxide Absorption into Aqueous Solutions of 2-Amino-2-methyl-1-propanol Using a Continuum Solvation Model. *J. Phys. Chem. A* **2011,** *115*, 3079-3086.
40. Gutowski, K. E.; Maginn, E. J., Amine-Functionalized Task-Specific Ionic Liquids: A Mechanistic Explanation for the Dramatic Increase in Viscosity upon Complexation with CO_2 from Molecular Simulation. *J. Am. Chem. Soc.* **2008,** *130*, 14690-14704.
41. García-Abuín, A.; Gómez-Díaz, D.; Navaza, J. M.; Rumbo, A., CO_2 capture by pyrrolidine: Reaction mechanism and mass transfer. *AIChE J.* **2014,** *60*, 1098-1106.
42. Gurkan, B. E.; de la Fuente, J. C.; Mindrup, E. M.; Ficke, L. E.; Goodrich, B. F.; Price, E. A.; Schneider, W. F.; Brennecke, J. F., Equimolar CO_2 Absorption by Anion-Functionalized Ionic Liquids. *J. Am. Chem. Soc.* **2010,** *132*, 2116-2117.
43. Bonenfant, D.; Mimeault, M.; Hausler, R., Determination of the Structural Features of Distinct Amines Important for the Absorption of CO_2 and Regeneration in Aqueous Solution. *Ind. Eng. Chem. Res.* **2003,** *42*, 3179-3184.
44. Lepaumier, H.; Picq, D.; Carrette, P.-L., New Amines for CO_2 Capture. II. Oxidative Degradation Mechanisms. *Ind. Eng. Chem. Res.* **2009,** *48*, 9068-9075.

45. Falk-Pedersen, O.; Dannström, H., Separation of carbon dioxide from offshore gas turbine exhaust. *Energy Convers. Manage.* **1997,** *38, Supplement*, S81-S86.
46. Lin, H.; Freeman, B. D., Materials selection guidelines for membranes that remove CO_2 from gas mixtures. *J. Mol. Struct.* **2005,** *739*, 57-74.
47. Merkel, T. C.; Freeman, B. D.; Spontak, R. J.; He, Z.; Pinnau, I.; Meakin, P.; Hill, A. J., Ultrapermeable, Reverse-Selective Nanocomposite Membranes. *Science* **2002,** *296*, 519-522.
48. Baker, R. W., *Membrane Technology and applications*. 2nd ed.; John Wiley & Sons Ltd.: Chichester, 2004.
49. Matsumoto, M.; Inomoto, Y.; Kondo, K., Selective separation of aromatic hydrocarbons through supported liquid membranes based on ionic liquids. *J. Membr. Sci.* **2005,** *246*, 77-81.
50. Kreiter, R.; Overbeek, J. P.; Correia, L. A.; Vente, J. F., Pressure resistance of thin ionic liquid membranes using tailored ceramic supports. *J. Membr. Sci.* **2011,** *370*, 175-178.
51. UOP, H. https://www.honeywell-uop.cn/wp-content/uploads/2011/02/UOP-Separex-Membrane-Technologytech-presentation.pdf. (accessed 30.06.2014).
52. Baker, R. W., Future directions of membrane gas separation technology. *Ind. Eng. Chem. Res.* **2002,** *41*, 1393-1411.
53. Basu, S.; Khan, A. L.; Cano-Odena, A.; Liu, C.; Vankelecom, I. F. J., Membrane-based technologies for biogas separations. *Chem. Soc. Rev.* **2010,** *39*, 750-768.
54. Kemperman, A. J. B.; Bargeman, D.; Van Den Boomgaard, T.; Strathmann, H., Stability of Supported Liquid Membranes: State of the Art. *Sep. Sci. Technol.* **1996,** *31*, 2733-2762.
55. Quinn, R.; Appleby, J. B.; Pez, G. P., New facilitated transport membranes for the separation of carbon dioxide from hydrogen and methane. *J. Membr. Sci.* **1995,** *104*, 139-146.
56. Scovazzo, P.; Visser, A. E.; Davis, J. H.; Rogers, R. D.; Koval, C. A.; DuBois, D. L.; Noble, R. D., Supported Ionic Liquid Membranes and Facilitated Ionic Liquid Membranes. In *Ionic Liquids*, American Chemical Society: 2002; pp 69-87.
57. Adibi, M.; Barghi, S. H.; Rashtchian, D., Predictive models for permeability and diffusivity of CH_4 through imidazolium-based supported ionic liquid membranes. *J. Membr. Sci.* **2011,** *371*, 127-133.

2.
Ionic liquids

"The world is full of obvious things
which nobody by any chance ever observes."

Sir Arthur Conan Doyle,
The Hound of the Baskervilles

2.1. Introduction

Ionic Liquids (ILs) are compounds that consist entirely of ions. ILs usually melt below 150 °C and are often already molten at room temperature (Room Temperature Ionic Liquids, RTILs).

ILs are usually composed of a bulky organic cation and an (in)organic anion (Figure 2.1). Among cations, the most commonly used are: *aza-heterocyclic* cations (e.g. imidazolium, piperidinium, pyridinium, pyrrolidinium or morpholinium cations); *ammonium* and *phosphonium* cations. Predominant anion species include *halides* (chloride, bromide, iodide), *carboxylate* anions (acetate), *fluorinated anions* (bis(trifluoromethylsulfonyl)imide, trifluoromethane sulfonate, trifluoroacetate), *nitrile-containing anions* (dicyanamide, tricyanomethanide) and sulfonate-containing anions (*p*-toluenesulfonate).

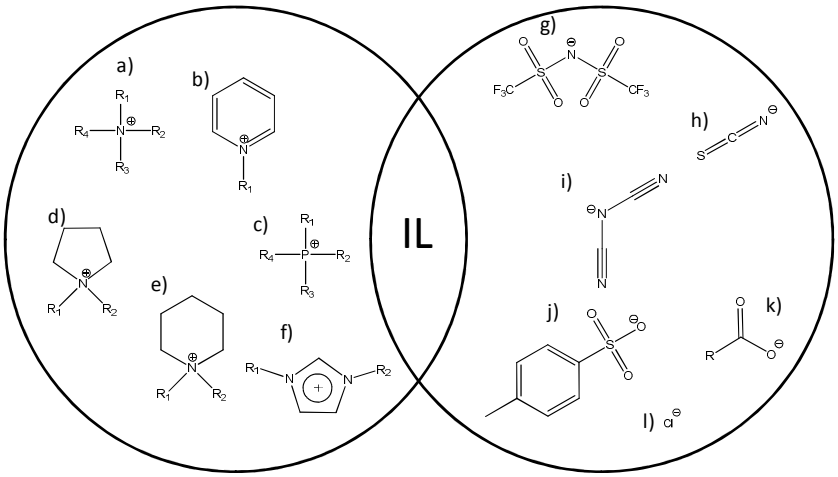

Figure 2.1: Commonly used constituent ions of ionic liquids. Cations: a) ammonium $[N_{wxyz}]^+$, b) pyridinium [R-Py]$^+$, c) Phosphonium $[P_{wxyz}]^+$, d) pyrrolidinium $[R_1,R_2\text{-Pyrr}]^+$, e) piperidinium $[R_1,R_2\text{-Pip}]^+$, f) imidazolium $[R_1,R_2\text{-Im}]^+$; Anions: g) bis(trifluoromethylsulfonyl)imide $[Tf_2N]^-$, h) thiocyanate $[SCN]^-$, i) dicyanamide $[DCA]^-$, j) *p*-toluenesulfonate $[TsO]^-$, k) carboxylate $[RCOO]^-$, l) chloride $[Cl]^-$

Formulas of ILs are composed of abbreviated names of cations and anions placed next to one another in square brackets. For example the name of a common IL, 1-ethyl-3-methylimidazolium bis(trifluoromethyl-sulfonyl)imide (Fig. 2.2) is abbreviated $[C_2mim][Tf_2N]$.

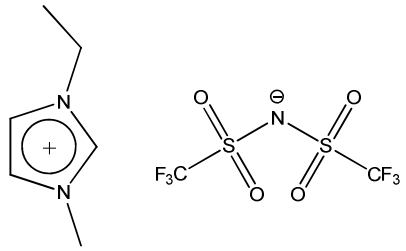

Figure 2.2: Structure of a common IL, 1-ethyl-3-methylimidazolium bis(trifluoromethylsulfonyl)imide, $[C_2mim][Tf_2N]$.

2.2. Properties of ILs

Many of the physical and chemical properties of ILs, such as the melting point, viscosity, thermal stability and affinity for other compounds, can be "tuned" to a certain extent, that is, they can be regulated by the choice of cation and anion to obtain ILs that fit the desired application. This is why ILs are sometimes referred to as "designer solvents". Whereas approximately 600 molecular solvents are known, it has been estimated that 10^{18} cation-anion permutations in ILs are theoretically possible. Virtually any combination of cation and anion can be used, provided the ions will not react with each other and provided the melting point of the resulting IL will not be too high.

2.2.1. Melting point

In general, the melting point of an ionic compound depends on its crystal lattice energy, which in turn depends on the intermolecular forces between the ions, their molecular symmetry and conformational freedom.[1] The ions of ILs, in contrast with the ions of inorganic salts, are mismatched in size and shape, preventing the occurrence of strong electrostatic interactions. For example, *N,N*-dimethylpyrrolidinium *p*-toluene sulfonate melts at 167 °C.[2] Lowering the symmetry of the cation by incorporating different substituents, replacing of the TsO^- anion by the bulky Tf_2N^- anion and eventually replacing of the pyrrolidinium cationic core by the imidazolium cation with a delocalized electronic system, systematically decreases the melting points of the resulting ILs (Fig 2.3).

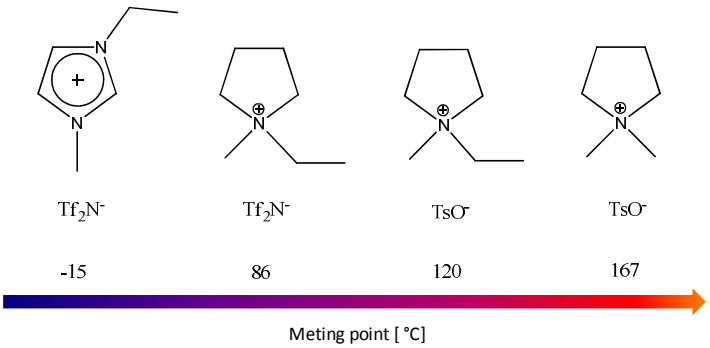

Figure 2.3: Melting point decrease of ionic liquids on lowering the symmetry, introduction of bulky and flexible anions and a delocalized cation.[2]

2.2.2. Viscosity

Apart from the melting point, viscosity is one of the parameters which determine the application and industrial utility of an IL. Viscosities of ILs range from about 15 cP ([C_2mim] [DCA], at 25 °C),[3] to about 3000 cP for instance for [$P_{(14)444}$][DBS],[4] that it from the viscosity of orange juice to that of honey. The mass transport through viscous ILs is impeded which is problematic in applications where stirring or bulk absorption is required (e.g. in extractions or gas absorption). On the other hand, high viscosity can be beneficial in other applications, where a layer of an ionic liquid should be stable under high pressure, such as IL-stationary phases in gas chromatography (Table 2.1).[5] Incorporation of long alkyl chains or halide anions to various cationic cores, as well as methyl group on the C2 atom of the imidazolium core increases viscosity of the resulting ILs.[6,7] The viscosity of ILs is also heavily influenced by the presence of impurities: alkali metal halides increase the IL viscosity while the presence of water or organic solvents dramatically decreases it.[8]

2.3. "Green" aspects of ILs

Ionic liquids are sometimes referred to as *green* solvents because they are non-volatile and because they can be recycled.[9] Indeed, in these

aspects they have the advantage over many molecular solvents. However, taking into account the toxicity, ILs are not always green. For example, imidazolium cations are structurally similar to histidine and therefore are potentially bioactive, while perfluorinated ILs are not easily biodegradable and can accumulate in the living species.[10-12] Moreover, some ILs can be unstable even in mild conditions and release toxic compounds. For example, $[C_4mim][PF_6]$ releases HF when heated in water.[13] Until all necessary toxicological tests are performed, all ILs should be treated as potentially toxic and they should be handled with special care.

2.4. Applications of ILs

Although the first ionic liquid was synthesized in 1914, their golden age began only in the late 1990s.[14,15] The boom for ILs came with the understanding that these compounds can be used in most versatile applications, solving long standing industrial problems or presenting more economic solutions to the currently applied processes. The combination of the ionic nature of ILs with their extremely low melting points, negligible vapour pressure, thermal stability, and high "tuneability" makes this class of compounds very interesting for a plethora of applications. Since ILs consist of ions, they can be used wherever mobile charges are needed, for example in electrochemistry, especially that they are often characterized by large electrochemical windows.[15] ILs are non-volatile, unless particularly harsh conditions are applied and they can thus serve as a replacement in all applications where volatility is an issue. The most important application of ILs paired with a property desired for the application, are listed in Table 2.1.

Table 2.1: Application of ionic liquids and their properties that enable their use in this application and examples of ILs.

Application	IL property	IL example
Gas absorption and separation[16,17]	High solubility of certain gases in ILs and low solubility of ILs in these gases [18]	$[C_4mim][Tf_2N]$
Storage of toxic gases[19]	Complexation of gases by ILs	$[C_4mim][BF_4]$
Metal ions extraction[20]	Affinity to certain metal ions	Cyphos® 101
Solvents for protein separation[21]	Affinity to certain proteins	$[P_{4444}][TF\text{-}Leu]$
Electrowetting[22]	High thermal stability, large electrochemical window	$[BrC_{10}BrC_{10}Im][Br]$
Lubricants and vacuum greases[23]	High thermal stability, low compressibility	$[C_2mim][BF_4]$
Stationary phases in gas chromatography (GC)[24]	High thermal stability and viscosity; affinity to certain analytes	[Bzmim][TfO]
Media for capillary electrophoresis (CE)[25]	High thermal stability and affinity to certain analytes	$[C_2mim][TFA]$
Solvents for polymers, e.g. cellulose[26]	Ability to interrupt hydrogen bond network	$[C_4mim][Cl]$
Reaction solvents and catalysts[27]	Recyclability, tuneability	$[C_4mim][PF_6]$

2.5. References

1. Dearden, J. C., The QSAR prediction of melting point, a property of environmental relevance. *Sci. Total Environ.* **1991,** *109–110*, 59-68.
2. Zhang, S.; Sun, N.; He, X.; Lu, X.; Zhang, X., Physical properties of ionic liquids: database and evaluation. *J. Phys. Chem. Ref. Data* **2006,** *35*, 1475-1517.
3. Larriba, M.; Navarro, P.; García, J.; Rodríguez, F., Liquid–Liquid Extraction of Toluene from Heptane Using [emim][DCA], [bmim][DCA], and [emim][TCM] Ionic Liquids. *Ind. Eng. Chem. Res.* **2013,** *52*, 2714-2720.
4. Ferguson, L.; Scovazzo, P., Solubility, Diffusivity, and Permeability of Gases in Phosphonium-Based Room Temperature Ionic Liquids: Data and Correlations. *Ind. Eng. Chem. Res.* **2007,** *46*, 1369-1374.
5. Poole, C. F.; Poole, S. K., Ionic liquid stationary phases for gas chromatography. *J. Sep. Sci.* **2011,** *34*, 888-900.
6. Mahurin, S. M.; Hillesheim, P. C.; Yeary, J. S.; Jiang, D.; Dai, S., High CO_2 Solubility, Permeability and Selectivity in Ionic Liquids with Tetracyanoborate Anion. *RSC Advances* **2012,** *2*, 11813-11819.
7. Wasserscheid, P. E., Welton, T. (Ed.), *Ionic Liquids in Synthesis*. 2002; Vol. 1.
8. Seddon, K. R.; Stark, A.; Torres, M.-J., Influence of chloride, water, and organic solvents on the physical properties of ionic liquids. *Pure Appl. Chem.* **2000,** *72*, 2275-2287.
9. Earle, M. J.; Seddon, K. R., Ionic liquids. Green solvents for the future. *Pure Appl. Chem.* **2000,** *72*, 1391-1398.
10. Anderson, E. B.; Long, T. E., Imidazole- and imidazolium-containing polymers for biology and material science applications. *Polymer* **2010,** *51*, 2447-2454.
11. Pretti, C.; Chiappe, C.; Baldetti, I.; Brunini, S.; Monni, G.; Intorre, L., Acute toxicity of ionic liquids for three freshwater organisms: Pseudokirchneriella subcapitata, Daphnia magna and Danio rerio. *Ecotoxicol. Environ. Saf.* **2009,** *72*, 1170-1176.
12. Hekster, F. M.; Laane, R. W.; de Voogt, P., Environmental and toxicity effects of perfluoroalkylated substances. In *Rev. Environ. Contam. Toxicol.*, Springer: 2003; pp 99-121.
13. Swatloski, R. P.; Holbrey, J. D.; Rogers, R. D., Ionic liquids are not always green: hydrolysis of 1-butyl-3-methylimidazolium hexafluorophosphate. *Green Chem.* **2003,** *5*, 361-363.
14. Wilkes, J. S.; Zaworotko, M. J., Air and water stable 1-ethyl-3-methylimidazolium based ionic liquids. *J. Chem. Soc., Chem. Commun.* **1992**, 965-967.
15. Plechkova, N. V.; Seddon, K. R., Applications of ionic liquids in the chemical industry. *Chem. Soc. Rev.* **2008,** *37*, 123-150.

16. Huang, J.; Riisager, A.; Wasserscheid, P.; Fehrmann, R., Reversible physical absorption of SO_2 by ionic liquids. *Chem. Commun.* **2006**, 4027-4029.
17. Neves, L. A.; Crespo, J. G.; Coelhoso, I. M., Gas permeation studies in supported ionic liquid membranes. *J. Membrane Sci.* **2010,** *357*, 160-170.
18. Huang, X.; Margulis, C. J.; Li, Y.; Berne, B. J., Why Is the Partial Molar Volume of CO_2 So Small When Dissolved in a Room Temperature Ionic Liquid? Structure and Dynamics of CO_2 Dissolved in [$Bmim^+$] [PF_6^-]. *J. Am. Chem. Soc.* **2005,** *127*, 17842-17851.
19. Tempel, D. J.; Henderson, P. B.; Brzozowski, J. R. Reactive liquid based gas storage and delivery systems. EP1486458 A2, 2007.
20. Wellens, S.; Thijs, B.; Binnemans, K., An environmentally friendlier approach to hydrometallurgy: highly selective separation of cobalt from nickel by solvent extraction with undiluted phosphonium ionic liquids. *Green Chem.* **2012,** *14*, 1657-1665.
21. Kohno, Y.; Saita, S.; Murata, K.; Nakamura, N.; Ohno, H., Extraction of proteins with temperature sensitive and reversible phase change of ionic liquid/water mixture. *Polym. Chem.* **2011,** *2*, 862-867.
22. Wanigasekara, E.; Zhang, X.; Nanayakkara, Y.; Payagala, T.; Moon, H.; Armstrong, D. W., Linear Tricationic Room-Temperature Ionic Liquids: Synthesis, Physiochemical Properties, and Electrowetting Properties. *ACS Appl. Mater. Interfaces* **2009,** *1*, 2126-2133.
23. Bermúdez, M.-D.; Jiménez, A.-E.; Sanes, J.; Carrión, F.-J., Ionic liquids as advanced lubricant fluids. *Molecules* **2009,** *14*, 2888-2908.
24. Anderson, J. L.; Armstrong, D. W., High-Stability Ionic Liquids. A New Class of Stationary Phases for Gas Chromatography. *Anal. Chem.* **2003,** *75*, 4851-4858.
25. Vaher, M.; Koel, M.; Kaljurand, M., Application of 1-alkyl-3-methylimidazolium-based ionic liquids in non-aqueous capillary electrophoresis. *J. Chromatogr. A* **2002,** *979*, 27-32.
26. Swatloski, R. P.; Spear, S. K.; Holbrey, J. D.; Rogers, R. D., Dissolution of Cellose with Ionic Liquids. *J. Am. Chem. Soc.* **2002,** *124*, 4974-4975.
27. Wasserscheid, P.; Keim, W., Ionic liquids-new" solutions" for transition metal catalysis. *Angew. Chem.* **2000,** *39*, 3772-3789.

3.

Supported Ionic Liquid Membranes (SILMs)

As mentioned in sections 1.2.4 and 2.4, low vapour pressure, high thermal stability and the ability to dissolve gases suggested the use of ILs in CO_2 absorption and separation. Although they are not yet industrially employed, Supported Ionic Liquids Membranes (1.2.4) make the best use of the special properties of ILs (non-volatility, thermal stability and higher surface tension) and are therefore often able to circumvent the instability problems inherent to SLMs.[1,2] To answer the question of which ILs are the most suitable for CO_2 separation on SILMs, the mechanism of gas separation and the reasons for the high CO_2 solubility in ILs on the molecular level have to be addressed first.

3.1. Solution-diffusion mechanism

Gas separation on SILMs is governed by the Solution-Diffusion mechanism: When a mixture of gases is directed onto a SILM, the gas of interest (e.g. CO_2) dissolves in the IL, diffuses through the IL and the porous support layer due to the pressure difference across the membrane, and desorbs on the permeate side (Fig 3.1).[3] The gas is then swept away by the permeate stream. An effective SILM is designed in such a way that the contaminant gas (e.g. N_2) is less soluble in the given IL and hence only a small fraction of it diffuses through the membrane.

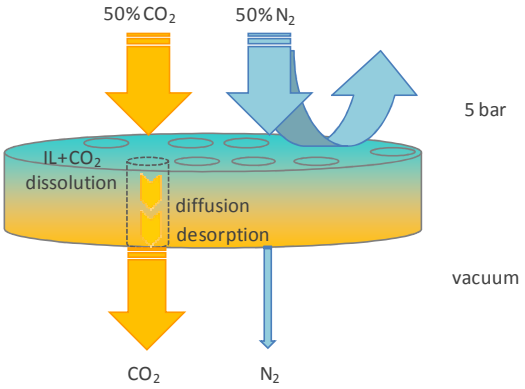

Figure 3.1: Separation of CO_2 from N_2 on a SILM. The blue colour represents the IL layer in the pores.

The ability of a membrane to permeate a gas, *membrane permeability*, P_i [Barrer, 10^{-10} cm^3 (STP) cm/cm^2 s cm Hg], is the product of the *solubility coefficient* S_i [cm^3 (STP)/cm^3 cm Hg] and the *diffusion coefficient* D_i [cm^2/s]:

$$P_i = S_i D_i \tag{3.1}$$

The solubility coefficient S_i indicates how well gas molecules dissolve in the membrane material; the diffusion coefficient D_i describes the ease of diffusion that is the mobility of gas molecules in the membrane material. The membrane *selectivity*, α_{ij}, or *permselectivity* (unitless) measures the ability of a membrane to separate two gases, and is equal to the ratio of the permeability of the more permeable gas to the less permeable one:

$$\alpha_{ij} = \frac{P_i}{P_j} \tag{3.2}$$

Taking into account Eq. 1, the selectivity can also be expressed as:

$$\alpha_{ij} = \frac{D_i}{D_j}\frac{S_i}{S_j} \tag{3.3}$$

The ratio D_i/D_j is the *diffusivity selectivity* and reflects the difference in ease of passing thorough the membrane for the two gases. The ratio S_i/S_j is the *solubility selectivity* and shows the relative solubility of both

gases in the membrane material, indicating their affinity to the substrate. The *performance* of the membrane is a collective term used to describe both permeability and selectivity.

3.1.1. Robeson plot

The graph presented in (Fig 3.2) is customary known as *Robeson plot* and is used to compare the performance of gas separation membranes made of different materials (e.g. purely polymeric membranes and SILMs).[4]

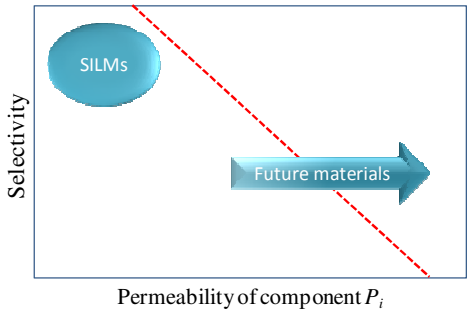

Figure 3.2: Robeson plot showing the performance of currently known SILMs.[5]

The selectivity α (α = P_i/P_j) is plotted against the permeability of the more permeable gas (P_i). The data points for all existing membranes are located below a critical line, called the "upper bound". An ideal membrane is characterized by high separation selectivity and high permeability of a given gas. In other words, the data point for this membrane would be situated in the upper right corner of the plot. Most membranes, however, exhibit a trade-off between selectivity and permeability, that is, when permeability increases, selectivity decreases.[6] More permeable membranes usually permit both gases, and, as a consequence their separation abilities decrease. Analogously, increased selectivity causes a decrease in permeability.[7] Area locating the data points for SILM systems is marked in a blue circle. Thus, SILMs (and polymeric membranes) exhibit high selectivities but rather low permeabilities, what is inherent to dense membranes.[5]

3.2. Designing ILs for SILMs

When designing ILs to create a SILM with the highest performance in CO_2 separation from N_2 or CH_4, diffusivity and solubility of both gases in the system can be adjusted.

3.2.1. Influencing the diffusion coefficient

In general, the diffusivity of all gases increases with decreasing viscosity of the IL and decreasing strength of specific gas-IL interactions.[6] It is important to note that too low viscosities can lead to similar problems as observed with SLMs: a layer of a less viscous IL will not be stable under pressure. Diffusivity is also affected to a certain extent by the molecular size of the gas. Since the kinetic diameters of the gases are as follows: CO_2 (3.4 Å), N_2 (3.6Å), CH_4 (3.8Å), the diffusivity of CO_2 is higher than that of CH_4 and similar to the one of N_2.[5,8-9] Additionally, diffusivity selectivity is proportional to the ratio of the molar volumes of the gases involved, and in the case of CO_2/N_2, and even CO_2/CH_4 separation, the diffusivity selectivity is close to one.[10] Therefore, apart from aiming at low viscosity ILs, the increase of IL diffusivity is less often addressed and selectivity of gas separation on SILMs is dominated by solubility selectivity.

3.2.2. Influencing the solubility coefficient

Due to its polar nature, CO_2 dissolves in ILs much better than for example nitrogen, oxygen, hydrogen or hydrocarbons that interact with ILs only by weak and nonspecific dispersion forces.[11,12,13] For instance, the N_2 molecule has a low quadrupole moment and a low polarizability and thus the proximity of IL ions cannot induce in it an electric dipole, while the CH_4 molecule has no dipole moment and no quadrupole moment.[13,14] Therefore, CO_2 solubility can be increased by using ILs equipped with polar groups that efficiently interact with this gas, while being neutral towards N_2 or CH_4. In contrast with diffusivity, the

possibilities to enhance CO_2 solubility are countless. The following sections will specify how to achieve the highest CO_2 solubility and what other factors besides the presence of the polar groups influence it.

3.2.3. Physical vs. chemical absorption

According to the solution-diffusion theory, the most effective ILs dissolve the largest amount of CO_2, but they do not bind gas molecules too strongly. This suggests the advantage of the use of physisorption over chemisorption.[15] Chemical absorption occurs in ILs which contain a significantly basic group, such as an amino group,[16] a superbasic moiety[17] or a carboxylate anion.[18] Although these ILs are efficient in CO_2 capture, due to the difficulty in releasing the gas, only a few examples of SILMs made with such ILs are known.[19,20] Physical dissolution is based on, inter alia, the interactions of the gas molecules with various polar moieties of the ILs.

3.2.4. Mechanism of physical gas dissolution in ILs

Results of several gas dissolution experiments revealed that this process in ILs cannot be exclusively related to the gas-IL interactions.[21-23] For instance, replacing a PF_6 anion by a Tf_2N anion in imidazolium ILs, improves not only the dissolution of CO_2 but also that of N_2 and H_2, both of which are both non-polar and should not interact with the Tf_2N anion better than with the PF_6.[21] The answer was to be found on the nanoscopic scale.

Various theoretical and experimental investigations revealed that the bulk of ILs is nanosegregated.[21,24] Anions, cationic cores and polar substituents form three-dimensional *polar domains*, while nonpolar substituent alkyl chains tend to aggregate in *nonpolar domains*.[21,25] A given IL can be thus seen as composed of polar and nonpolar solvents. When a gas dissolves in the IL, depending on its nature, it can locate in either type of the domains. For example C_3F_8 locates in nonpolar

domains of $[P_{66614}][Tf_2N]$ while CF_4 can be found in polar and nonpolar domains of this IL.[25]

Matching polarity is not the only requirement for efficient gas dissolution in ILs. Equally important is the availability of space (free volume) in which the gas can dissolve. *Free volume* of a substance, usually expressed as the fractional free volume (FFV, unitless), is the space filled by the substance that is not occupied by its atoms, and is therefore available for the gas molecules:

$$FFV = \frac{V - V_0}{V} \qquad 3.4$$

V is the specific volume of the substance [cm^3/g] at the temperature of interest (volume occupied by a unit of mass) and V_0 is the specific volume occupied by the molecules themselves [cm^3/g] at 0 K, estimated to be 1.3 times the Van der Waals volume of the molecule.

There is always some free volume present in an IL, although it is usually not big enough to accommodate the gas molecules.[21] Therefore, on contact with the gas, *cavities* are formed in the bulk of the IL. In contrast with molecular solvents, strong electrostatic interactions between the ions of the ILs allow only for a small volume expansion on gas absorption (for the phenomenon of IL swelling, see Chapter 5).[26] This is why spatial rearrangements of the ions are necessary to create the cavities. Flexible ions can provide the necessary space for the gas by changing their conformations. For example, pyrrolidinium cations, can adopt an *envelope* or a *twist* conformation, while Tf_2N anions can exhibit a *cis* or a *trans* conformation.[21,27-28] Rigid ions, such as BF_4, form cavities by small angular rearrangements.[26]

Since the ions of ILs vary in degree of conformational flexibility, charge density and symmetry they are able to accommodate the gas to a different extent. When bulk CO_2 absorption is desired, large cavities are needed. By contrast, when CO_2 separation is concerned, too big cavities (large FFV) promote dissolution of all gases including CH_4 and N_2.[29-6]

Once the voids are created, more specific interactions between the IL ions and the gas molecules occur.[21] In summary, according to the most recent findings, gas dissolution in ILs proceeds via the following steps:[21,26]

i) Creation of cavities (*free volume*) in the bulk of the IL to accommodate the approaching gas;
ii) Insertion of gas molecules into the cavities and occurrence of specific gas-IL interactions.

3.2.5. Designing a CO_2-phile

Several authors tried to define a perfect "CO_2-phile". According to Beckman, an ideal molecule with high CO_2-affinity is flexible, is characterized by high free volume, weak self interactions, and is able to act via multidendate interactions with CO_2 (both via the carbon and the oxygen atoms of the gas).[30] In the light of the newest discoveries concerning the mechanism of gas dissolution in ILs, the most up-to-date requirements for a CO_2-philic ILs are as following: an IL has to possess flexible ions of well adjusted polarity for efficient interactions with CO_2 and for the creation of cavities of the proper size and polarity.[21]

In the quest for ILs that provide high CO_2 separation selectivity on SILMs, various "building blocks" have been suggested. Since ILs are highly tuneable, both the cation and the anion can be independently chosen and functionalized, although chemical modifications are better suited for the cations.

Choice of cationic core

CO_2 absorption and separation on SILMs is greatly dominated by imidazolium ionic liquids, owning to their evident advantages:[5,31-33] (i) The delocalized charge of the ring prevents a formation of strong cation-anion interactions reducing the viscosity of the IL and making the ions available for the interactions with the gas molecules; (ii) The presence of

two tertiary nitrogen atoms on the imidazole ring allows for a facile independent functionalization; (iii) The starting imidazoles are inexpensive.

The appearance of many papers about imidazolium ILs due to the abovementioned reasons further stimulated the research in this direction. Less often explored ILs contain phosphonium, ammonium or pyrrolidinium cations.[34-36]

Choice of the functionalization

The idea to functionalize ILs with polar groups came from the CO_2-solubilizing abilities of common organic solvents possessing these groups, such as dimethylformamide, acetonitrile, dimethylsulfoxide and diethylene glycol (Fig. 3.2).[5]

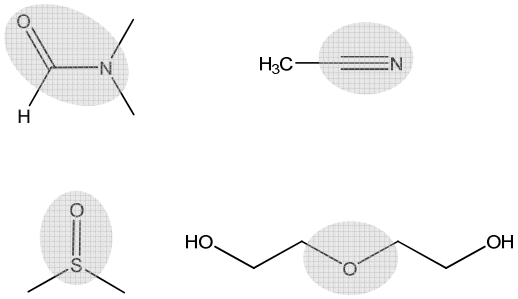

Figure 3.2: Structures of common solvents with CO_2 absorbing abilities. The moieties that define their performance and which are often incorporated into the structures of ILs are highlighted.

Studies of gas absorption in polymers led to the discovery that a polyether, poly(ethylene glycol), has excellent CO_2 solubilisation ability, much higher than the aliphatic polyethylene, and good CO_2/N_2 separation ability.[9,37] There are two reasons for this desirable effect. Firstly, the ether C-O groups strongly interact with CO_2 as observed by infrared spectroscopy (Chapter 5).[38] Secondly, ether linkages promote the creation of polar cavities because glycol chains are even more flexible than the alkyl chains.[39] Incorporation of an oligo(ethylene glycol) moiety

in the cation of an IL increases its performance by up to 75% compared to the corresponding IL with an alkyl chain, leading to ideal solubility selectivities as high as 33 for CO_2 /N_2 and 13 for CO_2 /CH_4 at 40 ºC, for methylimidazolium ILs with bis(trifluoromethylsulfonyl)imide anions.[31] High selectivity of SILMs and other membranes based on PEG-containing materials is mostly related to the difference in solubility between CO_2 and the contaminant non-polar gases and in the light of the new dissolution mechanism, size and polarity of the cavities.[9] In the case of imidazolium ILs functionalized with ether chains, the ether oxygen atoms interact with the imidazolium rings, causing a reduction of the FFV and enhancement of the CO_2 selectivity.[40,41] Moreover, this interaction disturbs cation-anion attraction, which, in turn, can make the ions more available for interplay with the gas molecules.[41]

Likewise, a nitrile group tethered to the IL cation can increase the CO_2 solubility and gas separation ability of a SILM by 30% in comparison with an alkyl analogue, most probably, as in the case of ether-functionalized ILs, due to the reduced FFV, creation of polar domains and specific IL-CO_2 interactions.[42,40] Also, anions containing several nitrile groups, such as dicyanamide, tricyanomethanide or tetracyanoborate, can be very efficient in CO_2 absorption and separation, significantly outperforming the most popular bis(trifluoro-methylsulfonyl) imide anion in 1-alkyl-3-methylimidazolium ILs.[8,10,14]

Choice of the anion

The bis(trifluoromethylsulfonyl)imide anion is a common choice in designing ILs for CO_2 separation from N_2 or CH_4, because it gives low viscosity ILs and provides high separation selectivities.[11,14,31,43] The efficiency of this anion, apart from its flexibility, is attributed to the delocalized charge and functionalization. The charge on the imide nitrogen atom is delocalized over the neighbouring sulfur atoms but not into the oxygen atoms, which, along with the CF_3 groups shield the

anion from interaction with cations.[44] ILs possessing an analogous non-fluorinated bis(methylsulfonyl)imide anion dissolve less CO_2 than Tf_2N ILs indicating the importance of the CF_3 groups.[45] The drawback of Tf_2N is its high price and toxicity, both due to the fluorination.

Another anion used in CO_2-absorbing ILs is *p*-toluenesulfonate (tosylate, TsO^-). Just like the Tf_2N anion, TsO^- possesses the sulfonyl ($–SO_2$ group). Ab initio calculations revealed that this group in DMSO may be responsible for high CO_2 solubility in this solvent.[46] The TsO^- anion has delocalized electrons not only at the toluyl ring but also at the sulfonyl group, which can contribute to the lower viscosity of its IL and makes CO_2-π interactions possible. For example, the IL triisobutyl-methylphosphonium *p*-toluenesulfonate exhibits CO_2 solubility comparable to $[C_4mim][PF_6]$ and $[C_4mim][BF_4]$, which are efficient in CO_2 absorption but unstable in the presence of water.[14] Additional proof for the interaction of tosylate-containing ILs came from their use in CO_2 sensors where $[C_4mim][TsO]$ exhibited a significantly higher response to CO_2 than the materials based on $[C_4mim][BF_4]$, possibly due to a higher solubility of CO_2 in the IL composed of a more bulky anion.[47]

3.2.6. Challenges in the synthesis of ILs for SILMs

Although many ILs have been already tested on SILMs and other types of IL-containing membranes, the search for industrially relevant ILs is still in progress. Moreover, the structure-performance relationship for ILs on SILMs is not yet sufficiently comprehended. The challenge of obtaining an IL perfect for SILM separation of CO_2 from N_2 or CH_4 is illustrated in Figure 3.1.

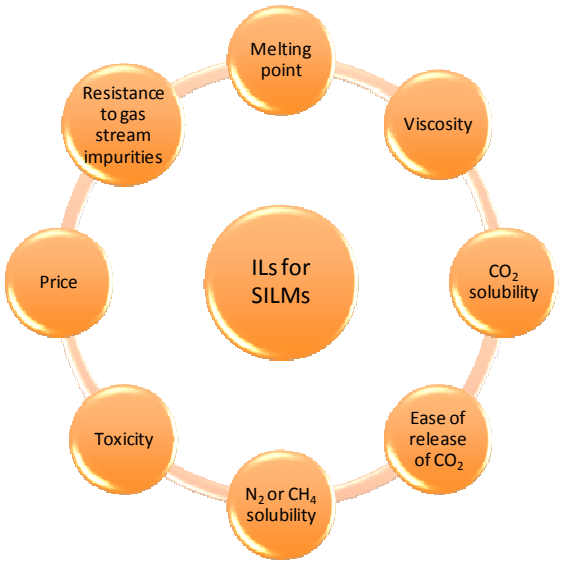

Figure 3.1 Aspects that have to be taken into account when designing an IL for CO_2 separation on SILMs from N_2 or CH_4.

3.3. References

1. Scovazzo, P.; Visser, A. E.; Davis, J. H.; Rogers, R. D.; Koval, C. A.; DuBois, D. L.; Noble, R. D., Supported Ionic Liquid Membranes and Facilitated Ionic Liquid Membranes. In *Ionic Liquids*, American Chemical Society: 2002; pp 69-87.
2. Adibi, M.; Barghi, S. H.; Rashtchian, D., Predictive models for permeability and diffusivity of CH_4 through imidazolium-based supported ionic liquid membranes. *J. Membr. Sci.* **2011,** *371*, 127-133.
3. Baker, R. W., *Membrane Technology and applications*. 2nd ed.; John Wiley & Sons Ltd.: Chichester, 2004.
4. Robeson, L. M., Correlation of separation factor versus permeability for polymeric membranes. *J. Membr. Sci.* **1991,** *62*, 165-185.
5. Bara, J. E.; Carlisle, T. K.; Gabriel, C. J.; Camper, D.; Finotello, A.; Gin, D. L.; Noble, R. D., Guide to CO_2 Separations in Imidazolium-Based Room-Temperature Ionic Liquids. *Ind. Eng. Chem. Res.* **2009,** *48*, 2739-2751.
6. Freeman, B. D., Basis of Permeability/Selectivity Tradeoff Relations in Polymeric Gas Separation Membranes. *Macromolecules* **1999,** *32*, 375-380.
7. Robeson, L. M., The upper bound revisited. *J. Membr. Sci.* **2008,** *320*, 390-400.

8. Camper, D.; Bara, J.; Koval, C.; Noble, R., Bulk-Fluid Solubility and Membrane Feasibility of Rmim-Based Room-Temperature Ionic Liquids. *Ind. Eng. Chem. Res.* **2006,** *45*, 6279-6283.
9. Lin, H.; Freeman, B. D., Materials selection guidelines for membranes that remove CO_2 from gas mixtures. *J. Mol. Struct.* **2005,** *739*, 57-74.
10. Mahurin, S. M.; Lee, J. S.; Baker, G. A.; Luo, H.; Dai, S., Performance of nitrile-containing anions in task-specific ionic liquids for improved CO_2/N_2 separation. *J. Membr. Sci.* **2010,** *353*, 177-183.
11. Anderson, J. L.; Dixon, J. K.; Brennecke, J. F., Solubility of CO_2, CH_4, C_2H_6, C_2H_4, O_2, and N_2 in 1-Hexyl-3-methylpyridinium Bis(trifluoromethylsulfonyl)imide: Comparison to Other Ionic Liquids. *Acc. Chem. Res.* **2007,** *40*, 1208-1216.
12. Anthony, J. L.; Maginn, E. J.; Brennecke, J. F., Solubilities and Thermodynamic Properties of Gases in the Ionic Liquid 1-n-Butyl-3-methylimidazolium Hexafluorophosphate. *J. Chem. Phys. B* **2002,** *106*, 7315-7320.
13. Prasad, B. R.; Senapati, S., Explaining the Differential Solubility of Flue Gas Components in Ionic Liquids from First-Principle Calculations. *J. Chem. Phys. B* **2009,** *113*, 4739-4743.
14. Anthony, J. L.; Anderson, J. L.; Maginn, E. J.; Brennecke, J. F., Anion Effects on Gas Solubility in Ionic Liquids. *J. Chem. Phys. B* **2005,** *109*, 6366-6374.
15. Mahurin, S. M.; Hillesheim, P. C.; Yeary, J. S.; Jiang, D.; Dai, S., High CO_2 Solubility, Permeability and Selectivity in Ionic Liquids with Tetracyanoborate Anion. *RSC Advances* **2012,** *2*, 11813-11819.
16. Bates, E. D.; Mayton, R. D.; Ntai, I.; Davis, J. H., CO_2 Capture by a Task-Specific Ionic Liquid. *J. Am. Chem. Soc.* **2002,** *124*, 926-927.
17. Wang, C.; Luo, H.; Jiang, D.-e.; Li, H.; Dai, S., Carbon Dioxide Capture by Superbase-Derived Protic Ionic Liquids. *Angew. Chem.* **2010,** *122*, 6114-6117.
18. Gurau, G.; Rodríguez, H.; Kelley, S. P.; Janiczek, P.; Kalb, R. S.; Rogers, R. D., Demonstration of Chemisorption of Carbon Dioxide in 1,3-Dialkylimidazolium Acetate Ionic Liquids. *Angew. Chem. Int. Ed.* **2011,** *50*, 12024-12026.
19. Myers, C.; Pennline, H.; Luebke, D.; Ilconich, J.; Dixon, J. K.; Maginn, E. J.; Brennecke, J. F., High temperature separation of carbon dioxide/hydrogen mixtures using facilitated supported ionic liquid membranes. *J. Membr. Sci.* **2008,** *322*, 28-31.
20. Hanioka, S.; Maruyama, T.; Sotani, T.; Teramoto, M.; Matsuyama, H.; Nakashima, K.; Hanaki, M.; Kubota, F.; Goto, M., CO_2 separation facilitated by task-specific ionic liquids using a supported liquid membrane. *J. Membr. Sci.* **2008,** *314*, 1-4.
21. Hu, Y.-F.; Liu, Z.-C.; Xu, C.-M.; Zhang, X.-M., The molecular characteristics dominating the solubility of gases in ionic liquids. *Chem. Soc. Rev.* **2011,** *40*, 3802-3823.

22. Kazarian, S. G.; Briscoe, B. J.; Welton, T., Combining ionic liquids and supercritical fluids: ATR-IR study of CO_2 dissolved in two ionic liquids at high pressures. *Chem. Commun.* **2000**, 2047-2048.
23. Seki, T.; Grunwaldt, J.-D.; Baiker, A., In Situ Attenuated Total Reflection Infrared Spectroscopy of Imidazolium-Based Room-Temperature Ionic Liquids under "Supercritical" CO_2. *J. Chem. Phys. B* **2008,** *113*, 114-122.
24. Antonietti, M.; Kuang, D.; Smarsly, B.; Zhou, Y., Ionic Liquids for the Convenient Synthesis of Functional Nanoparticles and Other Inorganic Nanostructures. *Angew. Chem. Int. Ed.* **2004,** *43*, 4988-4992.
25. Pison, L.; Canongia Lopes, J. N.; Rebelo, L. P. N.; Padua, A. A. H.; Costa Gomes, M. F., Interactions of Fluorinated Gases with Ionic Liquids: Solubility of CF_4, C_2F_6, and C_3F_8 in Trihexyltetradecylphosphonium Bis(trifluoromethylsulfonyl)amide. *J. Chem. Phys. B* **2008,** *112*, 12394-12400.
26. Huang, X.; Margulis, C. J.; Li, Y.; Berne, B. J., Why Is the Partial Molar Volume of CO_2 So Small When Dissolved in a Room Temperature Ionic Liquid? Structure and Dynamics of CO_2 Dissolved in [$Bmim^+$] [PF_6^-]. *J. Am. Chem. Soc.* **2005,** *127*, 17842-17851.
27. Fujimori, T.; Fujii, K.; Kanzaki, R.; Chiba, K.; Yamamoto, H.; Umebayashi, Y.; Ishiguro, S.-i., Conformational structure of room temperature ionic liquid N-butyl-N-methyl-pyrrolidinium bis(trifluoromethanesulfonyl) imide — Raman spectroscopic study and DFT calculations. *J. Mol. Liq.* **2007,** *131–132*, 216-224.
28. Lassègues, J. C.; Grondin, J.; Holomb, R.; Johansson, P., Raman and ab initio study of the conformational isomerism in the 1-ethyl-3-methyl-imidazolium bis(trifluoromethanesulfonyl)imide ionic liquid. *J. Raman Spectrosc.* **2007,** *38*, 551-558.
29. Turner, C. H.; Cooper, A.; Zhang, Z.; Shannon, M. S.; Bara, J. E., Molecular Simulation of the Thermophysical Properties of N-Functionalized Alkylimidazoles. *J. Chem. Phys. B* **2012,** *116*, 6529-6535.
30. Beckman, E. J., A challenge for green chemistry: designing molecules that readily dissolve in carbon dioxide. *Chem. Comm.* **2004,** *0*, 1885-1888.
31. Bara, J. E.; Gabriel, C. J.; Lessmann, S.; Carlisle, T. K.; Finotello, A.; Gin, D. L.; Noble, R. D., Enhanced CO_2 Separation Selectivity in Oligo(ethylene glycol) Functionalized Room-Temperature Ionic Liquids. *Ind. Eng. Chem. Res.* **2007,** *46*, 5380-5386.
32. Scovazzo, P.; Kieft, J.; Finan, D. A.; Koval, C.; DuBois, D.; Noble, R., Gas separations using non-hexafluorophosphate $[PF_6]^-$ anion supported ionic liquid membranes. *J. Membr. Sci.* **2004,** *238*, 57-63.
33. Uchytil, P.; Schauer, J.; Petrychkovych, R.; Setnickova, K.; Suen, S. Y., Ionic liquid membranes for carbon dioxide–methane separation. *J. Membr. Sci.* **2011,** *383*, 262-271.

34. Quinn, R.; Appleby, J. B.; Pez, G. P., New facilitated transport membranes for the separation of carbon dioxide from hydrogen and methane. *J. Membr. Sci.* **1995,** *104*, 139-146.
35. Cserjési, P.; Nemestóthy, N.; Bélafi-Bakó, K., Gas separation properties of supported liquid membranes prepared with unconventional ionic liquids. *J. Membrane Sci.* **2010,** *349*, 6-11.
36. Tomé, L. C.; Mecerreyes, D.; Freire, C. S. R.; Rebelo, L. P. N.; Marrucho, I. M., Pyrrolidinium-based polymeric ionic liquid materials: New perspectives for CO_2 separation membranes. *J. Membr. Sci.* **2013,** *428*, 260-266.
37. Okamoto, K.-I.; Umeo, N.; Okamyo, S.; Tanaka, K.; Kita, H., Selective permeation of carbon dioxide over nitrogen through polyethyleneoxide-containing polyimide membranes. *Chem. Lett.* **1993**, 225-228.
38. Nalawade, S. P.; Picchioni, F.; Marsman, J. H.; Janssen, L. P. B. M., The FT-IR studies of the interactions of CO_2 and polymers having different chain groups. *J. Supercrit.Fluid* **2006,** *36*, 236-244.
39. May, F.; Marcon, V.; Hansen, M. R.; Grozema, F.; Andrienko, D., Relationship between supramolecular assembly and charge-carrier mobility in perylenediimide derivatives: The impact of side chains. *J. Mater. Chem.* **2011,** *21*, 9538-9545.
40. Horne, W. J.; Shannon, M. S.; Bara, J. E., Correlating fractional free volume to CO_2 selectivity in [Rmim][Tf_2N] ionic liquids. *J. Chem. Thermodyn.* **2014**.
41. Smith, G. D.; Borodin, O.; Li, L.; Kim, H.; Liu, Q.; Bara, J. E.; Gin, D. L.; Nobel, R., A comparison of ether- and alkyl-derivatized imidazolium-based room-temperature ionic liquids: a molecular dynamics simulation study. *Phys. Chem. Chem. Phys.* **2008,** *10*, 6301-6312.
42. Carlisle, T. K.; Bara, J. E.; Gabriel, C. J.; Noble, R. D.; Gin, D. L., Interpretation of CO_2 Solubility and Selectivity in Nitrile-Functionalized Room-Temperature Ionic Liquids Using a Group Contribution Approach. *Ind. Eng. Chem. Res.* **2008,** *47*, 7005-7012.
43. Carvalho, P. J.; Álvarez, V. H.; Machado, J. J. B.; Pauly, J.; Daridon, J.-L.; Marrucho, I. M.; Aznar, M.; Coutinho, J. A. P., High pressure phase behavior of carbon dioxide in 1-alkyl-3-methylimidazolium bis(trifluoromethylsulfonyl)imide ionic liquids. *J. Supercrit.Fluid* **2009,** *48*, 99-107.
44. Golding, J.; MacFarlane, D.; Skelton, B.; White, A., Weak intermolecular interactions in sulfonamide salts: structure of 1-ethyl-2-methyl-3-benzyl imidazolium bis [(trifluoromethyl) sulfonyl] amide. *Chem. Commun.* **1998**, 1593-1594.
45. Pringle, J. M.; Golding, J.; Baranyai, K.; Forsyth, C. M.; Deacon, G. B.; Scott, J. L.; MacFarlane, D. R., The effect of anion fluorination in ionic liquids-physical properties of a range of bis(methanesulfonyl)amide salts. *New J. Chem.* **2003,** *27*, 1504-1510.

46. Raveendran, P.; Wallen, S. L., Cooperative C−H···O Hydrogen Bonding in CO_2−Lewis Base Complexes: Implications for Solvation in Supercritical CO_2. *J. Am. Chem. Soc.* **2002,** *124*, 12590-12599.
47. Borisov, S. M.; Waldhier, M. C.; Klimant, I.; Wolfbeis, O. S., Optical Carbon Dioxide Sensors Based on Silicone-Encapsulated Room-Temperature Ionic Liquids. *Chem. Mater.* **2007,** *19*, 6187-6194.

4.

Influence of Cation Type and Charge on the Performance of SILMs

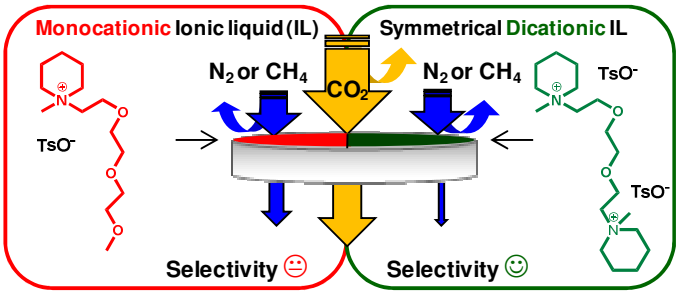

4.1. Introduction

Ionic liquids described so far in this thesis were *monocationic* and *monoanionic*, that is, their cations had a +1 charge and their anions had a -1 charge. There is a possibility to further tune ILs by assembling them from ions with double, triple or higher charge, to form so called oligoionic ILs (*oligocationic* and *oligoanionic* ILs). For example, a

---

This chapter is based on the article:

Separation of Carbon Dioxide from Nitrogen or Methane by Supported Ionic Liquid Membranes (SILMs): Influence of the Cation Charge of the Ionic Liquid. Hojniak, S. D.; Khan, A. L.; Holloczki, O.; Kirchner, B.; Vankelecom, I. F. J.; Dehaen, W.; Binnemans, K., *The Journal of Physical Chemistry B* **2013,** *117* (48), 15131-15140.

dicationic ionic liquid is generally made of two cations connected with a common linker (Fig. 4.1 a).

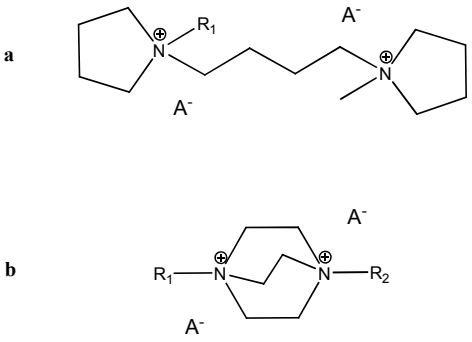

Figure 4.1: Examples of symmetrical dicationic ILs: a geminal IL (a) and an IL containing a dicationic core (b); A^- represents an anion.

The use of molecules containing two sites susceptible to quaternisation, such as DABCO (1,4-diazabicyclo[2.2.2]octane), allows a formation of a dication containing one core and two side chains (Fig. 4.1 b). Further functionalization can be achieved by replacing the alkyl spacer with an ether or thioether chain or by assembling the IL from different cations creating so called unsymmetrical ILs.[1-3] The physical and chemical properties of the oligocationic (di-, tri-cationic) ILs are generally similar to the properties of their monocationic analogues, although the former can be more thermally stable or more viscous than the latter. The higher viscosity is a result of stronger Coulombic forces occurring between doubly or triply charged ions than between single charges.[4] Although a high viscosity can limit gas diffusion across the membrane, it can also contribute to a higher pressure stability of a SILM.

Whilst prior to our publication presented in this chapter, the oligocationic ILs have not been tested in gas separation, *polyionic ILs* were already studied by many research groups.[5-10] Polyionic ILs, Poly(ILs), are polymers made of freestanding polymerizable ILs, which, as the name suggest, contain a functional group prone to polymerization (e.g. vinyl or acryloyl group).[7] During polymerization, a polymerizable IL

can be fabricated into a thin film of poly(IL), that directly serves as a membrane and usually exhibits good CO_2/N_2 and CO_2/CH_4 separation selectivities, but rather low permeabilities.[5,11,12]

In this chapter, we present the synthesis of monocationic ILs and symmetrical dicationic ILs, with imidazolium, pyrrolidinium, piperidinium or morpholinium cations, functionalized with a tri(ethylene glycol) chain. The glycol moiety is a common choice in ionic liquid functionalization when high CO_2 solubility and CO_2/N_2 or CO_2/CH_4 separation abilities are desired (3.2.5).[13] The ionic liquids were incorporated into SILMs and the selectivities of these SILMs for CO_2/N_2 and CO_2/CH_4 separations were measured. Quantum chemical calculations were used to investigate the difference in the interaction of CO_2 with monocationic and dicationic ILs.

4.2. Results and Discussion

4.2.1. Monocationic ionic liquids

Before the current CO_2 dissolution theory had been proposed (section 3.2.4), the solubility of CO_2 in ILs was attributed to the CO_2-anion interactions, with cations being merely "spectator" ions or regulators of the physical properties of ILs.[14-16] A few years later, cation-anion and CO_2-CO_2 interplays were added to the list of interactions responsible for the gas dissolution.[17-18] It is important to note that the majority of these observations was based on the studies of imidazolium ILs. Hong et al. showed that Tf_2N ILs with diversely functionalized cations (imidazolium, ammonium and pyrrolidinium) showed small but significant difference in CO_2 solubility.[19]

Our initial goal was to examine the influence of various, but identically functionalized cationic cores on CO_2 separation on SILMs. For this purpose we obtained a small library of *p*-toluenesulfonate ILs, all functionalized with a tri(ethylene glycol) moiety. Commonly used *N*-

methylated aza-heterocycles were chosen as cationic cores: *N*-methylpyrrolidine, *N*-methylpiperidine, *N*-methylmorpholine and *N*-methylimidazole (Fig. 4.2). The imidazolium IL was prepared as a reference for comparison with the ILs that have already been reported for gas separation.[12-13,20] Pyrrolidine and piperidine cores differ in ring size as well as in their conformations and were tested as examples of non-aromatic heterocycles. For example, even though the pyrrolidinium IL does not possess a delocalized charge, it can in certain cation-anion combinations, dissolve comparably much CO_2 as imidazolium ILs, due to the bigger flexibility of the pyrrolidinium ion and hence a higher free volume created.[19] Morpholine can be considered an oxygen-containing analogue of piperidine.

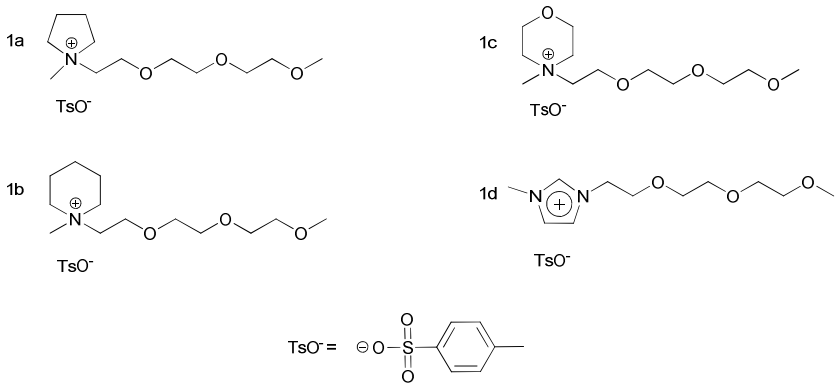

Figure 4.2: Monocationic tosylate ionic liquids functionalized with a glycol chain.

All the ionic liquids of this study contained the *p*-toluenesulfonate (tosylate) anion, for the following reasons: (i) the ease of synthesis and purity control by ^{1}H NMR spectroscopy; (ii) easier assessment of structure-property relationship and the influence of the ionic liquid on the membrane performance, when all the ILs have the same anion.

4.2.2. The influence of the cationic core on selectivity

The membrane measurements were performed by dr Asim Khan from the group of Prof. Ivo Vankelecom, COK, KU Leuven. The monocationic glycol-functionalized tosylate ionic liquids exhibit moderate mixed-gas selectivities, ranging from 15.2 for the pyrrolidinium IL **1a** to 17.6 for the morpholinium IL **1c** (Table 4.1, CO_2/N_2 system). Already these results confirm the theoretical predictions that cations can influence gas selectivity to a similar extent as anions.[21] For the CO_2/N_2 system, selectivity of the ILs increases in the following order: **1a <1d < 1b < 1c**.

Table 4.1: Gas separation mixed gas selectivities, viscosity and glass transition temperature for monocationic and dicationic ILs shown in Figure 4.1 and Figure 4.2.

Ionic liquid	$\alpha_{CO2/N2}$	$\alpha_{CO2/CH4}$	Viscosity [cP][a,b]	Glass transition[b] [°C]
1a	15.2	12.6	437	-59.6
1b	17.2	15.4	1536	-52.8
1c	17.6	14.2	4076	-43.7
1d	16.3	16.1	569	- 53.9
2a	27.9	22.4	>10000	-34.5
2b	24.1	20.2	solid	91[c]
2c	34.7	31.8	>10000	-18.1

[a]Measured at 25 °C. [b]All ionic liquids possess 300 to 400 ppm of water. [c]Melting point. Supercooled liquid at room temperature.

The pyrrolidinium IL **1a** had the poorest performance in this series. This is not surprising as functionalized pyrrolidinium-based ionic liquids exhibit lower solubilities for carbon dioxide than, for example, imidazolium ILs.[22,16] On the other hand, IL **1d** used in this study was

not the best in the investigated series although imidazolium ILs are generally considered the most efficient in gas absorption and separation.[23,24,25] One of the reasons for this result could be the existence of π-π interactions between the delocalized electrons in the imidazolium cation and in the *p*-toluenesulfonate anion, making these ions are less available for interaction with CO_2. It has also been shown that a glycol chain interacts with an imidazolium core to which it is appended.[26] This means that the ether oxygen atoms as well as the imidazolium ring are less available for interaction with CO_2 molecules.

Ionic liquids based on six-membered heterocyclic rings performed the best in the series (ILs **1b** and **1c**). The slightly better performance of the morpholinium IL over the piperidinium IL can be attributed to the additional Lewis-basic site on the oxygen atom of the morpholinium ring (see below: quantum chemical calculations). Since, however, the morpholinium ionic liquid **1c** possesses the highest viscosity in the series the selectivity increase is not very significant.

For the CO_2/CH_4 separations, the order of the ionic liquids arranged according to their increasing selectivity was the following: **1a** < **1c** < **1b** < **1d** (Table 4.1). It was therefore very different from the order observed for the CO_2/N_2 separations. While the pyrrolidinium IL **1a** remains the least effective for the gas separation, the imidazolium IL **1d** shows the highest selectivity. The changes can be related to the different properties of the contaminant gases: while nitrogen, just like carbon dioxide, possesses a quadrupole moment, methane does not.[27]

In general, the monocationic ionic liquids presented in this paper are more viscous than other ILs reported for gas separation purposes (Table 4.1).[13] For example IL **1a** has a viscosity of 437 cP, while an ionic liquid with the same cation but with the bis(trifluoromethylsulfonyl)imide anion has a viscosity of only 73 cP at 25 °C.[28] Generally, one aims to get a low viscosity as high viscosities limit mass transfer in the membrane and as a consequence decrease the

permeability for a given ionic liquid.[29] However, since the solution-diffusion is expected to be a dominating transport mechanism through a SILM, attention has to be given to the solubility factor as well. It can be expected that with increasing viscosity, gas molecules travel through the membrane more slowly and there can be more interaction between the ionic liquid and carbon dioxide.[30] As a result, gas solubility can increase and the product of solubility and diffusivity (gas permeability) may stay almost unaffected. On the other hand, in the light of the newest theories regarding CO_2 dissolution by creation of polar domains in ILs, a well adjusted polarity of an IL may be more important that the viscosity effects.[31]

4.2.3. Dicationic ILs – membrane performance

Subsequently, dicationic analogous of ILs **1a-d** were prepared. The rationale behind the synthesis of these compounds was to obtain higher concentrations of charges and groups able to interact with carbon dioxide per mol of IL. The dicationic ILs were symmetrical and consisted of two identical aza-heterocycles, for example two *N*-methyl-pyrrolidinium rings, connected to each other by a tri(ethylene glycol) linker (Fig 4.3). Also in this case the tosylate anions were chosen to enable the study of the structure-property relationship in mono- and dicationic ILs.

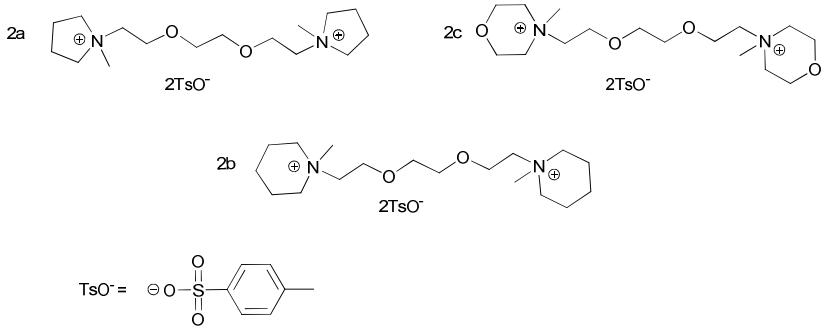

Figure 4.3: Dicationic tosylate ionic liquids functionalized with a glycol chain.

A dicationic imidazolium IL (an analogue of IL **1d**) would be a logical extension of the series, nevertheless, we did not include it, as this IL had already been reported by other authors.[1] Moreover, despite multiple trials it was impossible to prepare a good quality SILM from this compound.

Comparison of the selectivity results for mono- and dicationic ILs revealed an interesting regularity: the dicationic ILs always provide higher selectivities than the corresponding monocationic analogues (Table 4.1). The order of the dicationic ILs arranged according to their increasing performance is for both gas mixtures the following: **2b** < **2a** < **2c**. The morpholinium ionic liquid is thus the most effective, as it was the case for the monocationic ILs (for the CO_2/N_2 system), while the order pyrrolidinium versus piperidinium is reversed (for both systems). The selectivity difference between mono- and dicationic ionic liquids depends on the type of cationic core (Figure 4.4). For pyrrolidinium (**1a/2a**) and morpholinium (**1c/2c**) ILs, the selectivity nearly doubles when the charge doubles, while in the case of piperidinium ILs (**1b/2b**) the difference is much smaller. This phenomenon may be caused by the difference in strength of interaction between the dicationic molecules and the neighbouring anions as well as between the dicationic ionic liquids and CO_2. The selectivity increase is observed for both the CO_2/N_2 and CO_2/CH_4 system, although to a variable extent.

(a)

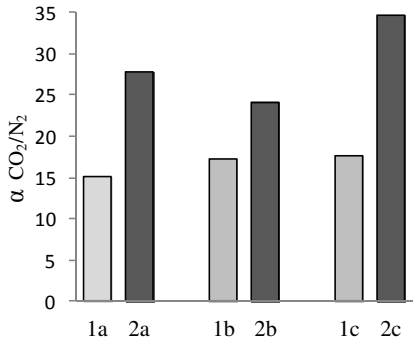

(b)

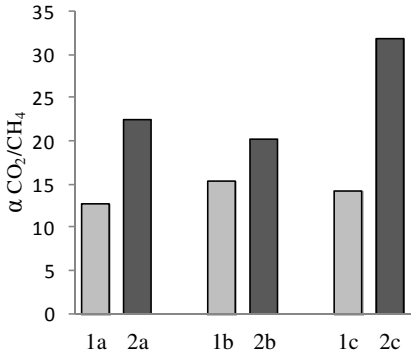

Figure 4.4: Comparison of the selectivities of monocationic (light grey) and dicationic (dark gray) ionic liquids for (a) the CO_2/N_2 system and (b) the CO_2/CH_4 system.

Mixed gas selectivity for dicationic ionic liquids ranges from 24.1 to 34.7 for CO_2/N_2, and from 20.2 to 31.8 for the CO_2/CH_4 gas mixture. The significant spread of the values can be related to the type of heterocycle used, and, as a consequence, to the conformation of the molecules in the solid state. Anderson *et al.* have shown that pyrrolidinium $[C_3(MPy)_2]^{2+}$ dications, connected by a 1,3-propylene spacer, experience three different conformations in the solid state.[16] As mentioned in the experimental section, the dicationic ILs used to prepare the SILMs were in the supercooled state and hence a certain degree of crystallinity might

have been present. As glycol chains may be considered even more flexible than alkyl chains,[32] the long ethyleneoxy chains used by us in the dicationic ILs can contribute to the existence of many conformations. As a result, the availability of interaction sites and the type and size of nanodomains may vary with the type of heterocycle.

The improvement of the performance for all the dicationic ILs on doubling the cationic charge cannot be caused by the reduced viscosity. On the contrary, dicationic ionic liquids are more viscous than the corresponding monocationic ILs and **2b** is even solid at room temperature.

Ideal vs. mixed gas selectivity

Gas separation selectivity is reported in the literature as either *ideal* or *mixed gas selectivity*.[33] *Ideal selectivity* refers to the selectivity value obtained from the ratio of pure gas permeabilities, that is, from two separate permeability measurements of the studied gases, where in each case only one gas is permeated through the membrane at a time.

The ideal selectivity is an intrinsic property of the membrane material and it provides insight into the interactions between ILs and the gas. It does not, however, present a realistic picture because possible interactions between the gases and their preferences for the membrane material are not taken into account.

Mixed gas selectivity is therefore calculated on the basis of the permeabilities obtained from a two-gas system. The mixed gas values tell a little less about the interaction between each component with the IL, but can indicate a possible competition between the gases for the membrane material. The mixed selectivity values are usually lower than those for the ideal selectivity, because of the impact of one gas on the other and competition of the gases for the membrane material.

Ideal selectivity is equal to the mixed gas selectivity when the gases barely interact with the membrane material. On the other hand,

when one of the gases is easily sorbed by the membrane, the permeability of the other can be seriously affected, as it for example happens in the case of CO_2/CH_4 separations.[33] In such cases the mixed gas selectivity can be then more than 50% smaller than the ideal selectivity. In the optimal situation, both ideal and mixed gas permeability should be reported and interpreted. As mixed gas data require a more complicated set-up, some research groups report only ideal selectivity data, which can be falsely higher than those in actual industrial mixed gas systems.

While the porous SILM supports do not influence the separation selectivity, the dense (non-porous) supports can enhance it. Therefore, before impregnating the support with ILs, it is important to determine its performance.

The data collected in pure gas experiments show a clear difference in the permeance of N_2 and CH_4 for the mono- and dicationic ILs (Table 4.2).

Table 4.2: Ideal (pure gas) permeance and selectivity for selected ionic liquids.

	Permeance of pure gasses (GPU)			Ideal selectivity	
IL	CO_2	N_2	CH_4	CO_2/N_2	CO_2/CH_4
1a	1.120	0.0726	0.0785	15.4	14.3
2a	0.930	0.0349	0.0368	26.6	25.2
1b	1.340	0.0684	0.0735	19.6	18.2
2b	0.980	0.0397	0.0406	24.6	24.1

While on doubling the cationic charge, the permeance of CO_2 decreased moderately (17% decrease for **1a** vs. **2a** and 27% for **1b** vs. **2b**), the permeance of N_2 and CH_4 dropped by approximately 50% (N_2: 50% decrease for **1a**/**2a**, 43% for **1b**/**2b**; CH_4: 57% for **1a**/**2a** and 43% for **1b** vs. **2b**). The effect of the increased selectivity is, from this perspective,

not directly related to the ability of dicationic ILs to facilitate CO_2 permeation, but to their potency to lower the permeance of N_2 and CH_4, while only slightly reducing the permeance of CO_2. Carlisle *et al.* and Mahurin *et al.* reported a very similar observation for the SILM performance of ionic liquids with nitrile-functionalized cations and tetracyanoborate anions, respectively.[34,35] Although the solubility of CO_2 (or permeability, in the paper of Mahurin), decreased on such functionalization, the solubility (permeability) of nitrogen and methane dropped even more, contributing to high CO_2/N_2 and CO_2/CH_4 separation selectivities. The positive influence of polar groups on CO_2 separation selectivities could be thus related to the ability of ILs to "repel" non-polar gases such as N_2 or CH_4 as well as to their beneficial interactions with CO_2 and for example free volume. These observations are consistent with the calculations showing that the free volume of simple imidazolium dicationic IL is approximately 3% smaller than the free volume of its monocationic analogue.[36] However, the dicationic ILs **2a**-**2c** are not of imidazolium type. It is possible that polar cavity formation is also promoted in these ILs.

The undeniably lower permeance of N_2 and CH_4 in the dicationic ILs could be partly related to the higher viscosity of these ILs. High viscosity permits facile diffusion only for gases that efficiently interact with an IL, changing the intramolecular interactions in the IL bulk and hence its operational viscosity. The distinctly quadrupolar nature of CO_2, the rationale for the use of ionic liquids in SILMs, allows this gas to interact better with ILs than N_2 and CH_4, which in contrast are attracted to the ILs only by weak and non-polar van der Waals interactions.[25] Moreover, small CO_2 molecules (3.4 Å) will penetrate the SILMs easier than larger molecules of N_2 (3.6Å) or CH_4 (3.8Å).[37,33]

4.2.4. Quantum chemical calculations

Quantum chemical calculations performed by dr. Oldamur Hollóczki (from the group of Prof. Barbara Kirchner, University of Leipzig) shed more light on the observed phenomena and provided an alternative explanation. The DFT (Density Functional Theory) method chosen, allows computing the electronic structure of interacting molecules (CO_2-IL).

The electrostatic potential maps for the ions were created on the basis of the electron density of a given ion. The commonly applied technique used for this purpose was to calculate how much energy is needed to move a proton from infinity to a given point on the surface of the ion.

The interaction energies were calculated on the basis of the binding energies of CO_2 molecules at a given site of the ion. More than 100 CO_2-ion binding configurations were considered for each ion and the interaction energy value for the most stable system (the most negative value) was chosen to be visualised in the figures presented below.

The calculations were performed on the morpholinium ILs **1c** and **2c** to investigate the difference in the interaction with CO_2 between monocationic and dicationic ILs. This particular pair of ILs was chosen as there was the biggest difference between the selectivity of mono/dicationic IL and in the same time both ILs performed the best within own series.

The electrostatic potential of the tosylate anion, common to both ILs, is shown in Figure 4.5. As expected, the negative charge of the anion is located mainly on the oxygen atoms of the sulfonate group and on the π-system of the aromatic ring. Accordingly, the positively polarized carbon atom of the carbon dioxide molecule interacts with the sulfonate group with a considerable interaction energy (-35.3 kJ/mol in the gas phase), in agreement with the general wisdom in IL research that the anion greatly contributes to the solvation of carbon dioxide.[14,38]

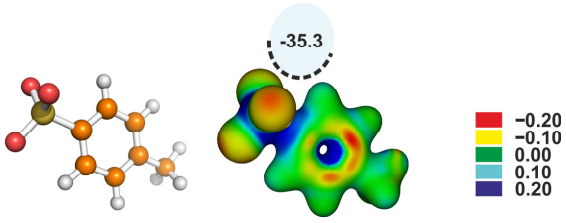

Figure 4.5: Electrostatic potential map of the anion and its interaction site with the CO_2 molecule, together with the corresponding interaction energy, blue circle (in kJ/mol; PBE/def-TZVPP).

It has been shown that the cation of ILs can also significantly interact with the carbon dioxide molecule, which has structural and in certain cases chemical consequences on the system.[21] This is in complete accordance with the experimental differences observed for the gas solubility and separation efficiency between the morpholinium ionic liquids **1c** and **2c**, that is, a mono- and a dicationic ionic liquid possessing the same anion.

Thus, after having quantified the importance of the anion in the solute-solvent interactions, the cation-CO_2 interplay was investigated (Figure 4.6). The electrostatic potential of the monocation **1c** shows a decreasing charge from the head group toward the tip of the side chain. While the ring atoms are highly polarized, the terminal methyl unit is almost completely neutral. Hence, while at the latter moiety only weak dispersion interactions and the interplay between the oxygen atoms of the ethylene glycol chains and the carbon atom of CO_2 is possible, closer to the morpholinium ring the negatively polarized oxygen atoms of the solute gas molecule may also interact with the positively charged head group atoms. Thus, the most favorable interaction site of this cation for the CO_2 molecule is at the junction of the side chain and the ring. Although the corresponding interaction energies are somewhat lower than those for CO_2 with the anion, they are of the same order of magnitude, and are, therefore, similarly important. On the other hand, the anion is also expected to be closer to the highly charged regions of

the cation in the liquid, therefore the CO_2 molecules accommodated here have a chance to approach both ions at the same time.

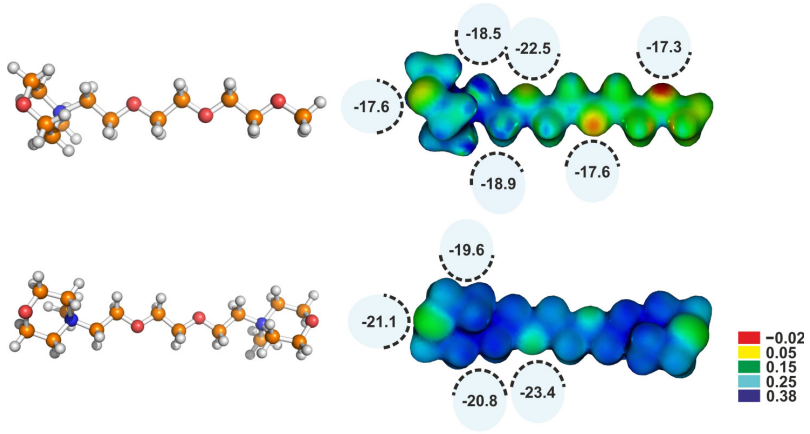

Figure 4.6: Electrostatic potential maps of the monocationic (top) and dicationic (bottom) morpholinium cations, together with the interaction sites and the corresponding interaction energies, in blue circles (in kJ/mol; PBE/def-TZVPP). Note that the dication is symmetrical.

The electrostatic potential of dication **2c** shows, interestingly, a completely different picture (Figure 4.6). The ethylene glycol linker between the two morpholinium rings is shorter than the side chain of the monocation, and the positive charge spans from one end of the molecule to the other without any non-polar domain. According to the considerations above, the orientation of the CO_2 molecule is more flexible around the dication, as shown by the very similar interaction energies all around this ion. This may indicate an easier diffusion of CO_2 around the dication, and hence within the corresponding ionic liquid. On the other hand, the fewer non-polar domains in the dicationic IL in comparison with the monocationic one should result in a less desirable environment for non-polar molecules, such as CH_4 and N_2. These two effects are in good agreement with the experimentally observed increased performance of the dicationic ionic liquid in terms of separation of CO_2 from CH_4 or N_2.

Taking into account the abovementioned observations, higher gas separation performance of the dicationic ILs **2a-c** is not as much related to the increased charge *per se*, but rather to the associated change in the electronic environment. One can speculate that unsymmetrical dicationic ILs may not possess similar properties unless the two head groups have comparable electron-withdrawing properties. On the other hand, (symmetrical) tricationic ionic liquids may help to achieve an extended positively charged region, and contribute to higher selectivity, provided their physical properties (e.g. melting point, viscosity) would be favorable. Poly(ILs) would be the subsequent natural candidates for even better performing systems. It has been shown, however, that although poly(ILs) provide better selectivities than their monomeric (monocationic) analogues, their selectivity values are usually not much higher than those presented here for the dicationic ionic liquids, suggesting a different charge distribution in the poly(ILs).[11, 10]

4.3. Conclusions

The synthesis and characterization of functionalized monocationic and dicationic ILs with tosylate anions have been described, as well as their use in SILMs in the separation of CO_2 from N_2 and CH_4. The cations were based on four different aza-heterocycles (pyrrolidine, piperidine, morpholine and imidazole) and were all functionalized with a tri(ethylene glycol) moiety. The ILs showed moderate to good gas separation selectivities, ranging from 15 to 34. Dicationic ILs gave doubled selectivities for CO_2/N_2 and CO_2/CH_4 separations when compared to their monocationic analogues. Pure gas permeance data along with quantum chemical calculations provided an explanation for this phenomenon. Firstly, a decrease in permeance of N_2 and CH_4 through the dicationic IL layer is observed, presumably due to their less favorable interactions of these ILs with the gases, while the permeance of CO_2 is reduced less significantly. Secondly, in the dicationic ILs the

number of interaction sites is bigger than in their monocationic analogues. The results clearly show that the electronic structure of the linear symmetrical dicationic ionic liquids is beneficial for interactions with CO_2 molecules. Moreover, the cation has a pronounced influence on the solubility of carbon dioxide in ILs. This means that future research in this area should also be directed to the design of linear dicationic ionic liquids with new (functionalized) cationic cores.

4.4. Experimental section

Sven Dewilde assisted the synthesis of the dimorpholinium ionic liquid. CHN analyses were recorded by Dirk Henot. DSC measurements were interpreted with the assistance of Jeroen Sniekers.

4.4.1. Syntheses

1-(2-(2-(2-Methoxyethoxy)ethoxy)ethyl)-1-methylpyrrolidinium p-toluenesulfonate (1a)

The compound was prepared via a method analogous to a literature procedure.[37] A mixture of 1-methylpyrrolidine (2.08 mL, 20.0 mmol) and tri(ethylene glycol) monomethyl ether monotosylate (5.0 g, 15.72 mmol) in acetonitrile (50 mL) was stirred at 120 °C for 3 h. The excess of 1-methylpyrrolidine and the solvent was evaporated *in vacuo* to give a light yellow oil in quantitative yield. ^{1}H NMR (300 MHz, $CDCl_3$): δ = 7.73 (d, 2H, *J* = 8.1 Hz), 7.12 (d, 2H, *J* = 8.1 Hz), 3.94–3.86 (m, 2H), 3.86–3.79 (m, 2H), 3.79–3.65 (m, 4H), 3.65–3.52 (m, 6H), 3.52–3.44 (m, 2H), 3.32 (s, 3H), 3.20 (s, 3H), 2.32 (s, 3H), 2.25-2.04 (m, 4H) ppm. ^{13}C NMR (75 MHz, $CDCl_3$): δ = 143.9, 139.1, 128.6, 125.8, 71.8, 70.3, 70.2, 70.1, 65.4, 65.3, 63.0, 59.0, 48.3, 21.4, 21.2 ppm. IR (ATR, cm^{-1}): 2877, 1457, 1353, 1189, 1117, 1031, 1010, 957, 882, 849, 817, 678, 562. CHN (M·1H_2O) [%] (calculated): C: 54.13 (54.13), H: 8.35 (8.37), N: 3.30 (3.32).

1-(2-(2-(2-Methoxyethoxy)ethoxy)ethyl)-1-methylpiperidinium *p*-toluenesulfonate (1b)

1-Methylpiperidine (2.5 mL, 21.0 mmol) and tri(ethylene glycol) monomethyl ether monotosylate (5.0 g, 15.7 mmol) in acetonitrile (70 mL) were stirred at 90 °C for 24 h. The excess of 1-methylpiperidine and the solvent was evaporated *in vacuo* to give a yellow oil in quantitative yield. ^{1}H NMR (300 MHz, $CDCl_3$): δ = 7.76 (d, 2H, *J* = 7.7 Hz), 7.13 (d, 2H, *J* = 7.7 Hz), 3.94 (m, 2H), 3.86 (m, 2H), 3.73–3.45 (m, 12H), 3.34 (s, 3H), 3.29 (s, 3H), 2.32 (s, 3H), 1.84 (m, 4H), 1.70 (m, 2H) ppm. ^{13}C NMR (75 MHz, $CDCl_3$): δ = 144.3, 139.4, 128.9, 126.2, 72.2, 70.6, 70.5, 70.4, 70.2, 65.0, 62.8, 62.4, 59.3, 48.8, 21.0, 20.5 ppm. IR (ATR, cm^{-1}): 3023, 2941, 2874, 1456, 1353, 1191, 1118, 1032, 1011, 943, 876, 849, 817, 678, 562. CHN ($M{\cdot}1H_2O$) [%] (calculated): C: 55.18 (55.15), H: 8.60 (8.56), N: 3.23 (3.22).

1-(2-(2-(2-Methoxyethoxy)ethoxy)ethyl)-1-methylmorpholinium *p*-toluenesulfonate (1c)

1-Methylmorpholine (1.23 mL, 11.2 mmol) and tri(ethylene glycol) monomethyl ether monotosylate (3.0 g, 9.43 mmol) in acetonitrile (70 mL) were stirred at 90 °C for 3 days. The excess of 1-methylmorpholine and the solvent was evaporated and the residue was dissolved in water and washed with dichloromethane. Evaporation of water gave a yellow oil. Yield: 2.53 g (64%). ^{1}H NMR (300 MHz, $CDCl_3$): δ = 7.76 (d, 2H, *J* = 7.9 Hz), 7.15 (d, 2H, *J* = 7.9 Hz), 4.12-3.93 (m, 8H), 3.86–3.74 (m, 2H), 3.71–3.61 (m, 4H), 3.57 (t, 4H, *J* = 4.2 Hz), 3.50 (t, 2H, *J* = 2.3 Hz), 3.49 (s, 3H), 3.34 (s, 3H), 2.33 (s, 3H) ppm. ^{13}C NMR (75 MHz, $CDCl_3$): δ = 143.8, 139.2, 128.7, 125.8, 71.8, 70.3, 70.1, 70.0, 64.6, 63.2, 61.0, 60.8, 58.9, 48.3, 21.3 ppm. IR (ATR, cm^{-1}): 3021, 2875, 1471, 1455, 1352, 1190, 1117, 1104, 1032, 1010, 957, 924, 881, 849, 817, 713, 678, 625, 568. CHN ($M{\cdot}1H_2O$) [%] (calculated): C: 51.99 (52.16), H: 8.10 (8.06), N: 3.25 (3.20).

1-(2-(2-(2-Methoxyethoxy)ethoxy)ethyl)-1-methylimidazolium *p*-toluenesulfonate (1d)

1-Methylimidazole (1.82 mL, 22.8 mmol) and tri(ethylene glycol) monomethyl ether monotosylate (8.0 g, 25.15 mmol) in acetonitrile (50 mL) were stirred at 70 °C for 48 h. The solvent was evaporated and the residue was dissolved in 50 mL of water and washed with dichloromethane (3×7 mL). Evaporation of water and traces of dichloromethane yielded a colourless oil. Yield: 6.21 g (68%). ^{1}H NMR (300 MHz, $CDCl_3$): δ = 9.75 (s, 1H), 7.77 (d, 2H, *J* = 7.9 Hz), 7.58 (s, 1H), 7.27 (s, 1H), 7.14 (d, 2H, *J* = 7.9 Hz), 4.46 (t, 2H, *J* = 4.4 Hz), 3.86 (s, 3H), 3.80 (t, 2H, *J* = 4.4 Hz), 3.64–3.55 (m, 6H), 3.55–3.50 (m, 2H), 3.34 (s, 3H), 2.32 (s, 3H) ppm. ^{13}C NMR (75 MHz, $CDCl_3$): δ = 143.7, 139.3, 138.2, 128.6, 125.9, 123.5, 122.6, 71.8, 70.3, 70.2, 70.1, 69.0, 59.0, 49.5, 36.3, 21.3 ppm. IR (ATR, cm^{-1}): 3148, 3099, 2873, 1573, 1461, 1351, 1192, 1119, 1033, 1011, 933, 849, 818, 762, 680, 654, 624, 569. CHN ($M{\cdot}1H_2O$) [%] (calculated): C: 49.26 (49.64), H: 7.22 (7.17), N: 6.39 (6.43).

1,8-Bis [1-methylpyrrolidinium)]-3,6-dioxaoctane di(*p*-toluene-sulfonate) (2a)

N-Methylpyrrolidine (5.44 mL, 52.3 mmol) and tri(ethylene glycol) ditosylate (8 g, 17.4 mmol) were stirred in acetonitrile (50 mL) at 75 °C for 60 h. The solvent and the excess of amine were evaporated to give an orange-brown oil in quantitative yield. ^{1}H NMR (300 MHz, $CDCl_3$): δ = 7.69 (d, 4H, *J* = 7.4 Hz), 7.13 (d, 4H, *J* = 7.4 Hz), 3.93 (m, 4H), 3.76 (m, 4H), 3.64 (m, 12H), 3.14 (s, 6H), 2.32 (s, 6H), 2.08 (m, 8H) ppm. ^{13}C NMR (75 MHz, $CDCl_3$): δ = 144.1, 139.3, 128.7, 125.7, 70.4, 65.4, 65.1, 63.2, 48.6, 21.3, 21.2 ppm. IR (ATR, cm^{-1}): 2949, 2876, 1646, 1456, 1355, 1181, 1120, 1033, 1010, 941, 875, 819, 712, 564. CHN ($M{\cdot}4H_2O$) [%] (calculated): C: 51.34 (51.41), H: 8.12 (8.05), N: 4.03 (4.00).

1,8-Bis [1-methylpiperidinium)]-3,6-dioxaoctane di(*p*-toluene-sulfonate) (2b)

N-Methylpiperidine (6.3 mL, 52.1 mmol) and tri(ethylene glycol) ditosylate (8g, 17.4 mmol) were refluxed in acetonitrile (40 mL) for 3 days. The solvent and the excess of amine were evaporated to give a yellow oil in quantitative yield. ^{1}H NMR (300 MHz, $CDCl_3$): δ = 7.71 (d, 4H, *J* = 8.0 Hz), 7.12 (d, 4H, *J* = 8.0 Hz), 3.98 (t, 4H, *J* = 4.2 Hz), 3.75 (t, 4H, *J* = 4.2 Hz), 3.67 (s, 4H), 3.47 (m, 8H), 3.24 (s, 6H), 2.33 (s, 6H), 1.77 (t, 8H, *J* = 5.6 Hz), 1.60 (m, 4H) ppm. ^{13}C NMR (75 MHz, $CDCl_3$): δ = 144.1, 139.2, 128.6, 125.8, 70.4, 64.5, 63.1, 61.9, 48.4, 21.3, 20.7, 20.1 ppm. IR (ATR, cm^{-1}): 3024, 2939, 2873, 1461, 1338, 1189, 1117, 1030, 1008, 943, 919, 888, 867, 815,716, 678, 559. CHN ($M{\cdot}1H_2O$) [%] (calculated): C: 57.30 (56.95), H: 8.11 (8.06), N: 4.17 (4.15).

1,8-Bis [1-methylmorpholinium)]-3,6-dioxaoctane di(*p*-toluene-sulfonate) (2c)

N-Methylmorpholine (1.72 mL, 15.6 mmol) and tri(ethylene glycol) ditosylate (3 g, 6.52 mmol) were refluxed in acetonitrile (30 mL) for 3 days. The solvent was evaporated and the resulting liquid was dried *in vacuo* at 60 °C to give a yellow oil in quantitative yield. ^{1}H NMR (300 MHz, $CDCl_3$): δ = 7.72 (d, 4H, *J* = 7.9 Hz), 7.16 (d, 4H, *J* = 7.9 Hz), 4.08 (m, 4H), 3.92 (m, 12H), 3.79 (m, 4H), 3.69-3.51 (m, 8H), 3.46 (s, 6H), 2.34 (s, 6H) ppm. ^{13}C NMR (75 MHz, D_2O): δ = 142.4, 139.5, 129.4, 125.3, 69.6, 63.6, 60.3 (2 signals), 48.0, 20.4 (2 signals) ppm. IR (ATR, cm^{-1}): 3013, 2963, 2919, 2875, 1473, 1457, 1186, 1117, 1031, 1009, 957, 923, 881, 817,713, 678, 625, 568. CHN ($M{\cdot}1H_2O$) [%] (calculated): C: 53.45 (53.08), H: 7.40 (7.42), N: 4.13 (4.13).

4.4.2. Membrane preparation and measurements

To prepare SILMs presented in this chapter, porous γ-alumina discs (25 mm diameter, 2 mm thickness, 3-5 nm pore size) from Pervatech were used as a support. Before coating with ionic liquids, the support was tested for potential gas separation properties by passing the two studied gas mixtures (CO_2/N_2 and CO_2/CH_4) through it. It was found to be non-selective and had only a minimal effect on the gas flux. Therefore, the selectivity and permeability values presented in this chapter are indicative of the performance of the "free" ILs.

Before the application of the IL on the support, the viscosity of the IL was adjusted by dilution with an appropriate volatile solvent (acetone or dichloromethane). The ionic liquid was then applied to the membrane surface using a micropipette. Excess liquid was removed from the surface using a lint-free wipe. The membrane was then spun at 1000 rpm in a spin-coater for 60 s, producing a visually uniform surface. The membrane was dried in an oven for 2 h to remove the excess of solvent. This process of spin-coating and drying was repeated three times to ensure complete coverage of the support with ionic liquid.

The gas permeation set-up consisted of a stainless steel module with a cavity to insert the membrane disk gripped with Viton® o-rings. The module, upstream and downstream parts were evacuated by a vacuum pump to remove residual air and other gases before measurement of the gas permeation properties. A feed gas at a flow rate of 1 L/min was introduced in the module. For mixed-gas measurements, mass flow controllers (MFC, Bronkhorst) were used to adjust the feed gas composition. The upstream pressure was adjusted using a back-pressure regulator. Gas permeabilities were measured by allowing the permeate gas to expand in a constant volume auxiliary cylinder connected to a Baratron® pressure transducer having a higher limit of 10 mbar (MKS Instruments GmbH, Germany). The rate of pressure

increase (dP/dt) was measured to calculate the gas permeability from the following equation:

$$P_i = \frac{273 \times 10^6}{760} \frac{y_i V}{AT\left(\frac{76}{14.7}\right) x_i P_1} \left(\frac{dP}{dt}\right) \quad 4.1$$

where y_i and x_i refer to the mole fraction of component i in the downstream and upstream, respectively. V is the downstream volume (cm^3), A is the membrane permeation area (cm^2), T is the operating temperature (K), and P_1 is the pressure of the feed gas (psi). The gas permeate composition was measured using a compact gas chromatograph (CGC, Interscience). The operation and data acquisition was carried out using a CGC-editor and Agilent EZchrom software. The mixed-gas selectivity was calculated by the ratio of downstream and upstream mole fractions of the two gases by the following equation:

$$\alpha_{ij} = \frac{\left(y_i / y_j\right)}{\left(x_i / x_j\right)} \quad 4.2$$

where y_i and y_j are the mole fractions of components i and j, respectively, in the downstream, and x_i and x_j are the mole fractions of components i and j, respectively, in the upstream.

4.4.3. DFT calculations

To achieve a better understanding of the factors influencing the selectivity of the separations at a microscopic level, DFT calculations were carried out for the experimentally investigated morpholinium derivatives. These calculations were performed by the TURBOMOLE 6.10 program package,[39] using the PBE functional with the def-TZVPP basis set, applying the dispersion correction D3 of Grimme *et al.*,[40] and the RI approach. At the fully optimized geometries the eigenvalues of the Hessian were checked, to characterize the nature of the obtained

stationary point. To reduce the number of possible conformations, only those with a straight side chain have been considered. Interaction energies between CO_2 and each ion have been obtained from gas phase calculations. Although it has been shown that the interaction energies are significantly overestimated in such gas phase, the data compared to those in systems having several cations and anions around the solute gas molecule,[41] and the trends in measured physical CO_2 solubilities are well reproduced by this approach.[42] Thus, while comparing the calculated interaction energy values themselves to experimental data is rather difficult, by comparing the calculated interaction energies to one another – in the light of the also traceable ion-CO_2 interaction sites and modes – valuable physical information can be obtained on the solution.

4.5. References

1. Jadhav, A. H.; Kim, H., Short oligo (ethylene glycol) functionalized imidazolium dicationic room temperature ionic liquids: Synthesis, properties, and catalytic activity in azidation. *Chem. Eng. J.* **2012,** *200–202*, 264-274.
2. Bhadani, A.; Singh, S., Synthesis and Properties of Thioether Spacer Containing Gemini Imidazolium Surfactants. *Langmuir* **2011,** *27*, 14033-14044.
3. Payagala, T.; Huang, J.; Breitbach, Z. S.; Sharma, P. S.; Armstrong, D. W., Unsymmetrical Dicationic Ionic Liquids: Manipulation of Physicochemical Properties Using Specific Structural Architectures. *Chem. Mater.* **2007,** *19*, 5848-5850.
4. Anderson, J. L.; Ding, R.; Ellern, A.; Armstrong, D. W., Structure and Properties of High Stability Geminal Dicationic Ionic Liquids. *J. Am. Chem. Soc.* **2004,** *127*, 593-604.
5. Hu, X.; Tang, J.; Blasig, A.; Shen, Y.; Radosz, M., CO_2 permeability, diffusivity and solubility in polyethylene glycol-grafted polyionic membranes and their CO_2 selectivity relative to methane and nitrogen. *J. Membr. Sci.* **2006,** *281*, 130-138.
6. Bara, J. E.; Camper, D. E.; Gin, D. L.; Noble, R. D., Room-Temperature Ionic Liquids and Composite Materials: Platform Technologies for CO_2 Capture. *Acc. Chem. Res.* **2009,** *43*, 152-159.
7. Tang, J.; Tang, H.; Sun, W.; Radosz, M.; Shen, Y., Poly(ionic liquid)s as new materials for CO_2 absorption. *J. Polym. Sci. A Polym. Chem.* **2005,** *43*, 5477-5489.

8. Li, P.; Pramoda, K.; Chung, T.-S., CO_2 separation from flue gas using polyvinyl-(room temperature ionic liquid)–room temperature ionic liquid composite membranes. *Ind. Eng. Chem. Res.* **2011,** *50*, 9344-9353.
9. Simons, K.; Nijmeijer, K.; Bara, J. E.; Noble, R. D.; Wessling, M., How do polymerized room-temperature ionic liquid membranes plasticize during high pressure CO_2 permeation? *J. Membr. Sci.* **2010,** *360*, 202-209.
10. Li, P.; Paul, D. R.; Chung, T.-S., High performance membranes based on ionic liquid polymers for CO_2 separation from the flue gas. *Green Chem.* **2012,** *14*, 1052-1063.
11. Bara, J. E.; Lessmann, S.; Gabriel, C. J.; Hatakeyama, E. S.; Noble, R. D.; Gin, D. L., Synthesis and Performance of Polymerizable Room-Temperature Ionic Liquids as Gas Separation Membranes. *Ind. Eng. Chem. Res.* **2007,** *46*, 5397-5404.
12. Scovazzo, P., Determination of the upper limits, benchmarks, and critical properties for gas separations using stabilized room temperature ionic liquid membranes (SILMs) for the purpose of guiding future research. *J. Membr. Sci.* **2009,** *343*, 199-211.
13. Bara, J. E.; Gabriel, C. J.; Lessmann, S.; Carlisle, T. K.; Finotello, A.; Gin, D. L.; Noble, R. D., Enhanced CO_2 Separation Selectivity in Oligo(ethylene glycol) Functionalized Room-Temperature Ionic Liquids. *Ind. Eng. Chem. Res.* **2007,** *46*, 5380-5386.
14. Aki, S. N. V. K.; Mellein, B. R.; Saurer, E. M.; Brennecke, J. F., High-Pressure Phase Behavior of Carbon Dioxide with Imidazolium-Based Ionic Liquids. *J. Chem. Phys. B* **2004,** *108*, 20355-20365.
15. Cadena, C.; Anthony, J. L.; Shah, J. K.; Morrow, T. I.; Brennecke, J. F.; Maginn, E. J., Why Is CO_2 So Soluble in Imidazolium-Based Ionic Liquids? *J. Am. Chem. Soc.* **2004,** *126*, 5300-5308.
16. Anthony, J. L.; Anderson, J. L.; Maginn, E. J.; Brennecke, J. F., Anion Effects on Gas Solubility in Ionic Liquids. *J. Chem. Phys. B* **2005,** *109*, 6366-6374.
17. Seki, T.; Grunwaldt, J.-D.; Baiker, A., In Situ Attenuated Total Reflection Infrared Spectroscopy of Imidazolium-Based Room-Temperature Ionic Liquids under "Supercritical" CO_2. *J. Chem. Phys. B* **2008,** *113*, 114-122.
18. Carvalho, P. J.; Coutinho, J. A., On the nonideality of CO_2 solutions in ionic liquids and other low volatile solvents. *J. Phys. Chem. Lett.* **2010,** *1*, 774-780.
19. Hong, G.; Jacquemin, J.; Deetlefs, M.; Hardacre, C.; Husson, P.; Costa Gomes, M. F., Solubility of carbon dioxide and ethane in three ionic liquids based on the bis{(trifluoromethyl)sulfonyl}imide anion. *Fluid Phase Equilib.* **2007,** *257*, 27-34.
20. Liang, L.; Gan, Q.; Nancarrow, P., Composite ionic liquid and polymer membranes for gas separation at elevated temperatures. *J. Membr. Sci.* **2014,** *450*, 407-417.

21. Hollóczki, O.; Kelemen, Z.; Könczöl, L.; Szieberth, D.; Nyulászi, L.; Stark, A.; Kirchner, B., Significant Cation Effects in Carbon Dioxide–Ionic Liquid Systems. *ChemPhysChem* **2013,** *14*, 315-320.
22. Torralba-Calleja, E.; Skinner, J.; Gutiérrez-Tauste, D., CO2 Capture in Ionic Liquids: A Review of Solubilities and Experimental Methods. *J. Chem.* **2013,** *2013*, 16.
23. Scovazzo, P.; Kieft, J.; Finan, D. A.; Koval, C.; DuBois, D.; Noble, R., Gas separations using non-hexafluorophosphate $[PF_6]^-$ anion supported ionic liquid membranes. *J. Membr. Sci.* **2004,** *238*, 57-63.
24. Adibi, M.; Barghi, S. H.; Rashtchian, D., Predictive models for permeability and diffusivity of CH_4 through imidazolium-based supported ionic liquid membranes. *J. Membr. Sci.* **2011,** *371*, 127-133.
25. Shannon, M. S.; Tedstone, J. M.; Danielsen, S. P. O.; Hindman, M. S.; Irvin, A. C.; Bara, J. E., Free Volume as the Basis of Gas Solubility and Selectivity in Imidazolium-Based Ionic Liquids. *Ind. Eng. Chem. Res.* **2012,** *51*, 5565-5576.
26. Smith, G. D.; Borodin, O.; Li, L.; Kim, H.; Liu, Q.; Bara, J. E.; Gin, D. L.; Nobel, R., A comparison of ether- and alkyl-derivatized imidazolium-based room-temperature ionic liquids: a molecular dynamics simulation study. *Phys. Chem. Chem. Phys.* **2008,** *10*, 6301-6312.
27. Stogryn, D. E.; Stogryn, A. P., Molecular multipole moments. *Mol. Phys.* **1966,** *11*, 371-393.
28. Abitelli, E.; Ferrari, S.; Quartarone, E.; Mustarelli, P.; Magistris, A.; Fagnoni, M.; Albini, A.; Gerbaldi, C., Polyethylene oxide electrolyte membranes with pyrrolidinium-based ionic liquids. *Electrochim. Acta* **2010,** *55*, 5478-5484.
29. Moganty, S. S.; Baltus, R. E., Regular Solution Theory for Low Pressure Carbon Dioxide Solubility in Room Temperature Ionic Liquids: Ionic Liquid Solubility Parameter from Activation Energy of Viscosity. *Ind. Eng. Chem. Res.* **2010,** *49*, 5846-5853.
30. Baltus, R. E.; Culbertson, B. H.; Dai, S.; Luo, H.; DePaoli, D. W., Low-Pressure Solubility of Carbon Dioxide in Room-Temperature Ionic Liquids Measured with a Quartz Crystal Microbalance. *J. Chem. Phys. B* **2003,** *108*, 721-727.
31. Hu, Y.-F.; Liu, Z.-C.; Xu, C.-M.; Zhang, X.-M., The molecular characteristics dominating the solubility of gases in ionic liquids. *Chem. Soc. Rev.* **2011,** *40*, 3802-3823.
32. May, F.; Marcon, V.; Hansen, M. R.; Grozema, F.; Andrienko, D., Relationship between supramolecular assembly and charge-carrier mobility in perylenediimide derivatives: The impact of side chains. *J. Mater. Chem.* **2011,** *21*, 9538-9545.
33. Baker, R. W., *Membrane Technology and applications*. 2nd ed.; John Wiley & Sons Ltd.: Chichester, 2004.
34. Mahurin, S. M.; Hillesheim, P. C.; Yeary, J. S.; Jiang, D.; Dai, S., High CO_2 Solubility, Permeability and Selectivity in Ionic Liquids with Tetracyanoborate Anion. *RSC Advances* **2012,** *2*, 11813-11819.

35. Carlisle, T. K.; Bara, J. E.; Gabriel, C. J.; Noble, R. D.; Gin, D. L., Interpretation of CO_2 Solubility and Selectivity in Nitrile-Functionalized Room-Temperature Ionic Liquids Using a Group Contribution Approach. *Ind. Eng. Chem. Res.* **2008,** *47*, 7005-7012.
36. Shirota, H.; Mandai, T.; Fukazawa, H.; Kato, T., Comparison between Dicationic and Monocationic Ionic Liquids: Liquid Density, Thermal Properties, Surface Tension, and Shear Viscosity. *J. Chem. Eng. Data* **2011,** *56*, 2453-2459.
37. Breck, D. W., *Zeolite Molecular Sieves: Structure, Chemistry, and Use*. J. Wiley & Sons: New York, 1974.
38. Anderson, J. L.; Dixon, J. K.; Brennecke, J. F., Solubility of CO_2, CH_4, C_2H_6, C_2H_4, O_2, and N_2 in 1-Hexyl-3-methylpyridinium Bis(trifluoromethylsulfonyl)imide: Comparison to Other Ionic Liquids. *Acc. Chem. Res.* **2007,** *40*, 1208-1216.
39. Ahlrichs, R.; Bär, M.; Häser, M.; Horn, H.; Kölmel, C., Electronic structure calculations on workstation computers: The program system turbomole. *Chem. Phys. Lett.* **1989,** *162*, 165-169.
40. Grimme, S.; Antony, J.; Ehrlich, S.; Krieg, H., A consistent and accurate ab initio parametrization of density functional dispersion correction (DFT-D) for the 94 elements H-Pu. *J. Chem. Phys.* **2010,** *132*, 154104.
41. Hollóczki, O.; Firaha, D. S.; Friedrich, J.; Brehm, M.; Cybik, R.; Wild, M.; Stark, A.; Kirchner, B., Carbene Formation in Ionic Liquids: Spontaneous, Induced, or Prohibited? *J. Chem. Phys. B* **2013,** *117*, 5898-5907.
42. Bhargava, B. L.; Balasubramanian, S., Probing anion–carbon dioxide interactions in room temperature ionic liquids: Gas phase cluster calculations. *Chem. Phys. Lett.* **2007,** *444*, 242-246.

5.

Separation of CO_2 from N_2 and CH_4 by Nitrile/Glycol-Difunctionalized Ionic Liquids

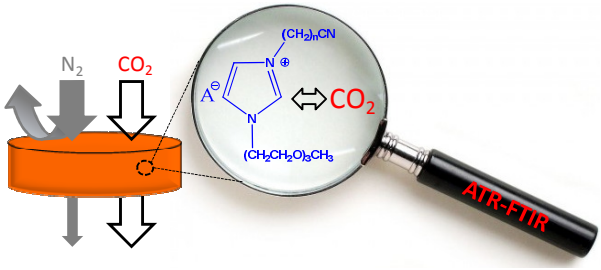

This chapter is based on the article:

Highly Selective Separation of Carbon Dioxide from Nitrogen and Methane by Nitrile/Glycol-Difunctionalized Ionic Liquids in Supported Ionic Liquid Membranes (SILMs), Sandra D. Hojniak, Ian P. Silverwood, Asim Laeeq Khan, Ivo F. J. Vankelecom, Wim Dehaen, Sergei G. Kazarian, and Koen Binnemans, The Journal of Physical Chemistry B, **2014** 118 (26), 7440-7449

5.1. Introduction

It has been mentioned in section 3.2.5 that ether chain and nitrile group are desirable moieties in the structures of ILs designed for the purpose of CO_2 separation from N_2 or CH_4. Flexible ether chains promote creation of the necessary cavities, while the ether oxygen atoms interact with CO_2 to dissolve the gas. In the case of imidazolium ILs, the ether oxygen atoms interact also with the imidazolium rings causing a decrease of the free volume that in turn leads to an enhancement of the CO_2 separation selectivity.[1-2] Moreover, this interaction disturbs cation-anion attraction, what in turn can make the ions more available for interplay with the gas.[1] Likewise, a nitrile group tethered to the IL cation can increase the CO_2 solubility and gas separation ability of a SILM by 30% in comparison with an alkyl analogue. Most probably, as in the case of ether-functionalized ILs, it contributes to FFV reduction, creation of polar domains and occurrence of specific IL-CO_2 interactions.[2-3]

In this chapter, new ILs with cationic cores containing both a nitrile functional group and a tri(ethylene glycol) monomethyl ether chain are presented. The ILs are incorporated into SILMs and the performance of these membranes for CO_2/N_2 and CO_2/CH_4 separations is measured. Moreover, the interactions of CO_2 molecules with these ILs are investigated by infrared spectroscopy.

5.1.1. Attenuated Total Reflection Spectroscopy

Attenuated Total Reflection Fourier Transform Infrared (FTIR-ATR) spectroscopy is a convenient technique to study the CO_2/IL systems.[4-5] In this method, a sample (e.g. pure IL) is spread on the ATR crystal. During the measurement, the IR beam is directed onto a crystal where it undergoes total internal reflection creating the evanescent wave (Fig 5.1). Total internal reflection occurs only if the refractive index (RI) of a crystal is significantly greater than that of the sample. For example, the RI of a diamond is 2.38 while of acetone is 1.33 and of common ILs is

around 1.4.[6] The evanescent wave progresses in the crystal extending beyond the surface of the crystal and penetrating the sample on the depth of a few micrometers.[7] When the frequency of the IR light corresponds to the vibrational frequency of the bond, absorption of the IR light occurs, which weakens or *attenuates* the wave, giving rise to an absorption spectrum.

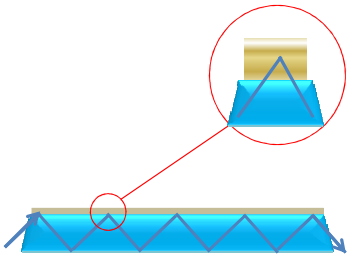

Figure 5.1: Evanescent wave in the ATR crystal (blue) penetrating the IL spread on the crystal (brown).

A very small depth of penetration as compared to transmission IR spectroscopy enables a study of highly absorbing samples.[8] On the other hand, such short path length requires an impeccable contact between the crystal and the sample (uniform and thick enough IL layer). ATR is suitable for the examination of liquids, solids and gases as well as for *in situ* reaction monitoring (in a flow cell). There are certain differences that should be accounted for when comparing spectra obtained via ATR or transmission IR spectroscopy. First of all, in ATR, the penetration depth, and hence the intensity of a band, is a function of wavelength: the longer the wavelengths of IR radiation the larger the depth of penetration and the intensity of the bands. In addition, in ATR the absorption maxima of bands are shifted by a few cm^{-1} in comparison to the transmission spectra and appear at lower wavenumbers.[9]

5.1.2. Infrared spectroscopy of carbon dioxide

Carbon dioxide is a linear triatomic molecule and therefore has four fundamental vibrations: *symmetric stretching*, *antisymmetric stretching*, *bending in-plane* and *bending out-of-plane* (Fig. 5.2).

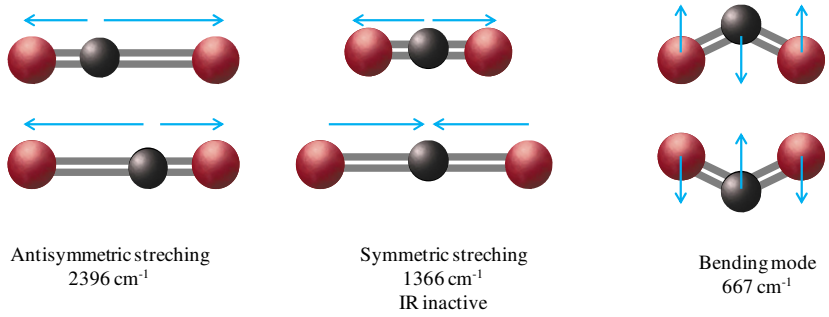

Figure 5.2: Fundamental vibrations of carbon dioxide molecule.

Since infrared radiation interacts with molecules whose dipole moment changes during the vibration, and in the CO_2 molecule no such change occurs during the symmetric stretching, this vibration is infrared inactive. Furthermore, the two bending modes are degenerate, thus they occur at the same vibrational frequency and appear in the spectrum as one band. In consequence, only the band corresponding to the antisymmetric stretching mode (denoted ν_3) at around 2396 cm^{-1}, and the bending mode band at 673 cm^{-1} (ν_2) will be observed in the spectrum of gaseous CO_2 (Fig 5.3, blue spectrum).

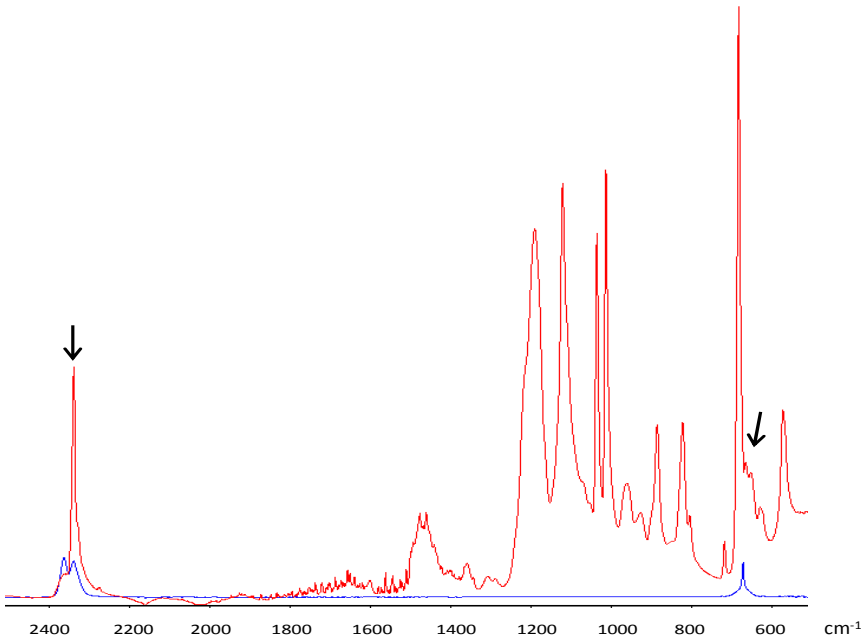

Figure 5.3: Comparison of the IR spectrum of: pure gaseous CO_2 (blue) and IL exposed to CO_2 (red). The arrows indicate the CO_2 in the spectrum of the IL.

The v_3 band has a fine vibration-rotation structure, which is visible only in the gas phase and at low pressures.[10]

The CO_2 molecule has two Lewis basic sites on the electron-rich oxygen atoms and a Lewis acidic site on the electron-poor carbon atom. It can therefore readily interact with other Lewis acids or bases, such as ions of ionic liquids. In the presence of an absorbing medium (a polymer, a solvent, an IL) two major changes occur in the spectrum of CO_2. First of all, the band of the antisymmetric stretching, appears at the characteristic frequency of 2336 cm^{-1}.[11] Moreover, the structure of the band is different from the gas phase CO_2: the band has a shoulder on the lower wavenumber side and the vibration-rotation structure is not visible anymore. The second change in the spectrum of CO_2 concerns the v_2 band which may broaden or split on interaction with the absorbent. This change may not be immediately visible (Fig. 5.3, red spectrum) due to the overlap with the bands of the IL. In order to isolate the v_2 band (as

it is presented in Fig. 5.9, further in the text), it is often necessary to perform a baseline correction or to subtract the spectrum of pure IL from the spectrum of the IL exposed to CO_2.

The width of the bending mode band of CO_2 (v_2) is directly proportional to the strength of interactions and can provide information about the type and strength of interaction of CO_2 molecule with the absorbing medium.[4,12] Spectra of ILs also alter when ILs are exposed to the gas.

5.1.3. Infrared study of CO_2-IL systems

Study of the changes in the spectra of CO_2 and ILs allows a simultaneous quantification of the following phenomena:[4]

(i) Gas solubility in ILs
(ii) Strength of interactions between ILs and CO_2 molecules
(iii) IL swelling (volume expansion on gas introduction)

(i) The approximate gas solubility in ILs can be determined on the basis of the Beer-Lambert law from the absorbance of the antisymmetric stretching (v_3) band of CO_2 molecules dissolved in ILs.[4] (ii) Strength of the CO_2- IL interaction is, as mentioned above, proportional to the width of the v_2 band of CO_2 and can be associated with a certain type of non-covalent interaction such as Lewis acid-base or dipole-dipole interaction.[12] (iii) When ILs are subjected to the gas, the bulk of the IL expands. In such swollen IL, the ions are further apart and the evanescent wave probes less ions on its way. In consequence, the absorbance of the IL bands decreases but the absorbance of the bands of CO_2 increases as more and more gas appears in the system.[13] Swelling is expressed in terms of percentage of volume expansion, as compared to the non-swollen IL. Table 5.1 summarizes the spectral changes associated with the three phenomena:

Table 5.1: Spectral changes associated with CO_2 absorption, CO_2-IL interactions and IL swelling.

Phenomenon	Spectral change(s)
Gas dissolution in ILs	Increase of intensity of the $v_3(CO_2)$ band
CO_2-IL interaction	Broadening and/or splitting of the $v_2(CO_2)$ band
IL swelling	Decrease of intensity of all the bands of ionic liquid and increase of intensity of the $v_3(CO_2)$ band

5.2. Results and discussion

5.2.1. SILM performance of monocationic ILs

The membrane measurements were performed by dr Asim Khan from the group of Prof. Ivo Vankelecom, COK, KU Leuven. High CO_2 separation selectivities of SILMs made with ILs functionalized with a glycol or a nitrile group[14,3] encouraged us to place these two moieties on one cationic core. Although the double functionalization is synthetically more challenging than monofunctionalization, it has the advantage of introducing desired properties from both moieties into the overall characteristics of the resulting IL: In imidazolium ILs, both tri(ethylene glycol) and nitrile groups favour creation of small polar cavities and enhance CO_2 separation selectivity.[2] ILs containing a nitrile group in their cation can often have a high melting.[15] Flexible glycol chains disturb the tight packing of the ions decreasing the glass transition temperature of the IL and ensure its fluidity far below room temperature (Table 5.2).

Table 5.2: Viscosities, glass transition temperatures and refractive indices of ILs.

IL	Viscosity (cP)[a]	Glass transition temperature (°C)	Refractive Index[a]
1a[b]	2048	-40.0	-
1b	437	-59.6	1.55
2a	6881	-33.8	1.55
2b	1969	-43.3	1.55
2c	857	-49.9	1.50
2d[b]	569	-53.9	1.50
3	>8000	-23.6	1.55

[a]measured at 25 °C; [b]data from ref.[16]

All ILs presented in this paper possess a nitrile group on an alkyl linker of a variable length and a tri(ethylene glycol) monomethyl ether moiety. The cationic cores are based on pyrrolidine and imidazole (Figures 5.4-5.6).

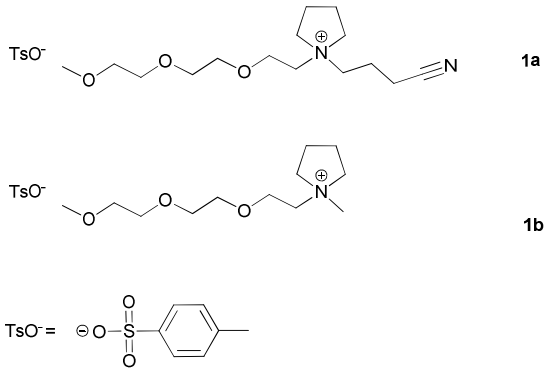

Figure 5.4: Pyrrolidinium ILs 2a-b.

The ILs **1b** and **2d** (Figure 5.4 and 5.5) have been reported previously and can be considered the "only-glycol" analogues of the difunctionalized ILs **1a** and **2a-2c**, respectively.[16] Their performance can be used as a

reference to determine the influence of difunctionalization in ILs **1a** and **2a**-**2c**. The presence of the same anion (*p*-toluenesulfonate) in all ILs of this study enables a direct comparison of the influence of cations on the SILM performance.

The anions were introduced via a quaternisation reaction with tri(ethylene glycol) *p*-toluenesulfonate, which (unlike for instance tetracyanoborate anion) contains protons, that enable a convenient measurement of the cation-anion ratio by ^{1}H NMR spectroscopy.

Table 5.3: Mixed gas permeances and mixed gas selectivities at 25 °C.

	Mixed gas permeance (GPU)[a]				Mixed gas selectivity	
IL	CO_2	N_2	CO_2	CH_4	CO_2/N_2	CO_2/CH_4
1a[b]	3.15	0.09	3.21	0.10	35.0	32.1
1b	1.06	0.07	1.13	0.09	15.1	12.6
2a	1.74	0.05	1.72	0.05	37.6	34.5
2b	3.49	0.09	3.52	0.10	38.2	35.2
2c	1.87	0.05	1.76	0.05	37.5	35.2
2d[b]	3.23	0.19	3.20	0.20	16.3	16.0
3	2.12	0.05	2.17	0.06	39.3	36.2

[a] 1 Gas Permeation Unit (GPU) = 1×10^{-6} cm^3 (STP)/(cm^2 s cmHg)

[b] data from ref [16]

Pyrrolidinium ionic liquids

A pyrrolidinium IL functionalized with a tri(ethylene glycol) monomethyl ether chain and a nitrile group on a three-carbon atom (C3) linker was obtained as a first example of a difunctionalized IL (Figure

5.4, compound **1a**). This IL provided a good CO_2/N_2 separation selectivity of 35.0 (Table 5.3). The selectivity of an analogous *p*-toluenesulfonate IL with an identical glycol chain and a methyl group (C1), but no nitrile moiety (**1b**), was only 15.1.[16] This difference was caused by the nearly tripled CO_2 permeance of IL **1a** in comparison with IL **1b** and a very similar N_2 permeance for both compounds (Table 5.3). Analogous observations apply to the CO_2/ CH_4 system.

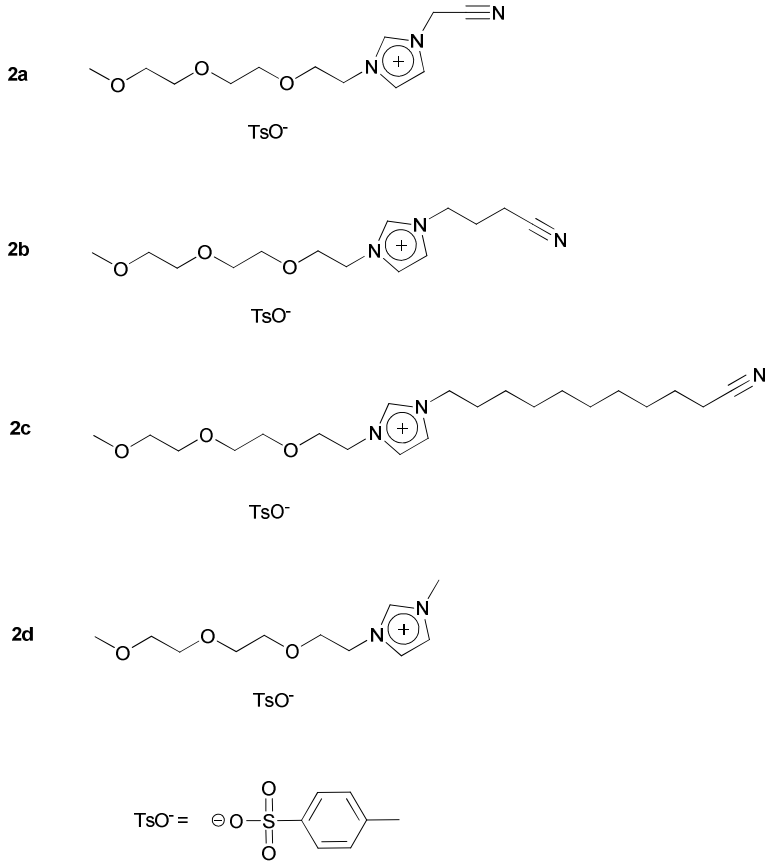

Figure 5.5: Monocationic imidazolium ILs 2a-d.

Imidazolium ionic liquids

Compounds **2a**, **2b** and **2c** represent a series of imidazolium ILs that differ only with a length of the alkyl spacer connecting the nitrile group to the cationic core. The spacer contains one (C1), three (C3) or ten (C10) methylene groups (Figure 5.5). The difference in the linker length is reflected in the selectivity to a much lesser extent than expected. All imidazolium ILs perform similarly, reaching mixed gas selectivity of 38.2 for compound **2b** and slightly lower values for the two other ILs (Table 5.3).

Similarly to the case of the pyrrolidinium ILs, the selectivities of the difunctionalized ILs **2a**-**c** are more than two times higher than the selectivities of their "only-glycol" imidazolium analogue, **2d**. In contrast with the pyrrolidinium ILs, the permeance of CO_2 increased on difunctionalization only for IL **2b** (vs. IL **2d**) and significantly dropped for ILs **2a** and **2c**.

Regardless of this difference, the high selectivity achieved by the SILMs covered with ILs **2a**-**c** is caused to a great extent by the decrease in permeances of N_2 and CH_4 in comparison with IL **2d**. Permeances of both contaminant gases dropped twice for IL **2b** and four times for ILs **2a** and **2c** (Table 5.3). These results suggest that the nitrile group is involved in rejection of the contaminant gases. A similar behaviour was reported by Carlisle *et al.* for systems with nitrile-functionalized imidazolium cations and by Mahurin *et al.* for ILs with the tetracyanoborate anion.[3,17] In both cases, solubility of CO_2 (or permeability)[17] decreased upon such functionalization, but the solubility (permeability) of N_2 and CH_4 dropped even more, resulting in high CO_2/N_2 and CO_2/CH_4 separation selectivities. It is interesting to note that of all difunctionalized imidazolium compounds, ILs **2a** (C1) and **2c** (C10) exhibit the lowest permeance of CO_2, N_2 and CH_4, while IL **2b** (C3)

shows the highest permeance of CO_2 and moderate permeance of N_2 and CH_4.

In the case of IL **2a**, the aromatic cations, anions and the cyano groups can participate in the formation of strong π-π interactions.[18] As a result, IL **2a** has a high viscosity which partly explains the lower permeance of all gases through a SILM covered with this IL (Table 5.2). The effect is even more pronounced for N_2 and CH_4 molecules, which are larger than CO_2 molecules and do not interact with the IL.[19] A decrease in FFV expected for an IL with an ether chain and a nitrile group on a very short spacer,[2] is consistent with the enhanced selectivity and reduced permeances of IL **2a** in comparison with IL **2d**.

The use of much longer alkyl chains of IL **2c** was chosen to increase CO_2 permeance, nevertheless, IL **2a** performs very similarly to IL **2c**.[20] The result contrary to our expectations, suggests an existence of other effects related most probably to the co-presence of the ether chain and the alkyl chain. Higher permeance of all gases and higher selectivity was observed for SILMs made of IL **2b**. The three-carbon atom linker of this IL appears to have just the right length to balance the strong π-π interactions which cause high viscosity in IL **2a** and the unfavourable effect related to the long alkyl spacer in IL **2c**. The longer spacer of IL **2b** is more flexible and prevents the formation of strong intramolecular bonds what is reflected in much lower viscosity of this IL.

The permeance of CO_2 for ILs **2a** and **2c** decreased proportionally to the permeance of the contaminant gases, therefore the selectivity remained very similar to that of IL **2b**. IL **2d** permeates twice as much N_2 and CH_4 than any of the difunctionalized imidazolium ILs and nearly as much CO_2 as IL **2b**. The high free volume created by the glycol chain and the simultaneous absence of a polar nitrile group result in a permeation of all three gases and a lower selectivity overall.

5.2.2. SILM performance of dicationic ILs

In order to achieve yet higher gas separation selectivities, IL **3** was designed (Figure 5.6). It combines the effective double functionalization described above (a glycol chain and a nitrile group), with a dicationic structure. According to our previous study, symmetrical dicationic ILs provide up to two times higher selectivities than monocationic ILs (Chapter 4).[16]

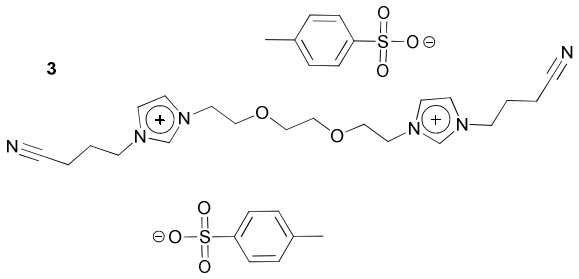

Figure 5.6: Dicationic imidazolium IL 3.

A SILM covered with IL **3** reached the highest selectivity of all ILs (39.3). Yet, this value was only slightly higher than the selectivity of its monocationic analogue – IL **2b** (38.2). The extremely high viscosity of IL **3** strongly decreased the CO_2 permeance. Consequently, only a small increase in selectivity was observed when compared to IL **2b**, characterized by much higher CO_2 permeance. Nevertheless, the highest selectivity of IL **3** and the twice lower permeance of N_2 and CH_4 through IL **3** versus IL **2b** is in agreement with our previously published findings, namely – the highly polar nature of dicationic ILs, manifested in the spread positive charge of the dications, aids a facile permeation of strongly quadrupolar CO_2 but does not easily permit less polar gases (N_2 and CH_4).[16] Recent findings show that apart from the highly polar nature of dicationic ILs, decreased free volume of these compounds may play a significant role in gas separations, as there is an inverse correlation between FFV and CO_2 separation selectivity from N_2 or CH_4.[2]

5.2.3. In situ FTIR-ATR study of the IL-CO_2 system

The FTIR-ATR measurements were performed with the help of dr Ian Silverwood from the group of Prof. Sergei Kazarian, Imperial College, London, UK. FTIR-ATR spectra shed more light on the interpretation of selectivity and mixed gas permeance data, both for mono- and dicationic ILs. IL swelling, CO_2 absorption and CO_2-IL interactions have been studied for the imidazolium ILs **2a**, **2b**, **2c**, and **3**, the imidazolium "only glycol" IL **2d**.

Table 5.4: Properties extracted from the infrared spectra of the ILs at 20 bar.

IL	Gas absorption (mmol/cm^3)	Swelling (%)	v_2 (CO_2) bandwidth (cm^{-1})
2a	1.85	3.4	27.6
2b	1.99	7.1	24.6
2c	n.d.[a]	n.d.[a]	24.7
2d	1.88	n.d.[a]	21.0
3	0.91	1.8	25.1

[a] n.d.: Data not available due to the disappearance of the IL layer from the diamond crystal, presumably due to the low viscosity of the compounds.

The concentrations of CO_2 dissolved in the studied ILs are presented in Table 5.4 and spectra of the ILs before and after equilibration in CO_2 atmosphere are shown in Figures 5.7-5.8. According to the data, the dicationic IL **3** solubilises the least CO_2, even though it provides the best selectivity overall. Stronger Coulombic interaction between the doubly charged ions in dicationic compounds, hold the ions closer together creating less free volume available for CO_2 molecules. Similarly functionalized, but monocationic IL **2b** has a much lower viscosity, and therefore solubilises the largest amount of CO_2.

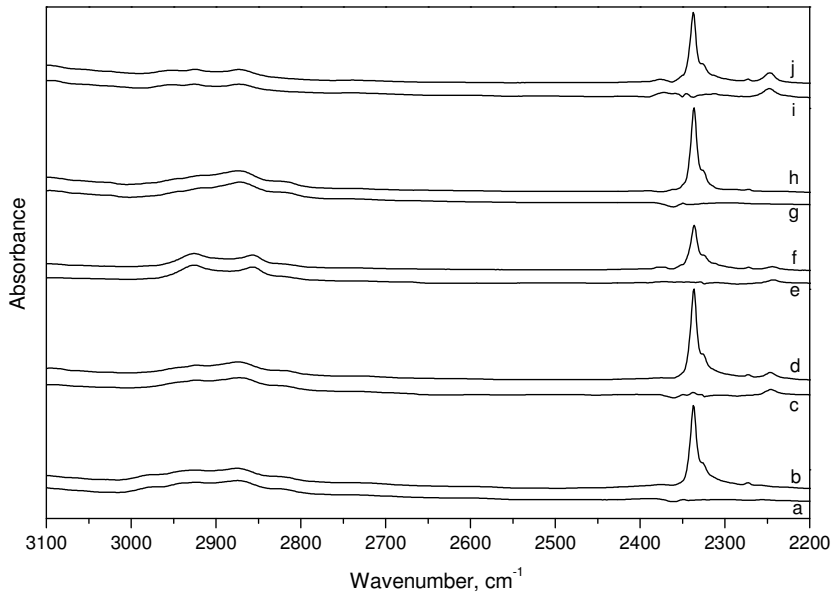

Figure 5.7: FTIR-ATR spectra of imidazolium ILs before and after equilibration in CO_2 atmosphere at 20 bar in the region of 3100–2200 cm^{-1}. a) IL 2a; b) IL 2a + CO_2; c) IL 2b; d) IL 2b + CO_2; e) IL 2c; f) IL 2c + CO_2; g) IL 2d; h) IL 2d + CO_2; i) IL 3; j) IL 3 + CO_2.

Despite the large difference in CO_2 permeance between ILs **2a** and **2b**, there is only a small difference in their CO_2 solubility, as the solubility was measured at the equilibrium where the high viscosity of IL **2a** is less of an issue. The imidazolium "only-glycol" IL **2d** dissolves comparably as much CO_2 as the nitrile- functionalized ILs, thus no clear trend is visible when CO_2 solubility in these two types of ILs is compared. The data further support the hypothesis that the high selectivity of the difunctionalized ILs is caused to a great extent by the rejection of N_2 and CH_4, rather than by more beneficial IL-CO_2 interactions, as these would be reflected in higher gas solubility.

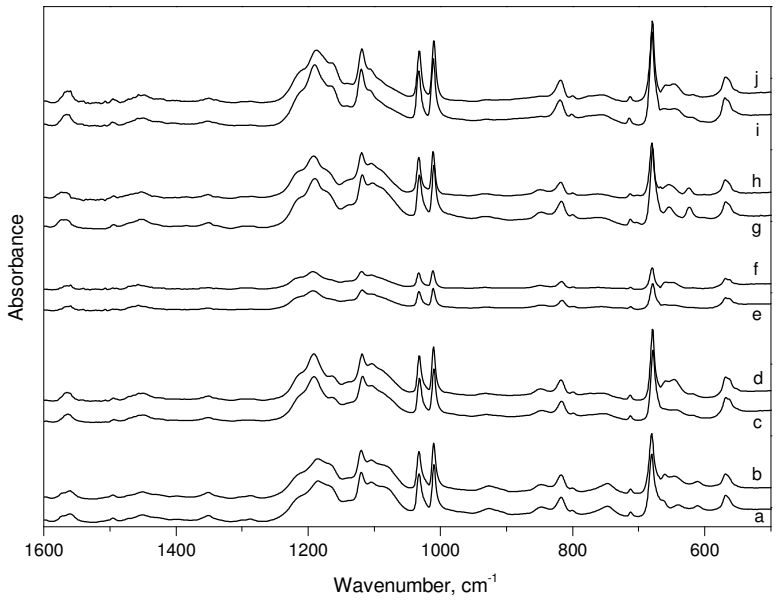

Figure 5.8: FTIR-ATR spectra of imidazolium ILs before and after equilibration in CO_2 atmosphere at 20 bar in the region of 1600–500 cm^{-1}. a) IL 2a; b) IL 2a + CO_2; c) IL 2b; d) IL 2b + CO_2; e) IL 2c; f) IL 2c + CO_2; g) IL 2d; h) IL 2d + CO_2; i) IL 3; j) IL 3 + CO_2.

The ILs presented here solubilise a similar amount of CO_2 as [C_4mim][PF_6] (Table 5.4) which dissolves approximately 1.5-2.5 mmol/cm^3 of the gas depending on the type of the measurement method used.[20,21] These are not particularly high values, therefore, these nitrile- and glycol-containing ILs are not suitable for bulk CO_2 absorption.

SILMs are less affected by swelling than pure polymeric membranes, nevertheless, swelling can alter mechanical stability and permeance of the membrane.[22] The extent of swelling can influence selectivity as follows: (i) negligible swelling stands for strong interactions between the ions and unless a sufficient initial free volume is present, there is less chance for CO_2 interactions with the IL; (ii) moderate increase of free volume on swelling facilitates gas diffusion into the IL layer of the SILM, what can result in more favourable IL-CO_2

interactions, and consequently in higher gas solubility and higher selectivity, provided enough polar cavities are formed;[23] (iii) extensive swelling increases permeance of both gases, lowering the selectivity. A simultaneous "dilution" of moieties able to interact with the gas, per unit volume, lowers the performance even further.[24]

At the pressure of 20 bar, the imidazolium IL **2a** swelled only 3.4%, what is consistent with the strong cation-anion interactions and high viscosity of this IL. This is also true for the dicationic IL **3**, which swells the least of all ILs: 1.8%. IL **2b** reached 7.1% of its initial volume and this was the highest value observed. This moderate swelling of IL **2b** facilitated CO_2 diffusion through the membrane and resulted in high permeance. On pressurization, the absorbance of ILs **2c** and **2d** drastically decreased, what is normally associated with a very high swelling. Here, however, it was accompanied by a decrease in CO_2 solubility, indicating the disappearance of the IL from the measuring surface of ATR crystal, probably due to the lower viscosity of these compounds. Under pressure, a small amount of IL moved away of the diamond surface to the surrounding area.

For comparison, [C_4mim][PF_6] swells approximately 6% at 20 bar, which is more than the majority of the ILs presented here but less than IL **2b**.[11] A molecular solvent, liquid poly(ethylene glycol), PEG 400, unrestricted by ionic interactions, swells 16% at 53 bar.[25]

By comparing the membrane and infrared data, it can be shown that the SILM containing IL **2b** performs the best, because it is characterized by the highest CO_2 permeance, the highest CO_2 solubility, and the highest but still moderate swelling. In contrast with our previous results, where dicationic ILs performed twice as well as monocationic ones, the selectivity of the dicationic IL **3** improves only slightly in comparison with its monocationic analogue, IL **2b**.[16] This is most probably related to the high viscosity of IL **3** and the exceptional performance of IL **2b**.

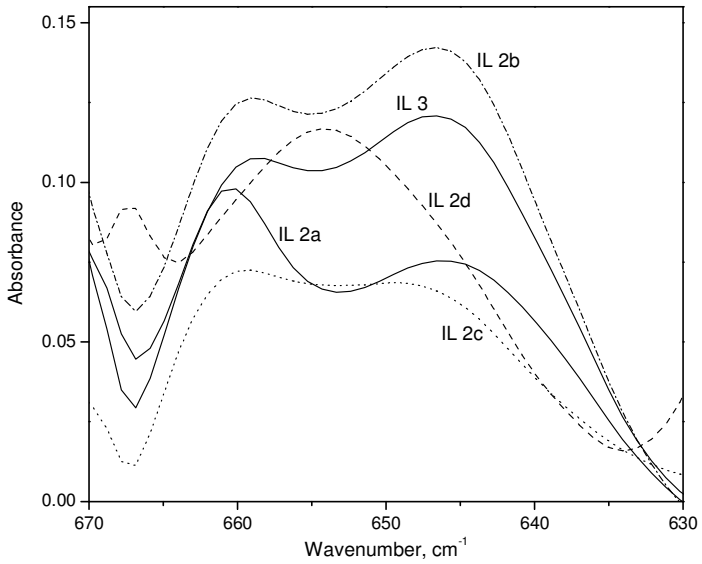

Figure 5.9: FTIR-ATR spectra of CO_2 dissolved in different imidazolium ILs in the v_2 band region.

Broadening and splitting of the bending mode band of CO_2 (v_2) in the presence of ILs, indicates a removal of a degeneracy of this mode associated with the interaction of CO_2 and ions of the studied ILs.[12,26,27] Figure 5.9 presents spectra of CO_2 dissolved in different ILs in the v_2 band region. The bandwidths, measured as an average half width (FWHM, Full Width at Half Maximum), range for the studied ILs from 21 to 28 cm^{-1}. The correlation between the $v_2(CO_2)$ and the amount of dissolved gas has been proposed by Kazarian *et al.* for the case of polymeric samples.[12]

Despite significant differences in gas solubility, the nitrile-containing monocationic ILs **2b** and **2c** and the dicationic IL **3** display similar bandwidths of *ca.* 25 cm^{-1}. IL **2a** shows much broader bandwidth of about 28 cm^{-1}. The FWHM of the "only-glycol" IL **2d** is much lower: 21 cm^{-1}.

The occurrence of such broad bands is not surprising *per se*. Band broadening stems from the interaction between CO_2 and functional groups localized on anions and cations, such as ethers, carbonyl groups

and aromatic systems.[4,12,27] Depending on the interacting moiety and its environment, the strength of interaction may vary, resulting in different FWHMs. The ILs presented in this paper possess multiple interaction sites, such as the *p*-toluenesulfonate anion, the imidazolium ring, the nitrile group and the tri(ethylene glycol) chain. A concurrent presence of more than one interacting group in these difunctionalized compounds may therefore result in the bandwidths of 21–28 cm^{-1}. Larger bandwidths values for the difunctionalized ILs can be explained by the higher strength of certain interactions that occur due to the presence of the nitrile group. Nevertheless, the values are not reflected in higher gas solubilities. The particularly large bandwidth value for IL **2a** suggests that the low CO_2 permeance through this IL may be also related to the slow desorption of CO_2 from the SILM, due to the strong CO_2-IL interactions.

Kazarian *et al.* reported band widths for [C_4mim][PF_6] and [C_4mim][BF_4] ILs, which were 15 cm^{-1} and 19 cm^{-1}, respectively.[4] The difference of 4 cm^{-1} was attributed to the different strength of interactions between the anions and CO_2 molecules. The interaction of anions with CO_2 has been well documented in the literature so also in the case of the ILs reported here there is no doubt that such interactions contribute to the band broadening.[20] Since, however, all the ILs presented here contain the same *p*-toluenesulfonate anion, the observed changes in FWHMs must be related to the dissimilar cations. The $v_2(CO_2)$ bandwidth can be affected by direct cation-CO_2 interactions,[28] or indirectly, by cation-anion interactions of various strength that influence the anion-CO_2 and cation-CO_2 interactions. When designing CO_2-philic ILs, cations should be as carefully chosen as anions, not only to adjust the physical properties of ILs (e.g. imidazolium cations generally ensure low viscosity) but also to enable CO_2 dissolution.[16, 28]

For the majority of the ILs presented here the CO_2 bending mode band is split, indicating the appearance of two new bending mode bands

(Figure 5.9). Only for IL **2d** is the v_2 band not split. It may be related to the smaller difference in wavenumber between the two new bands and hence a lower resolution.

Previous examinations of several common molecular solvents and polymers showed that the v_2 band of CO_2 splits into two bands in solvents that possess a lone electron pair.[29,26,12,27] In polymers containing a pyridine ring, a simultaneous contribution from the two interacting sites (the nitrogen atom and the aromatic ring), made it difficult to observe the v_2 band splitting. Instead, a broadening of the band was observed. Surprisingly, this was not the case with the *p*-toluenesulfonate anion (sulfonyl group and a toluoyl ring), even though, the existence of the two possible CO_2-binding sites have been proven theoretically.[16] Nalawade *et al.* reported that the splitting of the v_2 (CO_2) interacting with PEG 6000 was visible only at and above 60 bar. It was attributed to weak interactions between the ether groups and the CO_2 molecules.[27] This could indicate that the band splitting visible for ILs presented here at the lower pressure of 20 bar, results from the interactions with other functional groups than with the ether chain.

None of the spectral bands of the ILs showed any significant shifts or broadening, what implies a weak, physical binding of CO_2, as well as no profound influence of CO_2 on the structures of the ILs (Figures 5.7 and 5.8). The broadening of the CO_2 bending mode described above (Figure 5.9), results nevertheless from such interactions, even if they are not visible in the spectrum of the ILs themselves. Additionally, the lack of changes cannot be a proof that such interactions do not exist: only very small band shifts (ca. 0.5 cm^{-1}) appear in the spectrum of a widely known CO_2 absorber, PEG 6000 on the contact with the gas and a pressure of 60 bar is necessary to reveal them.[27]

Similarly, there were also no changes observed in the nitrile stretching band of the ILs, even though the nitrile group clearly

contributes to the performance of the SILMs. This observation suggests once again that the nitrile moiety does not facilitate CO_2 solubilisation or diffusion but rather prevents N_2 and CH_4 from passing through the membrane. The nitrile bands were fairly symmetrical, before and after CO_2 introduction.

Lethesh *et al.* studied polarization of the nitrile group in nitrile-functionalized pyridinium ILs.[15] The partial negative charge on the nitrile nitrogen atom was found to increase with increasing alkyl spacer length and the effect was especially pronounced for short chains (less than 3 carbons). The presumably significant dipole moment of the nitrile groups in ILs **2b**, **2c** and **3** could help to visualise the CO_2-nitrile interaction in the infrared. Nevertheless, there have been no changes observed in the spectra of any of the ILs after CO_2 has been introduced, neither in the short spacer salts **2a** or **2b** and **3**, nor in the long chain IL **2c**.

Romanos *et al.* examined imidazolium tricyanomethanide (TCM) ILs, in the presence of CO_2 by Raman spectroscopy. No changes were found in the nitrile stretching band of these compounds, even though the TCM ILs proved to be very efficient in CO_2 separation on SILMs.[30-32]

In conclusion, examination of the band corresponding to the vibration of –CN group did not reveal any significant interactions between this group and CO_2 molecules. It may indicate a stronger influence of the –CN group on the ν_2 band of CO_2, than the CO_2 effect on the –CN band. Even though no significant changes in the structure of the ILs can be traced, the larger FWHMs of the difunctionalized ILs suggest the occurrence of the weak specific IL-CO_2 interactions.

5.3. Conclusions

Novel difunctionalized ionic liquids containing a tri(ethylene glycol) monomethyl ether chain and a nitrile group on a pyrrolidinium or imidazolium cation were synthesized and incorporated into SILMs. The

difunctionalized ILs exhibited higher CO_2/N_2 and CO_2/CH_4 separation selectivities (mixed gas) of up to 40, which is *ca*. 2.3 times than their analogues functionalized only with a glycol group. The nitrile-and glycol-ILs benefit from the room temperature fluidity ensured by the glycol chain and high separation selectivities provided by both the glycol chain and the nitrile group. The working principle of the nitrile group is different for the pyrrolidinium and imidazolium compounds. In the case of pyrrolidinium ILs, introduction of the nitrile group increases the CO_2 permeance, while the permeances of the contaminant gases rise negligibly, resulting in high gas separation selectivity. For imidazolium ILs, the presence of a nitrile group does not always increase the CO_2 permeance nor does it increase the CO_2 solubility, as showed by in situ FTIR-ATR spectroscopy. High selectivities of the difunctionalized imidazolium ILs are caused by the largely reduced permeances of N_2 and CH_4, presumably due to the ability of the polar nitrile group to reject the contaminant gases. The CO_2 solubilities in the novel ILs were comparable to those of monofunctionalized ILs and ranged from 0.91 to 1.99 mmol/cm^3. Also IL-CO_2 interactions were studied by the in situ FTIR-ATR spectroscopy. The nitrile-containing ILs were found to interact stronger with the gas, which was reflected in larger v_2 bandwidths of CO_2 dissolved in these ILs. Although no changes were observed in the nitrile bands of the difunctionalized ILs, the appearance of the CO_2 spectra proved the existence of IL-CO_2 interactions related to the presence of the nitrile group on the cation. The broadening of the $v_2(CO_2)$ may be a result of a direct –CN-CO_2 interaction not visible at the applied pressure, or indirect cation-anion interactions that influence the contact between the *p*-toluenesulfonate anions or cations and CO_2. The dicationic, difunctionalized IL achieved the highest selectivity in the series (39.3 for CO_2/N_2 system). Nevertheless, it was only slightly better than that of its monocationic analogue, possibly due to the high viscosity of the dicationic IL and the exceptional performance of the monocationic

IL which was characterized by the highest CO_2 permeance, CO_2 solubility and swelling in the series.[16]

5.4. Experimental part

5.4.1. Syntheses

For the synthesis of IL precursors see: Electronic Supporting Information. The synthesized ILs are very hygroscopic and their exposure to ambient air during CHN sample preparation always resulted in absorption of water.

1-(3-Cyanopropyl)-1-[2-[2-(2-methoxyethoxy)ethoxy]ethyl] pyrrolidinium *p*-toluenesulfonate (1a)

A mixture of 4-(*N*)-pyrrolidinylbutyronitrile (1.39 g, 10.0 mmol) and tri(ethylene glycol) monomethyl ether monotosylate (3.0 g, 9.43 mmol) in acetonitrile (50 mL) was stirred at 80 °C for 72 h. After evaporation of the solvent, the residue was dissolved in water (70 mL) and washed with dichloromethane (20 mL). Removal of water *in vacuo* yielded a dark orange oil. Yield: 3.71 g (89%). ^{1}H NMR (300 MHz, $CDCl_3$): δ = 7.73 (d, 2H, *J* = 8.1 Hz), 7.15 (d, 2H, *J* = 8.1 Hz), 3.91–3.64 (m, 8H), 3.64–3.54 (m, 8H), 3.54–3.47 (m, 2H), 3.34 (s, 3H), 2.58 (t, 2H, *J* = 6.8 Hz), 2.34 (s, 3H), 2.26–2.12 (m, 6H) ppm. ^{13}C NMR (75 MHz, $CDCl_3$): δ = 143.7, 139.5, 128.8, 125.8, 118.9, 71.8, 70.3, 70.3, 70.1, 65.3, 63.8, 58.9, 58.9, 59.0, 21.6, 21.3, 19.9, 14.2 ppm. IR (cm^{-1}): 2879, 2246 (nitrile), 1459, 1353, 1191, 1118, 1032, 1010, 929, 849, 818, 713, 679, 564. CHN ($M \cdot H_2O$) [%](calculated): C: 57.27 (57.87), H: 8.07 (7.95), N: 6.19 (6.14).

1-(2-(2-(2-Methoxyethoxy)ethoxy)ethyl)-1-methylpyrrolidinium *p*-toluenesulfonate (1b)

The compound was prepared via a method analogous to a literature procedure.[14] A mixture of 1-methylpyrrolidine (2.08 mL, 20.0 mmol) and

tri(ethylene glycol) monomethyl ether monotosylate (5.0 g, 15.72 mmol) in acetonitrile (50 mL) was stirred at 120 °C for 3 h. The excess of 1-methylpyrrolidine and the solvent was evaporated *in vacuo* to give a light yellow oil in quantitative yield (6.34 g). ^{1}H NMR (300 MHz, $CDCl_3$): δ = 7.73 (d, 2H, *J* = 8.1 Hz), 7.12 (d, 2H, *J* = 8.1 Hz), 3.94–3.86 (m, 2H), 3.86–3.79 (m, 2H), 3.79–3.65 (m, 4H), 3.65–3.52 (m, 6H), 3.52–3.44 (m, 2H), 3.32 (s, 3H), 3.20 (s, 3H), 2.32 (s, 3H), 2.25–2.04 (m, 4H) ppm. ^{13}C NMR (75 MHz, $CDCl_3$): δ = 143.9, 139.1, 128.6, 125.8, 71.8, 70.3, 70.2, 70.1, 65.4, 65.3, 63.0, 59.0, 48.3, 21.4, 21.2 ppm. IR (cm^{-1}): 2877, 1457, 1353, 1189, 1117, 1031, 1010, 957, 882, 849, 817, 678, 562. CHN (M·H_2O) [%] (calculated): C: 54.13 (54.13), H: 8.35 (8.37), N: 3.30 (3.32).

1-(Cyanomethyl)-3-[2-[2-(2-methoxyethoxy)ethoxy]ethyl] imidazolium *p*-toluenesulfonate (2a)

A mixture of 1-(cyanomethyl)imidazole (2.0 g, 18.7 mmol) and tri(ethylene glycol) monomethyl ether monotosylate (5.94 g, 18.7 mmol) in acetonitrile (50 mL) was stirred at 82 °C for 72 h. After evaporation of the solvent, the residue was dissolved in water (150 mL) and washed with dichloromethane (15 mL). Removal of water *in vacuo* yielded a dark orange oil. Yield: 6.20 g (78 %). ^{1}H NMR (300 MHz, $CDCl_3$): *δ* = 9.80 (s, 1H), 7.73 (d, 2H, *J* = 8.0 Hz), 7.67 (s, 1H), 7.64 (s, 1H), 7.16 (d, 2H, *J* = 8.0 Hz), 5.76 (s, 2H), 4.39 (t, 2H, *J* = 4.5 Hz), 3.79 (t, 2H, *J* = 4.5 Hz), 3.64–3.48 (m, 8H) 3.35 (s, 3H), 2.34 (s, 3H) ppm. ^{13}C NMR (75 MHz, $CDCl_3$): *δ* = 143.2, 139.8, 138.3, 128.9, 125.8, 124.0, 122.4, 113.7, 71.8, 70.3, 70.2, 70.1, 68.5, 58.9, 50.0, 37.1, 21.3 ppm. IR (cm^{-1}): 2876, 2166 (nitrile), 1561, 1451, 1351, 1288, 1186, 1119, 1032, 1009, 928, 848, 817, 750, 712, 679, 611, 563. CHN (M·H_2O) [%] (calculated): C: 51.51 (51.45), H: 6.60 (6.59), N: 9.80 (9.47).

1-(3-Cyanopropyl)-3-[2-[2-(2-methoxyethoxy)ethoxy] ethyl]imidazolium *p*-toluenesulfonate (2b)

A mixture of 1-(3-cyanopropyl)imidazole (1.5 g, 11.1 mmol) and tri(ethylene glycol) monomethyl ether monotosylate (3.88 g, 12.2 mmol) in acetonitrile (50 mL) was stirred at 80 °C for 48 h. After evaporation of the solvent, the residue was dissolved in water (100 ml) and washed with dichloromethane (3 × 5 mL). Removal of water *in vacuo* yielded a dark orange oil. Yield: 4.63 g (92%). ^{1}H NMR (300 MHz, $CDCl_3$): δ = 9.92 (s, 1H), 7.76 (d, 2H, *J* = 8.0 Hz), 7.61 (s, 1H), 7.39 (s, 1H), 7.16 (d, 2H, *J* = 8.0 Hz), 4.50 (t, 2H, *J* = 7.1 Hz), 4.44 (t, 2H, *J* = 4.5 Hz), 3.82 (t, 2H, *J* = 4.5 Hz), 3.66–3.48 (m, 8H), 3.36 (s, 3H), 2.56 (t, 2H, *J* = 6.9 Hz), 2.34 (s, 3H), 2.30 (m, 2H) ppm. ^{13}C NMR (75 MHz, $CDCl_3$): δ = 143.5, 139.6, 137.6, 128.8, 158.8, 123.6, 122.1, 118.7, 71.8, 70.3, 70.2, 70.1, 68.8, 58.9, 49.7, 48.2, 26.1, 21.3, 14.2 ppm. IR (cm^{-1}): 3125, 3094, 2875, 2245 (nitrile), 1565, 1190, 1117, 1031, 1009, 850, 818, 562. CHN ($M \cdot 1H_2O$) [%] (calculated): C: 54.08 (53.49), H: 7.19 (7.05), N: 9.05 (8.91).

1-(10-Cyanodecyl)-3-[2-[2-(2-methoxyethoxy)ethoxy] ethyl]imidazolium p-toluenesulfonate (2c)

A mixture of 1-(10-cyanodecyl)imidazole (0.5 g, 2.14 mmol) and tri(ethylene glycol) monomethyl ether monotosylate (0.75 g, 2.36 mmol) in acetonitrile (40 mL) was stirred at 70 °C for 68 h. After evaporation of the solvent, the residue was dissolved in water (100 mL) and washed with dichloromethane (3 × 10 mL). The dichloromethane phase was then washed with water to recover a part of the product dissolved therein. Combination of the two water extracts, followed by evaporation, yielded a dark orange oil. Yield: 0.39 g (32 %). ^{1}H NMR (300 MHz, $CDCl_3$): *δ* = 9.94 (s, 1H), 7.79 (d, 2H, *J* =8.0 Hz), 7.63 (s, 1H), 7.15 (d, 2H, *J* = 8.0 Hz), 7.11 (s, 1H), 4.57 (t, 2H, *J* =4.4 Hz), 4.22 (t, 2H, *J* =7.5 Hz), 3.87 (t, 2H, *J* = 4.5 Hz), 3.69–3.50 (m, 8H), 3.37 (s, 3H), 2.34 (s, 3H), 2.33 (t, 2H, *J* =7.5 Hz), 1.88 (m, 2H), 1.64 (m, 2H), 1.43 (m, 2H), 1.28 (m, 10H) ppm. ^{13}C

NMR (75 MHz, $CDCl_3$): δ = 143.6, 139.2, 137.9, 129.4, 128.6, 125.9, 123.7, 120.8, 119.9, 71.9, 70.3, 70.2, 70.1, 69.2, 59.0, 50.0, 49.6, 30.1, 29.0, 29.0, 28.8, 28.6, 28.5, 26.2, 25.3, 21.3, 17.1 ppm. IR (cm^{-1}): 3140, 3096, 2925, 2856, 2243 (nitrile), 1599, 1564, 1456, 1351, 1191, 1119, 1105, 1033, 1011, 930, 848, 817, 758, 680, 565. CHN ($M \cdot H_2O$) [%] (calculated): C: 58.74 (59.03), H: 8.70 (8.31), N: 7.26 (7.38).

1-(2-(2-(2-Methoxyethoxy)ethoxy)ethyl)-1-methylimidazolium *p*-toluenesulfonate (2d)

1-Methylimidazole (1.82 mL, 22.8 mmol) and tri(ethylene glycol) monomethyl ether monotosylate (8.0 g, 25.15 mmol) in acetonitrile (50 mL) were stirred at 70 °C for 48 h. The solvent was evaporated and the residue was dissolved in 50 mL of water and washed with dichloromethane (3 × 7 mL). Evaporation of water and traces of dichloromethane yielded a colourless oil. Yield: 6.21 g (68%). ^{1}H NMR (300 MHz, $CDCl_3$): δ = 9.75 (s, 1H), 7.77 (d, 2H, J = 7.9 Hz), 7.58 (s, 1H), 7.27 (s, 1H), 7.14 (d, 2H, J = 7.9 Hz), 4.46 (t, 2H, J = 4.4 Hz), 3.86 (s, 3H), 3.80 (t, 2H, J = 4.4 Hz), 3.64–3.55 (m, 6H), 3.55–3.50 (m, 2H), 3.34 (s, 3H), 2.32 (s, 3H) ppm. ^{13}C NMR (75 MHz, $CDCl_3$): δ = 143.7, 139.3, 138.2, 128.6, 125.9, 123.5, 122.6, 71.8, 70.3, 70.2, 70.1, 69.0, 59.0, 49.5, 36.3, 21.3 ppm. IR (cm^{-1}): 3148, 3099, 2873, 1573, 1461, 1351, 1192, 1119, 1033, 1011, 933, 849, 818, 762, 680, 654, 624, 569. CHN ($M \cdot H_2O$) [%] (calculated): C: 49.26 (49.64), H: 7.22 (7.17), N: 6.39 (6.43)

1,8-Bis[1-(3-cyanopropylimidazolium-1-yl)]-3,6-dioxaoctane di(p-toluenesulfonate) (3)

A mixture of 1-(3-cyanopropyl)imidazole (1.03 g, 7.62 mmol) and tri(ethylene glycol) ditosylate (1.75 g, 3.81 mmol) in acetonitrile (50 mL) was stirred at 80 °C for 72 h. After evaporation of the solvent, the residue was dissolved in water (150 mL) and placed in the fridge for 1 h. The white precipitate of tri(ethylene glycol)diosylate was filtered off and

the mother liquor was washed with dichloromethane (3 × 15 mL). Removal of water *in vacuo* yielded a light yellow glassy solid. Yield: 1.25 g (45 %). ^{1}H NMR (300 MHz, D_2O): δ = 8.89 (s, 2H), 7.68 (d, 4H, J = 8.0 Hz), 7.57 (s, 4H), 7.36 (d, 4H, J = 8.0 Hz), 4.40 (t, 4H, J = 4.8 Hz), 4.35 (t, 4H, J = 6.9 Hz), 3.88 (t, 4H, J = 4.9 Hz), 4.49 (s, 4H), 2.58 (t, 4H, J = 6.9 Hz), 2.39 (s, 6H), 2.26 (m, 4H) ppm. ^{13}C NMR (75 MHz, D_2O): δ = 142.4, 139.5, 136.0, 129.4, 125.3, 123.1, 122.3, 119.9, 69.5, 68.4, 49.1, 48.2, 24.9, 20.4, 13.7 ppm. IR (cm^{-1}): 3098, 2924, 2872, 2247 (nitrile), 1565, 1449, 1350, 1188, 1119, 1032, 1010, 819, 755, 713, 680, 565. CHN ($M{\cdot}2H_2O$) [%] (calculated): C: 53.34 (53.39), H: 6.33 (6.33), N: 10.75 (10.99).

5.4.2. Instruments and methods

Chemicals were purchased from Acros Organics (Geel, Belgium) or from Sigma-Aldrich (Diegem, Belgium). All chemicals were used as received, without further purification. ^{1}H and ^{13}C NMR spectra were recorded on a Bruker Avance 300 spectrometer. The water content of the ILs dried overnight under vacuum at 50 °C was determined by the coulometric Karl Fischer titrator (Mettler-Toledo, model DL39). Due to their hygroscopic nature all ILs contained 300 to 400ppm of water. The viscosity of the ILs was measured with a Brookfield DV-II + Pro Cone/ plate set-up viscometer, equipped with a thermostatted sample cell purged with dry nitrogen gas. Differential scanning calorimetry (DSC) measurements were performed on a Mettler-Toledo DSC822e module, at a scan rate of 10 °C per minute in a helium atmosphere.

Membrane preparation and measurements

Porous γ-alumina discs (25 mm diameter, 2 mm thickness, 3–5 nm pore size) from Pervatech were used as support material for the ILs in the SILMs. In comparison to polymeric supports, alumina supports with such wide pores do not influence the gas separation properties of the ILs under study. Before coating the support with ILs, it was tested by

passing the two studied gas mixtures (CO_2/N_2 and CO_2/CH_4) through it. The support was found to be non-selective to the gas mixtures and had only a minimal effect on the gas flux. Before the application of the IL on the support, the viscosity of the IL was adjusted by dilution with an appropriate volatile solvent (acetone or dichloromethane). The IL was applied to the membrane surface using a micropipette. Excess liquid was removed from the surface using a lint-free cloth. The membrane was then spun at 1000 rpm in a spin-coater for 60 s, producing a visually uniform surface. The membrane was dried in an oven for 2 hours at 50° C to remove the excess of solvent. This process of spin-coating and drying was repeated three times to ensure complete coverage of the support with IL.

The gas permeation set-up consisted of a stainless steel module with a cavity to insert the membrane disk gripped with Viton® O-rings. The module, upstream and downstream parts were evacuated by a vacuum pump to remove residual air and other gases before measurement of the gas permeation properties. A feed gas at a flow rate of 1 L/min was introduced in the module. For mixed-gas measurements, mass flow controllers (MFC, Bronkhorst) were used to adjust the feed gas composition. The upstream pressure was adjusted using a back-pressure regulator. Gas permeances were measured by allowing the permeate gas to expand in a constant volume auxiliary cylinder connected to a MKS Baratron pressure transducer with a higher limit of 10 mbar. The rate of pressure increase (dP/dt) was measured to calculate the gas permeability from the following equation:

$$P_i = \frac{273\times 10^6}{760}\,\frac{y_i V}{AT\left(\frac{76}{14.7}\right)x_i P_1}\left(\frac{dP}{dt}\right) \qquad 5.1$$

where y_i and x_i refer to the mole fraction of component i in the downstream and upstream, respectively. V is the downstream volume (cm^3), A is the membrane permeation area (cm^2), T is the operating

temperature (K), and P_1 is the pressure of the feed gas (psi). The gas permeate composition was measured using a compact gas chromatograph (CGC, Interscience). The operation and data acquisition was carried out using CGC-editor and Agilent EZchrom software. The mixed-gas selectivity was calculated by the ratio of downstream and upstream mole fractions of the two gases by the following equation:

$$\alpha_{ij} = \frac{\left(y_i/y_j\right)}{\left(x_i/x_j\right)} \quad 5.2$$

where y_i and y_j are the mole fractions of components i and j, respectively, in the downstream, x_i and x_j are the mole fractions of components i and j, respectively, in the upstream. The permeation measurements for each membrane coupon were repeated at least three times, and an average of all these values was used for further analysis.

Infrared measurements and methods

Infrared spectra were recorded at 2 cm^{-1} resolution on a Bruker Equinox-55 FTIR spectrometer equipped with an MCT detector, a Golden Gate ATR accessory (Specac, Ltd., UK) and a miniature high-pressure flow cell which details have been described previously.[33-35] Gas pressure was applied using a high pressure generator from HiP and the gas handling system used 1/16" stainless steel tubing throughout. For the measurement, the diamond reflection element was covered with a layer of IL, taking care that the sample thickness exceeded the penetration depth of the infrared radiation. The sample was dried on the diamond at 80 °C in a gentle flow of nitrogen gas (99.998% purity) until the water stretching band at 3500 cm^{-1} has maximally decreased in intensity. The sample was then cooled to 25 °C under a static nitrogen atmosphere. The tubing connected to the gas reservoir and the gas cell, were purged three times with CO_2 (99.8% purity). Afterwards, the cell and the entire

system were charged with CO_2 at the desired pressure, thermostatted at 25 °C and left for equilibration, which took approximately 90 min at each pressure. The system was considered equilibrated when no changes in absorbance of the CO_2 bands or in absorbance of bands of the IL were observed for at least 15 min.

Whilst the membrane measurements were performed at a pressure of 5 bar of mixed gasses, all infrared spectra were recorded at the pressure of 20 bar. This was done because the spectral changes at the pressure of 5 bar were found to be very small and were seriously affected by the baseline correction and spectral subtraction. Good quality spectra were obtained using 128 scans in the 4000–500 cm^{-1} range. For determination of the bandwidth, a manual spectra subtraction of the pure gas phase CO_2 spectrum from the spectra of the CO_2-saturated IL was performed along with a baseline correction, using OPUS 6.5 software. The average bandwidth was measured as the width of the bending mode band at ca. 660 cm^{-1} at half of its height. The method for swelling determination has been developed by Kazarian *et al.* [13] . Swelling of a material can be calculated on the basis of the Lambert-Beer Law.[11] In the absence of the gas, the absorption of a selected band of the material can be described by the following equation:

$$A_0 = \varepsilon\, c_0\, d_{e,u} \qquad 5.3$$

Where A_0 is the absorbance of the sample before introduction of the gas, ε is the extinction coefficient, c_0 is the initial concentration of the IL and $d_{e,u}$ is the effective thickness of the IL layer penetrated by the non-polarized light. Since the band shape may change with changing pressure, it is advisable to report the absorbance as integrated absorbance rather than band height. With an assumption that the refractive index and the molar absorptivity do not change significantly with the increasing concentration of CO_2, the $d_{e,u}$ also does not and the absorbance of the selected band after gas introduction is given by:

$$A = \varepsilon \, c \, d_{e,u} \quad (5.4)$$

Similarly, if an IL initially occupies volume V_0, and it expands by ΔV but the number of moles of the IL remains constant, the concentrations before (c_0) and after (c) gas introduction look as follows:

$$c_0 = n/V_0 \quad (5.5)$$

$$c = n/ V_0 + \Delta V \quad (5.6)$$

Therefore:

$$\frac{c_0}{c} = \frac{V_0 + \Delta V}{V_0} = 1 + \frac{\Delta V}{V_0} = 1 + \sigma \quad (5.7)$$

where σ is swelling. Taking into account the Lambert-Beer law, we obtain the ultimate swelling equation:

$$\sigma = \frac{A_0}{A} \frac{d_{e,u}}{d_{e,u}} - 1 = \frac{A_0}{A} - 1 \quad (5.8)$$

The obtained σ value is often expressed in percentage.

In this chapter the assessment of the swelling of the ILs was achieved using the integrated absorbance of the band of the tri(ethylene glycol) chain at 1031 cm^{-1} at atmospheric pressure and 20 bar of CO_2.

The band absorbance of the antisymmetric stretching band of CO_2 at 2336 cm^{-1} (measured as the height of the band), and the molar absorptivity value for this band at high pressures were used to determine the concentration of the gas dissolved in the ILs.[36] Refractive indices of the compounds were measured at 25 °C and atmospheric pressure, using an analog refractometer N° 516871 (Bellingham & Stanley Ltd.).

The effective pathlength was calculated on the basis of the equation provided by Flichy *et al.*[8] Despite non-negligible initial water content, the estimation of the concentration of CO_2 dissolved in ILs was

reliable. Aki *et al.* studied the influence of water on CO_2 adsorption in ILs and reported that for [C_4mim][Tf_2N] even saturation of the sample with water had essentially no effect on CO_2 solubility.[20] Even though the influence of water could be more pronounced in case of the more hydrophilic ILs presented here,[37] the water content of the dried IL samples was negligible in comparison with a water-saturated sample.

5.5. References

1. Smith, G. D.; Borodin, O.; Li, L.; Kim, H.; Liu, Q.; Bara, J. E.; Gin, D. L.; Nobel, R., A comparison of ether- and alkyl-derivatized imidazolium-based room-temperature ionic liquids: a molecular dynamics simulation study. *Phys. Chem. Chem. Phys.* **2008,** *10*, 6301-6312.
2. Horne, W. J.; Shannon, M. S.; Bara, J. E., Correlating fractional free volume to CO_2 selectivity in [Rmim][Tf_2N] ionic liquids. *J. Chem. Thermodyn.* **2014**.
3. Carlisle, T. K.; Bara, J. E.; Gabriel, C. J.; Noble, R. D.; Gin, D. L., Interpretation of CO_2 Solubility and Selectivity in Nitrile-Functionalized Room-Temperature Ionic Liquids Using a Group Contribution Approach. *Ind. Eng. Chem. Res.* **2008,** *47*, 7005-7012.
4. Kazarian, S. G.; Briscoe, B. J.; Welton, T., Combining ionic liquids and supercritical fluids: ATR-IR study of CO_2 dissolved in two ionic liquids at high pressures. *Chem. Commun.* **2000**, 2047-2048.
5. Seki, T.; Grunwaldt, J.-D.; Baiker, A., In Situ Attenuated Total Reflection Infrared Spectroscopy of Imidazolium-Based Room-Temperature Ionic Liquids under "Supercritical" CO_2. *J. Chem. Phys. B* **2008,** *113*, 114-122.
6. Seki, S.; Tsuzuki, S.; Hayamizu, K.; Umebayashi, Y.; Serizawa, N.; Takei, K.; Miyashiro, H., Comprehensive Refractive Index Property for Room-Temperature Ionic Liquids. *J. Chem. Eng. Data* **2012,** *57*, 2211-2216.
7. Harrick, N. J., Study of Physics and Chemistry of Surfaces from Frustrated Total Internal Reflections. *Phys. Rev. Lett.* **1960,** *4*, 224-226.
8. Flichy, N. M. B.; Kazarian, S. G.; Lawrence, C. J.; Briscoe, B. J., An ATR−IR Study of Poly (Dimethylsiloxane) under High-Pressure Carbon Dioxide: Simultaneous Measurement of Sorption and Swelling. *J. Phys. Chem. B* **2002,** *106*, 754-759.
9. Averett, L. A.; Griffiths, P. R.; Nishikida, K., Effective path length in attenuated total reflection spectroscopy. *Anal. Chem.* **2008,** *80*, 3045-3049.
10. Hollas, M. J., *Modern Spectroscopy*. 4th ed.; John Wiley & Sons Ltd: Chichester, England, 2004.
11. Sakellarios N., I.; Kazarian S., G., In Situ IR Spectroscopic Study of the CO_2- Induced Swelling of Ionic Liquid Media. In *Ionic Liquids III A:*

Fundamentals, Progress, Challenges, and Opportunities, American Chemical Society: 2005; Vol. 901, pp 89-101.
12. Kazarian, S. G.; Vincent, M. F.; Bright, F. V.; Liotta, C. L.; Eckert, C. A., Specific Intermolecular Interaction of Carbon Dioxide with Polymers. *J. Am. Chem. Soc.* **1996,** *118*, 1729-1736.
13. Sakellarios, N. I.; Kazarian, S. G., Solute partitioning between an ionic liquid and high-pressure CO_2 studied with in situ FTIR spectroscopy. *J. Chem. Thermodyn.* **2005,** *37*, 621-626.
14. Bara, J. E.; Gabriel, C. J.; Lessmann, S.; Carlisle, T. K.; Finotello, A.; Gin, D. L.; Noble, R. D., Enhanced CO_2 Separation Selectivity in Oligo(ethylene glycol) Functionalized Room-Temperature Ionic Liquids. *Ind. Eng. Chem. Res.* **2007,** *46*, 5380-5386.
15. Lethesh, K. C.; Van Hecke, K.; Van Meervelt, L.; Nockemann, P.; Kirchner, B.; Zahn, S.; Parac-Vogt, T. N.; Dehaen, W.; Binnemans, K., Nitrile-Functionalized Pyridinium, Pyrrolidinium, and Piperidinium Ionic Liquids. *J. Chem. Phys. B* **2011,** *115*, 8424-8438.
16. Hojniak, S. D.; Khan, A. L.; Holloczki, O.; Kirchner, B.; Vankelecom, I. F. J.; Dehaen, W.; Binnemans, K., Separation of Carbon Dioxide from Nitrogen or Methane by Supported Ionic Liquid Membranes (SILMs): Influence of the Cation Charge of the Ionic Liquid. *J. Chem. Phys. B* **2013,** *117*, 15131-15140.
17. Mahurin, S. M.; Hillesheim, P. C.; Yeary, J. S.; Jiang, D.; Dai, S., High CO_2 Solubility, Permeability and Selectivity in Ionic Liquids with Tetracyanoborate Anion. *RSC Advances* **2012,** *2*, 11813-11819.
18. Fei, Z.; Zhao, D.; Pieraccini, D.; Ang, W. H.; Geldbach, T. J.; Scopelliti, R.; Chiappe, C.; Dyson, P. J., Development of Nitrile-Functionalized Ionic Liquids for C−C Coupling Reactions: Implication of Carbene and Nanoparticle Catalysts. *Organometallics* **2007,** *26*, 1588-1598.
19. Breck, D. W., *Zeolite Molecular Sieves: Structure, Chemistry, and Use*. J. Wiley & Sons: New York, 1974.
20. Aki, S. N. V. K.; Mellein, B. R.; Saurer, E. M.; Brennecke, J. F., High-Pressure Phase Behavior of Carbon Dioxide with Imidazolium-Based Ionic Liquids. *J. Chem. Phys. B* **2004,** *108*, 20355-20365.
21. Andanson, J.-M.; Jutz, F.; Baiker, A., Supercritical CO_2/Ionic Liquid Systems: What Can We Extract from Infrared and Raman Spectra? *J. Chem. Phys. B* **2009,** *113*, 10249-10254.
22. Cichowska-Kopczyńska, I.; Joskowska, M., Dębski, B., Łuczak, J., ; Aranowski, R., Influence of Ionic Liquid Structure on Supported Ionic Liquid Membranes Effectiveness in Carbon Dioxide/Methane Separation. *J. Chem.* **2013,** *2013*, 10.
23. Hu, Y.-F.; Liu, Z.-C.; Xu, C.-M.; Zhang, X.-M., The molecular characteristics dominating the solubility of gases in ionic liquids. *Chem. Soc. Rev.* **2011,** *40*, 3802-3823.
24. Lin, H.; Freeman, B. D., Materials selection guidelines for membranes that remove CO_2 from gas mixtures. *J. Mol. Struct.* **2005,** *739*, 57-74.

25. Guadagno, T.; Kazarian, S. G., High-Pressure CO_2-Expanded Solvents: Simultaneous Measurement of CO_2 Sorption and Swelling of Liquid Polymers with in-Situ Near-IR Spectroscopy. *J. Chem. Phys. B* **2004,** *108*, 13995-13999.
26. Meredith, J. C.; Johnston, K. P.; Seminario, J. M.; Kazarian, S. G.; Eckert, C. A., Quantitative Equilibrium Constants between CO_2 and Lewis Bases from FTIR Spectroscopy. *J. Phys. Chem.* **1996,** *100*, 10837-10848.
27. Nalawade, S. P.; Picchioni, F.; Marsman, J. H.; Janssen, L. P. B. M., The FT-IR studies of the interactions of CO_2 and polymers having different chain groups. *J. Supercrit.Fluid* **2006,** *36*, 236-244.
28. Hollóczki, O.; Kelemen, Z.; Könczöl, L.; Szieberth, D.; Nyulászi, L.; Stark, A.; Kirchner, B., Significant Cation Effects in Carbon Dioxide–Ionic Liquid Systems. *ChemPhysChem* **2013,** *14*, 315-320.
29. Jamróz, M. H.; Dobrowolski, J. C.; Bajdor, K.; Borowiak, M. A., Ab initio study of the $\nu(CO_2)$ mode in EDA complexes. *J. Mol. Struct.* **1995,** *349*, 9-12.
30. Romanos, G. E.; Zubeir, L. F.; Likodimos, V.; Falaras, P.; Kroon, M. C.; Iliev, B.; Adamova, G.; Schubert, T. J. S., Enhanced CO_2 Capture in Binary Mixtures of 1-alkyl-3-methylimidazolium Tricyanomethanide Ionic Liquids with Water. *J. Chem. Phys. B* **2013,** *117*, 12234-12251.
31. Mahurin, S. M.; Lee, J. S.; Baker, G. A.; Luo, H.; Dai, S., Performance of nitrile-containing anions in task-specific ionic liquids for improved CO_2/N_2 separation. *J. Membr. Sci.* **2010,** *353*, 177-183.
32. Labropoulos, A. I.; Romanos, G. E.; Kouvelos, E.; Falaras, P.; Likodimos, V.; Francisco, M.; Kroon, M. C.; Iliev, B.; Adamova, G.; Schubert, T. J. S., Alkyl-methylimidazolium Tricyanomethanide Ionic Liquids under Extreme Confinement onto Nanoporous Ceramic Membranes. *J. Phys. Chem. C* **2013,** *117*, 10114-10127.
33. Kazarian, S. G.; Flichy, N. M. B.; Coombs, D.; Poulter, G., Potential of ATR-IR spectroscopy in applications to supercritical fluids and liquefied gases. *Am. Lab.* **2001,** *33*.
34. Hasell, T.; Armstrong, J. A.; Jelfs, K. E.; Tay, F. H.; Thomas, K. M.; Kazarian, S. G.; Cooper, A. I., High-pressure carbon dioxide uptake for porous organic cages: comparison of spectroscopic and manometric measurement techniques. *Chem. Commun.* **2013,** *49*, 9410-9412.
35. Silverwood, I. P.; Keyworth, C. W.; Brown, N. J.; Shaffer, M. S. P.; Williams, C. K.; Hellgardt, K.; Kelsall, G. H.; Kazarian, S. G., An Attenuated Total Reflection Fourier Transform Infrared (ATR FT-IR) Spectroscopic Study of Gas Adsorption on Colloidal Stearate-Capped ZnO Catalyst Substrate. *Appl. Spectrosc.* **2014,** *68*, 88-94.
36. Maiella, P. G.; Schoppelrei, J. W.; Brill, T. B., Spectroscopy of Hydrothermal Reactions. Part XI: Infrared Absorptivity of CO_2 and N_2O in Water at Elevated Temperature and Pressure. *Appl. Spectrosc.* **1999,** *53*, 351-355.
37. Huddleston, J. G.; Visser, A. E.; Reichert, W. M.; Willauer, H. D.; Broker, G. A.; Rogers, R. D., Characterization and comparison of hydrophilic

and hydrophobic room temperature ionic liquids incorporating the imidazolium cation. *Green Chem*. **2001,** *3*, 156-164.

6.

Metal-containing ILs for separation of CO_2 from N_2

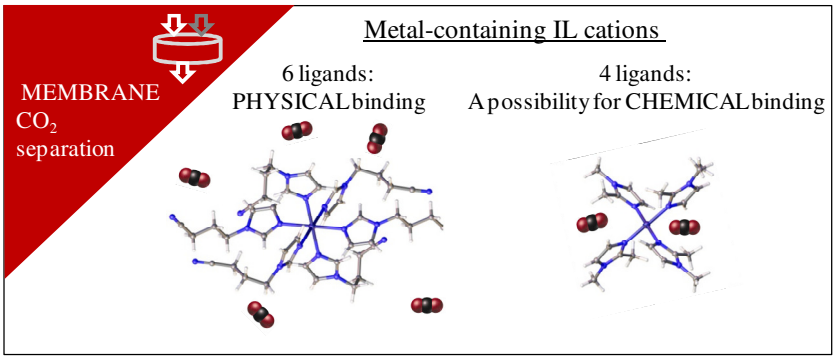

6.1. Introduction

6.1.1. Polymer-IL blend membranes

Supported ionic liquid membranes made of porous material impregnated with ILs, as well as films made of poly(ionic liquids) and free ILs bound in polymeric ILs, are promising in CO_2 separation. Nevertheless, they all suffer from the common problem of instability under industrially relevant pressures.[1-6] Additionally, preparation of these membranes often involves complex organic synthesis and polymerization techniques. A relatively new approach to incorporate ILs into membranes is by mere blending of a polymer solution with an IL to obtain IL-polymer blends. In such arrangement, the IL ions are trapped inside the polymer matrix rather than being held in the membrane pores and consequently the membranes prepared via this method are more resistant to pressure differences.[7] The method is not yet very popular, as shown by the small number of publications on this topic.[7-17] A disadvantage of such

membranes is their low permeability and therefore the necessity to perform gas separations at higher temperatures (35-200 °C).[17] The dissolution of CO_2 in a polymer blend membrane can be achieved by either a physical or a chemical interaction with the ILs, with the former being less efficient but easily reversible, and the latter being more selective but often suffering from too slow desorption kinetics.[18]

6.1.2. Metal-based CO_2 absorption and separation

In the search for alternative CO_2-absorbing materials, transition metal compounds in combination with ILs have been explored.

The initial inspiration came from nature: A zinc-containing enzyme, carbonic anhydrase, catalyses the reversible hydration of CO_2 to form bicarbonate ions (HCO_3^-). The Zn^{2+} ion is coordinated to three imidazole rings of histidine residues and to one water molecule. Due to the coordination to the metal ion, the O-H bond of the water molecule becomes polarized. It enables proton abstraction and appearance of a hydroxide ion, which reacts with CO_2 forming HCO_3^- ions. On a microgram scale, carbonic anhydrase has been successfully employed in CO_2 sequestration where it acted as a catalyst for calcium carbonate formation.[19] Carbonic anhydrase, however, has two major limitations: the enzyme is active in a relatively narrow temperature range (4-30 °C) and only above pH 7.[20,21] Bhaduri and Siller discovered that nickel nanoparticles are able to catalyse CO_2 hydration on the basis of an analogous mechanism, but independently of the pH.[22]

Liu *et al.* examined the absorption of CO_2 in a mixture of the ionic liquid 1-ethyl-3-methylimidazolium bis(trifluoromethyl-sulfonyl)imide, [C_2mim][Tf_2N], and zinc(II) bis(trifluoromethyl-sulfonyl)imide salt, Zn($Tf_2N)_2$, in the molar ratio 1:1.[23] The addition of the zinc(II) salt resulted in formation of bonds between the zinc(II) centre and CO_2 molecules. This increased the gas solubility more than twenty times, as compared with the pure [C_2mim][Tf_2N].

Rather than dissolving a metal salt in an IL, it is also possible to design metal-containing ILs. The metal can be a part of either the cation or the anion of the ionic liquid, or both.[24-28] [29-32] Metal-containing ILs with the metal centre as part of the cation (so-called *liquid metal salts*) have been successfully used for high-rate electrodeposition.[33-35]

Albo *et al.* studied separation of carbon dioxide from nitrogen and air with SILMs made of polymeric supports impregnated with phosphonium ionic liquids where a metal ion was a part of an anion: $[P_{66614}]_2[CoCl_4]$, $[P_{66614}][FeCl_4]$, $[P_{66614}]_2[MnCl_4]$ and $[P_{66614}]_3[GdCl_6]$. The SILM containing the manganese(II) compound showed the highest selectivity.

Metallic copper nanoparticles dispersed in $[C_6mim][NO_3]$ were used by Lee *et al.*, to separate CO_2 from N_2 and CH_4 by polysulfone membranes.[36] The increased separation selectivity in comparison with the pure IL system was attributed to the facilitated transport of CO_2, due to the reversible interaction of the partially positively charged nanoparticles with the gas molecules. Zarca *et al.* prepared PVDF SILMs impregnated with a solution of $[C_6mim][NO_3]$ and copper(I) chloride for separation of carbon monoxide from nitrogen.[37] The high selectivity was a result of the formation of a π-complex between carbon monoxide and the anion $[CuCl_3]^{2-}$ in a reversible reaction, to give $[(Cu(CO)Cl)]_3^{2-}$.

In this chapter we evaluated the performance of polymer-IL blend membranes prepared with novel ILs containing metal-based complex cations in CO_2/N_2 separation.

6.2. Results and discussion

The design of the ILs presented in this chapter has been based on two different approaches. In the first approach, hexacoordinate complexes, able to bind CO_2 solely on the physical basis, were explored. In the second approach, tetra- and pentacoordinate complexes with a

coordination vacancy were studied as potential direct (chemical) CO_2-binding agents.

6.2.1. Approach 1: Hexacoordinated ILs – physical CO_2 binding

The hexacoordinate metal-containing ionic liquids were composed nickel (II)-, zinc (II)- or manganese (II)-containing cations with functionalised imidazole ligands and bis(trifluoromethylsulfonyl)imide anions (Figures 6.1, 6.2 and Table 6.1). In this approach, the metal ion served as a scaffold to accommodate six CO_2-philic imidazole moieties (ligands) per mole of the salt, in contrast with one mole of imidazolium moieties present for example in a $C_n$mim IL.

The CO_2 molecules can interact with the functionalised imidazole rings and the anions only in a non-covalent way. Therefore, the gas dissolution in these ILs is a physical process.

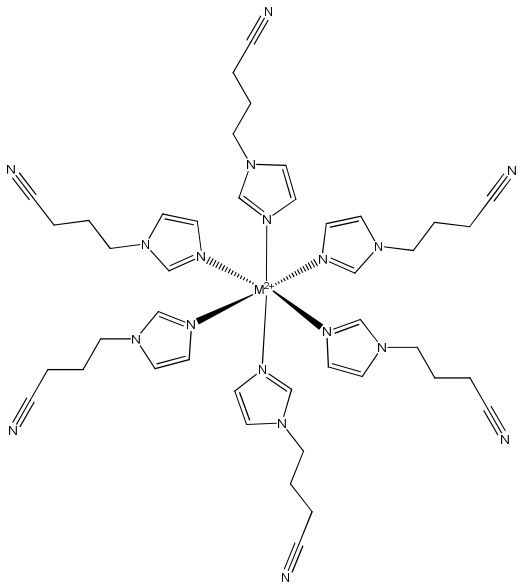

Figure 6.1: Schematic representation of the structure of the metal salt cation containing only nitrile substituents on imidazole ligands.

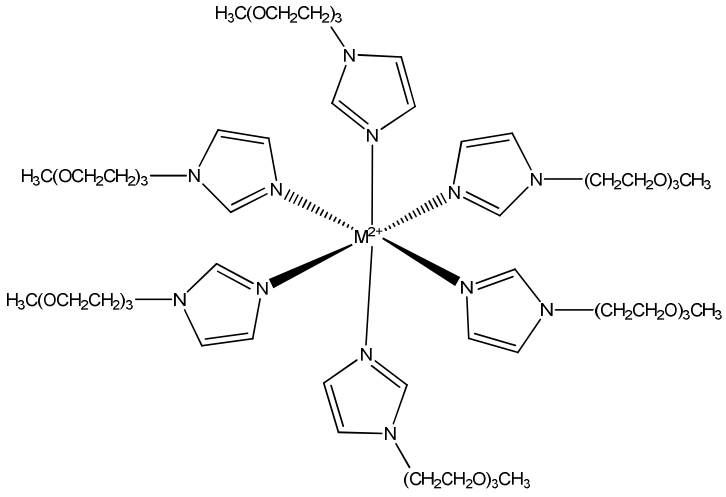

Figure 6.2: Schematic representation of the structure of the metal salt cation containing only glycol substituents on imidazole ligands.

Cations with three different divalent metal ions were prepared, each of them containing a glycol or a nitrile-functionalized imidazole or their combinations (Table 6.1).

The cations containing three and six glycol-functionalized imidazoles were liquid below room temperature. There was a large difference in the melting points between the $[M(C_3CNIm)_6][Tf_2N]_2$ ILs, even though structures of these ILs are isomorphous (Section 6.2.3). **$[Ni(C_3CNIm)_6][Tf_2N]_2$** melts at 82 °C, **$[Zn(C_3CNIm)_6][Tf_2N]_2$** at 44 °C and **$[Mn(C_3CNIm)_6]$ $[Tf_2N]_2$** at 74°C. The much lower melting points for zinc salts has been already observed in alkylimidazole metals salts and were believed to be caused by the gradual dissociation of two ligands in the zinc(II) complexes that did not occur for nickel(II) complexes.[38-39]

Table 6.1: Melting point and glass transition temperature of the metal-containing ILs presented in this work. TEG: tri(ethylene glycol); dmIm: 1,2-dimethylimidazole.

Ionic liquid	Melting point (°C)	Glass transition temp. (°C)
$[Ni(C_3CNIm)_6][Tf_2N]_2$	82	-
$[Ni(C_3CNIm)_3(TEGIm)_3][Tf_2N]_2$	-	-37
$[Ni(TEGIm)_6][Tf_2N]_2$	-	-54
$[Zn(C_3CNIm)_6][Tf_2N]_2$	44	-
$[Zn(C_3CNIm)_3(TEGIm)_3][Tf_2N]_2$	-	-49
$[Zn(TEGIm)_6][Tf_2N]_2$	-	-56
$[Mn(C_3CNIm)_6][Tf_2N]_2$	74	-
$[Ni(dmIm)_4][Tf_2N]_2$	120	-
$[Ni(dmIm)_5][Tf_2N]_2$	89	-

The imidazole ligands and bis(trifluoromethylsulfonyl)imide anions were selected because they effectively contribute to the increased performance in gas separation application.[18,40-44] Moreover, free *N*-functionalised imidazoles can also be used as media for physical CO_2 absorption and separation, often out-performing similarly functionalised imidazolium ILs.[45,46] The choice of imidazole functionalisation was suggested by the high CO_2 separation efficiency of imidazolium ILs containing tri(ethylene glycol) chain,[41,47] a nitrile group[48] or both these moieties at once.[49]

Membrane preparation and measurements were done by doctoral student Lu Soon Chien from the group of Prof. Ivo Vankelecom, COK, KU Leuven. The membranes were made of the amorphous polysulfone polymer (PSf, Fig. 6.3) containing 10 wt. % of the ILs. PSf membranes

are among the most popular polymeric membranes reported in the literature, because they provide good permeabilities and selectivities in gas separation, along with high thermal, chemical and plasticization resistance.[50]

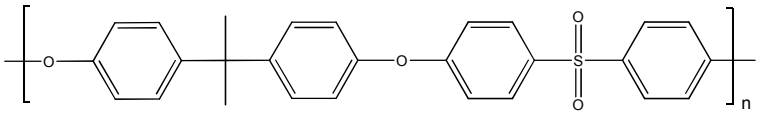

Figure 6.3: Chemical structure of Udel® P-1835 polysulfone used in membrane preparations.

The membranes prepared with this method, although visually uniform, may contain micro-defects or areas with uneven distribution of the IL in the polymer that can significantly decrease gas separation performance. Therefore, at least two different fragments of the membrane were tested for each IL-PSf blend (except for ILs $[Zn(C_3CNIm)_6][Tf_2N]_2$ and $[Zn(C_3CNIm)_3(TEGIm)_3][Tf_2N]_2$). For each blend membrane, the highest selectivity value was chosen for interpretation, as it corresponds to the most defect-free membrane. Table 6.2 gives an overview of the selectivities and permeances for CO_2/N_2 (50:50 vol. %) separation at 35 °C.

Table 6.2: Performance of PSf membranes blended with 10 wt. % IL

Membrane	Selectivity	CO_2 Permeance (GPU*10^{-3})	N_2 Permeance (GPU*10^{-3})
Pure PSf	25.1	14.3	0.566
	26.0	11.5	0.435
$[Ni(TEGIm)_6][Tf_2N]_2$	24.1	11.4	0.477
	20.2	11.3	0.572
	27.5	11.5	0.417
$[Ni(C_3CNIm)_3(TEGIm)_3][Tf_2N]_2$	30.7	14.4	0.469

$[Ni(C_3CNIm)_6][Tf_2N]$	18.7	14.2	0.745
	30.1	14.4	0.477
	25.2	14.3	0.566
	27.9	11.5	0.417
$[Zn(C_3CNIm)_6][Tf_2N]_2$	27.1	17.3	0.626
$[Zn(C_3CNIm)_3(TEGIm)_3][Tf_2N]_2$	20.6	11.4	0.56
$[Zn(TEGIm)_6][Tf_2N]_2$	23.5	11.4	0.489
	27.7	11.5	0.417
$[Mn(C_3CNIm)_6][Tf_2N]_2$	20.2	14.2	0.715
	28.7	11.5	0.405
$[Ni(dmIm)_4][Tf_2N]_2$	28.3	14.4	0.507
	29.3	14.4	0.492
	26.8	11.5	0.429
$[Ni(dmIm)_5][Tf_2N]_2$	26.3	11.5	0.435
	27.5	14.4	0.522
	23.9	14.3	0.596

The selectivity of the pure PSf membrane was 25.1-26.0, while the literature values are between 22.4 and 24.5,[51] which confirms the quality of the experimental data and indicates the experimental error of approximately 2 units of selectivity. The selectivities for blend membranes lower than the selectivity of the pure polymer (such as α = 20), were caused by the abovementioned imperfections.

Among nickel(II)-containing salts, **$[Ni(C_3CNIm)_3(TEGIm)_3][Tf_2N]_2$** of mixed functionalisation and the nitrile-functionalised **$[Ni(CNIm)_6][Tf_2N]_2$** showed the highest selectivity of 32 and 30, respectively (Table 6.2). The glycol-functionalised **$[Ni(TEGIm)_6][Tf_2N]_2$** exhibited similar but slightly lower selectivity of 28, suggesting that the glycol chain functionalisation may be less favorable than nitrile functionalisation in nickel(II)-containing ILs. Among zinc(II)-containing ILs, the highest selectivity was obtained for

the glycol-functionalised IL **[Zn(TEGIm)$_6$][Tf$_2$N]$_2$** and the nitrile-functionalised IL **[Zn(C$_3$CNIm)$_6$][Tf$_2$N]$_2$**. The structure-selectivity relationship for zinc salts was thus different than for the nickel(II) salts, although the difference may be attributed to the quality of the membrane pieces chosen for the measurement rather than to the actual performance of the ILs. Due to the lack of data for the mixed-ligand Zn IL, no further conclusions can be drawn here. The manganese(II)-containing IL, **[Mn(C$_3$CNIm)$_6$][Tf$_2$N]$_2$** showed selectivity of 29, that is, higher than Zn-containing ILs.

Although nickel(II) ILs appear to be more efficient for separation of CO_2 from N_2 than zinc(II) or manganese(II) ILs, it should be noted that they are also more toxic. Zinc(II) and manganese(II) compounds show toxic effects only after exposure to elevated concentrations of these salts or on accumulation by repeated exposure, while nickel(II) complex are always harmful (toxic to internal organs and carcinogenic).[52,53]

6.2.2. Approach 2: Tetra- and pentacoordinate ILs – a possibility for chemical CO_2 binding

In the second approach, the possibility of a direct interaction of metallic center with CO_2 was explored by designing nickel (II) ILs containing complex cations with a coordination vacancy, that is, tetra- and pentacoordinate complex cations.

CO_2 molecules can coordinate to metallic centres via oxygen atoms and/or carbon atoms.[54] Metal complexes with a coordination vacancy or an easily displaced ligand bind CO_2 in a variety of geometries, two of which are shown in Fig 6.4. Many of these complexes, especially where the binding occurs via the oxygen atom, are unstable and their isolation requires a strictly inert atmosphere.[54] The instability of these complexes can favour fast desorption of CO_2 necessary for a smooth operation of a membrane.

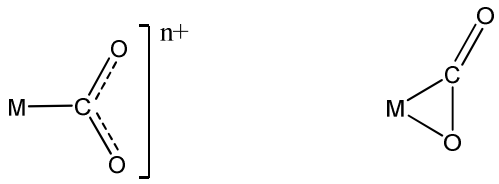

η_1–CO_2 η_2–CO_2

Figure 6.4: Examples of possible complexes of CO_2 with transition metals.[54-55]

In theory, when less than six coordination places are occupied by ligands, the remaining sites could be available for CO_2 molecules. Two gas molecules could interact with a square planar complex – one from above and one from below its plane, whilst one gas molecule could be attached to a metal ion in a pentacoordinated complex.

Obtaining a stable square planar nickel complex was not straightforward. For example, mixing four equivalents of N-alkylimidazole ligand with one equivalent of $Ni(Tf_2N)_2$ salt, yielded a blue complex. The colour suggested hexacoordination, indicating that the two remaining coordination sites were occupied by other molecules, for example solvent (ethanol) or water molecules. In order to hinder the formation of the 1:6 complexes, a more bulky ligand, 1,2-dimethylimidazole, was chosen. Mixing this ligand with $Ni(Tf_2N)_2$ in 4:1 ratio yielded orange **$[Ni(dmIm)_4][Tf_2N]_2$** (Fig. 6.5), that did not change colour in air or in ethanol, as the steric hindrance caused by the adjacent methyl groups obstructed binding of the solvent molecules. Crystal structure studies confirm that **$[Ni(dmIm)_4]$ $[Tf_2N]_2$** exhibited square planar geometry (Section 6.2.3).

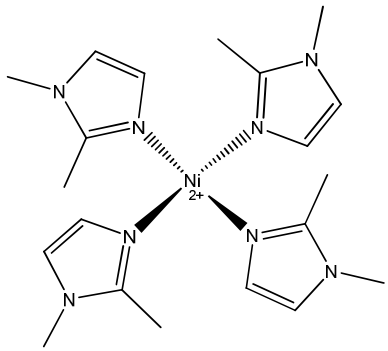

Figure 6.5: Structure of the tetracoordinated complex cation, $[Ni(dmIm)_4][Tf_2N]_2$.

The selectivity of the membranes containing **$[Ni(dmIm)_4][Tf_2N]_2$** was 29, thus slightly lower than for some of the hexacoordinate ILs. The lower performance can be caused by the following probable reasons: i) The complex does not bind CO_2 due to steric hindrance; ii) The complex binds CO_2 irreversibly and becomes saturated in the first stage of the measurement thereby making the membrane at equilibrium separate CO_2 merely on the physical basis; iii) The tetracoordinate complex has less moieties able to interact with CO_2 and this is the reason for its lower performance.

In order to determine the impact of the possible metal-CO_2 interactions on the membrane performance, UV-VIS-NIR absorption spectra of the PSf membrane containing **$[Ni(dmIm)_4][Tf_2N]_2$** with and without CO_2 were obtained with the help of Roman Matthessen and Pieter Vanelderen, both from COK, KU Leuven.

Due to the significant opacity of the membrane, the diffuse reflectance spectroscope was used instead of the classical transmission instrument. A membrane was degassed in the oven at 60 °C for 15 min, submitted to 5 bar of CO_2 (99.7% purity) for 3 min and then placed in the spectrophotometer at atmospheric pressure. The spectra of the membranes before and after exposure to the gas (Fig 6.6) showed no significant differences (peak shift or intensity change), indicating no

permanent gas binding that could affect membrane permeability of this gas.

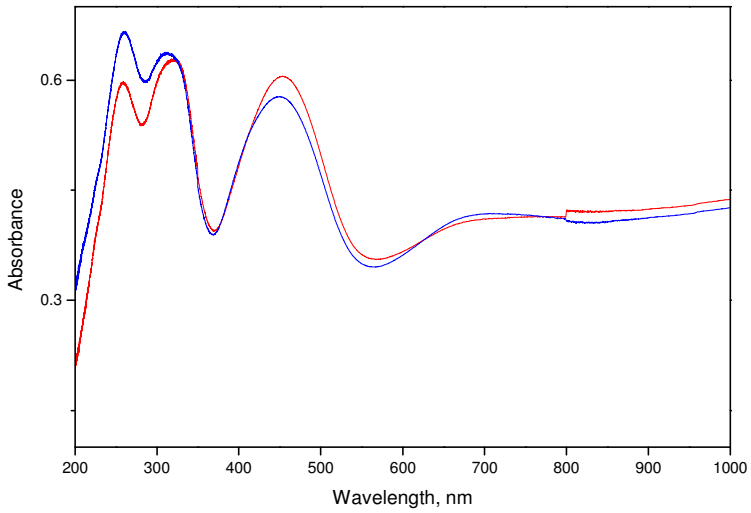

Figure 6.6: UV-VIS-NIR absorption spectrum of the PSf membrane containing $[Ni(dmIm)_4][Tf_2N]_2$ without CO_2 (red) and with CO_2 (blue).

Possible, weak CO_2-IL interactions were observed in the ^1H NMR spectra. Square planar nickel complexes are usually diamagnetic and give rise to narrow peaks in NMR. On the other hand, hexacoordinate (octahedral) and pentacoordinate nickel complexes are generally paramagnetic.[56] ^1H NMR spectra of the square planar $[Ni(dmIm)_4][Tf_2N]_2$ complex in a non-coordinating solvent, namely, dichloromethane-d_2, were taken with and without CO_2. Some peak broadening was observed in the spectrum of the pure IL (Fig. 6.7), which was most probably caused by the small quantity of paramagnetic impurities present in the sample and undetected by the characterization methods. The ^1H spectrum recorded after flushing the sample with CO_2 showed much more of the paramagnetic character, as indicated by the significantly broaden peaks.

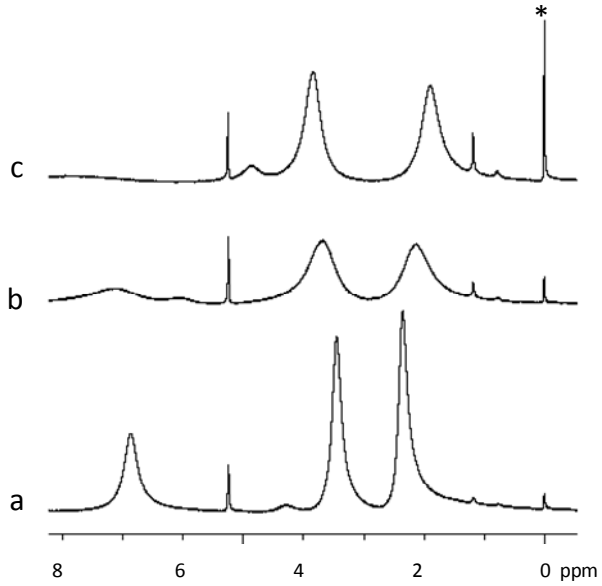

Figure 6.7: ^{1}H NMR spectrum of $[Ni(dmIm)_4][Tf_2N]_2$ in dichloromethane-d_2 before (a), and after flushing the solution with CO_2 (b), and after partial CO_2 desorption (c). (*) Indicates the silicone grease impurity from the CO_2 tubing.

In order to check if the line broadening was caused by the increase of paramagnetism of the sample on gas binding, rather than by the occurrence of paramagnetic impurities, a spectrum was taken after evaporating CO_2 from the sample. The spectrum after CO_2 desorption has recovered some of its previous character as the line broadening was significantly smaller, although the conversion was not complete. Possible presence of acidic impurities formed due to the traces of water in the system could also influence the spectra.

^{13}C NMR study of the IL-CO_2 system did not reveal any changes that could indicate CO_2 binding (Fig 6.8). Although after gas introduction the peak of $^{13}CO_2$ appeared at 125 ppm, the position of the peak in pure CD_2Cl_2 +CO_2 was the same, suggesting no change of the electronic environment for the carbon atoms in the IL and hence no strong binding.

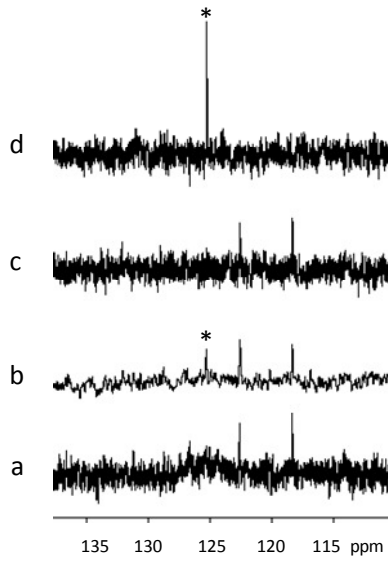

Figure 6.8: ^{13}C NMR spectrum of $[Ni(dmIm)_4][Tf_2N]_2$ in dichloromethane-d_2 before flushing the solution with carbon dioxide (a), after flushing (b), and after CO_2 desorption (c). Spectrum (d) corresponds to pure CD_2Cl_2 with CO_2. The stars indicate the $^{13}CO_2$ peak.

The UV-VIS-NIR and the NMR spectra showed that possible CO_2 binding is too weak to be the reason for the lower performance of the tetracoordinate IL. Therefore, permanent CO_2 binding or non-existent binding cannot be the reasons for the lower performance of this tetracoordinate IL in comparison with the hexacoordinate ILs.

In order to determine how the number of physically interacting ligands influences the membrane performance, we tried to prepare an IL with six 1,2- dimethylimidazole ligands. Due to the steric reasons, a hexacoordinate complex did not form and instead a pentacoordinate complex with one free ligand was obtained. Therefore, in the next step, $Ni(Tf_2N)_2$ was mixed with only five equivalents of the ligand to yield emerald green **$[Ni(dmIm)_5][Tf_2N]_2$** (Fig 6.9).

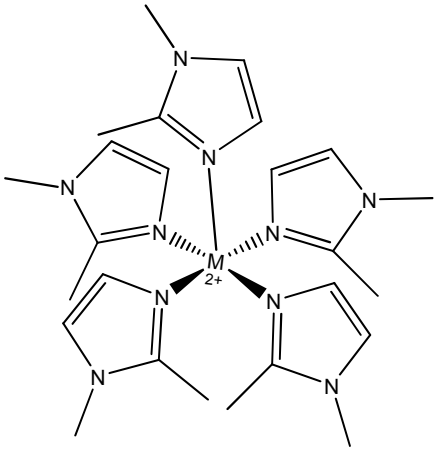

Figure 6.9: Structure of the pentacoordinate complex cation, $[Ni(dmIm)_5][Tf_2N]_2$.

The selectivity of this IL was slightly lower than that of the square planar $[Ni(dmIm)_4][Tf_2N]_2$ (28 vs. 29, respectively). One would assume that in the absence of strong chemical binding, the presence of an additional ligand will significantly increase the performance by providing an additional site for the interaction with CO_2. It is possible that the value lower by 1 unit is still within the limits of the experimental error. In either case, the lower performance of the ILs with a coordination vacancy (in comparison with the hexacoordinate ILs), is, in the absence of sufficient CO_2 binding, most probably caused by the smaller number of ligands in these complexes and therefore a smaller number of sites available for interaction with CO_2.

The obtained membranes gave moderate selectivities of up to 32. What is surprising, however, is the small difference of the selectivities provided by the blend membranes and the pure PSf membrane. The presence of the imidazole moieties and Tf_2N anions should alone provide good separation selectivities, and yet, the influence of these groups on the performance seems to be very small.[46,57]

The reason for the low performance could be however macroscopic, being the insufficient compatibility of the ILs and the PSf

(see: DSC method, section 6.4). Low compatibility means in practice that the IL, instead of blending in, forms "droplets" in the polymer matrix. This in turn means, that the area effectively covered by the specialized CO_2-separating medium (the IL) is very small in comparison with the area provided by the pure PSf, providing explanation for similar to the selecitivity of pure PSf and IL-polymer blends.

This issue should be addressed in further studies, by increasing the content of the IL or by choosing another polymer type for the blends.

An attempt has been made to measure the performance of the ILs spread on a porous support that does not contribute to gas separation. Such data would give an answer to the question of the absolute performance of these ILs. Unfortunately, the experiment did not succeed, as the gas pressure pushed the ILs out from the pores.

6.2.3. Crystal structures

The crystal structure determination experiments and data refinement were performed by dr. Neil Brooks from the group of Prof. Koen Binnemans (KU Leuven). For the ILs used in the first approach, crystals of **$[Ni(C_3CNIm)_6][Tf_2N]_2$** and **$[Zn(C_3CNIm)_6][Tf_2N]_2$** were grown from the melt after solvent evaporation in vacuum. Cooling of the products with solid carbon dioxide for 15 min induced the crystallization process. Crystals of **$[Mn(C_3CNIm)_6][Tf_2N]_2$** could be obtained by recrystallisation from ethanol. The structures of the three complexes were determined by X-ray crystallography and were found to be isomorphous with each other. Due to this similarity, only the crystal structure of **$[Mn(C_3CNIm)_6][Tf_2N]_2$** is shown in Figure 6.10.

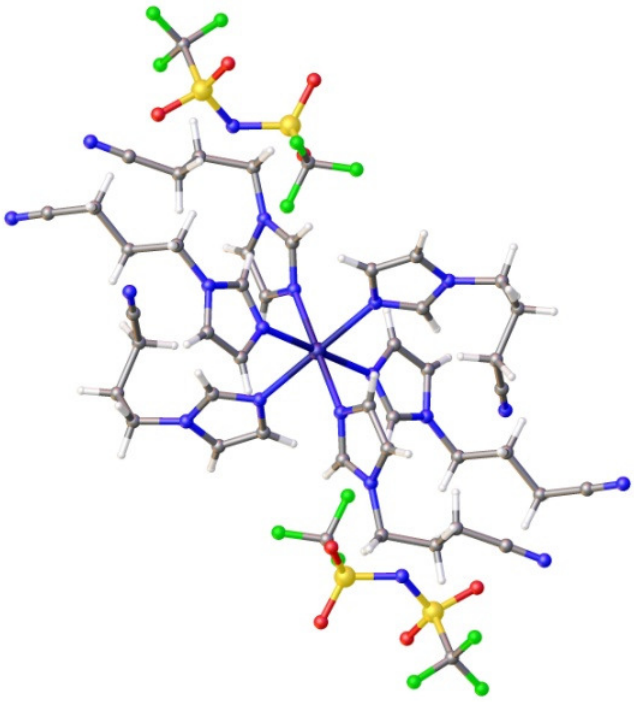

Figure 6.10: Crystal structure of $[Mn(C_3CNIm)_6][Tf_2N]_2$.

In the asymmetric unit there is half of one crystallographic octahedral M^{2+} centre, three C_3CNIm ligands and one Tf_2N anion. Two of the ligands have the substituent alkyl chains arranged in a staggered conformation, whereas the other ligand has a kink in the chain between the second and third carbon atom. In the nickel(II) and zinc(II) complexes, the Tf_2N anion and one of the alkyl chains are rotationally disordered. In the manganese(II) complex, no disorder was observed. The metal-nitrogen bond distances increase in the order Mn > Zn > Ni, which reflects the larger ionic radius of Mn^{2+} compared to that of Zn^{2+} and Ni^{2+} (Table 6.3).

Table 6.3: Selected bond lengths and angles in the crystal structures of $[Ni(C_3CNIm)_6][Tf_2N]_2$, $[Zn(C_3CNIm)_6][Tf_2N]_2$ and $[Mn(C_3CNIm)_6]$ $[Tf_2N]_2$.

	M–N/Å	N–M–N/°
$[Ni(C_3CNIm)_6][Tf_2N]_2$	2.136(3)	*cis*: 89.97(12),
	2.127(3)	88.62(12), 89.81(12)
	2.121(3)	*trans*: 180.0
$[Zn(C_3CNIm)_6][Tf_2N]_2$	2.1830(11)	*cis*: 89.69(4), 90.28(4),
	2.1697(11)	88.67(4)
	2.1997(11)	*trans*: 180.0
$[Mn(C_3CNIm)_6][Tf_2N]_2$	2.2666(11)	*cis*: 90.58(4), 89.86(4),
	2.2791(11)	88.80(4)
	2.2848(11)	*trans*: 180.0

Since the ionic radius of high-spin Mn(II) is 0.83 Å and only 0.67 Å for low-spin Mn(II), the Mn–N bond lengths suggest high-spin electron configuration ($t_{2g}^3e_g^2$).[58,59] The ionic radii for Zn(II) and Ni(II) are 0.74 Å and 0.69 Å, respectively.[59] The packing diagram shows $[Mn(C_3CNIm)_6]^{2+}$ cations stacked in the crystallographic *b* direction with the anions filling the spaces in between the cations (see: Experimental, Fig. 6.13). Since the structures of **$[Ni(C_3CNIm)_6][Tf_2N]_2$** and **$[Zn(C_3CNIm)_6]$ $[Tf_2N]_2$** are isomorphous, the packing is the same. Weak C–H···O/F interactions were observed between the anion and the alkyl substituents, which ranged in the manganese complex from 2.525 Å to 2.567 Å. Additionally, weak C–H···N interactions involving the hydrogen atoms of the alkyl chains and the nitrile nitrogen atoms of the neighboring ligands were found, which range from 2.553 Å to 2.593 Å. Due to the disorder in the nickel(II) and zinc(II) structures no reliable hydrogen bonding information can be obtained.

The crystals for the **$[Ni(dmIm)_4][Tf_2N]_2$** and **$[Ni(dmIm)_5][Tf_2N]_2$** were grown from the melt after solvent

evaporation in vacuum. Cooling of the products with solid carbon dioxide for 15 min was required for crystallization to begin. In the **[Ni(dmIm)$_4$][Tf$_2$N]$_2$** complex, the Ni^{2+} ion is coordinated by four dmIm ligands in a square-planar geometry. In the asymmetric unit, there is half of one crystallographic square M^{2+} centre, two dmIm ligands and one Tf_2N anion. The Tf_2N anion and one of the ligands are disordered.

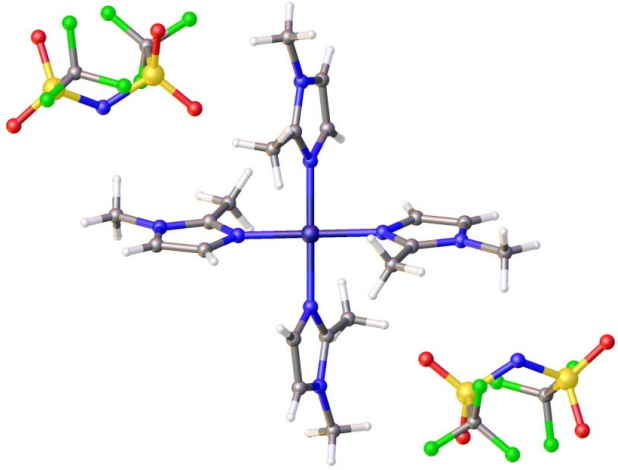

Figure 6.11: View of the structure of $[Ni(dmIm)_4][Tf_2N]_2$ (disorder omitted for clarity).

The metal-nitrogen distances and N–Ni–N angles are listed in Table 6.4.

Table 6.4: Selected bond lengths and angles in the crystal structures of $[Ni(dmIm)_4][Tf_2N]_2$ and $[Ni(dmIm)_5][Tf_2N]_2$

	Ni–N/Å	N–Ni–N/°
$[Ni(dmIm)_4][Tf_2N]_2$	1.906(3) 1.900(3) 1.897(14) 1.897(13)	*cis*:, 91.24(11), 91.23(11), 88.76(11), 95.5(5), 84.5(5), *trans*: 180.0, 179.998(1)
$[Ni(dmIm)_5][Tf_2N]_2$	2.077(2) 2.089(2) 2.084(2) 2.076(2) 2.038(2)	86.28(9), 89.70(9), 89.70(9), 88.26(9), 89.13(9), 98.86(9), 97.05(9), 100.07(9), 103.11(9), 160.99(9), 159.70(9)

In the asymmetric unit of the **$[Ni(dmIm)_5][Tf_2N]_2$** complex**,** there is one crystallographic M^{2+} pentacoordinate centre and two Tf_2N^- anions. There is no disorder present in the ligands, however, the anions are disordered just like in the case of **$[Ni(dmIm)_4][Tf_2N]_2$**.

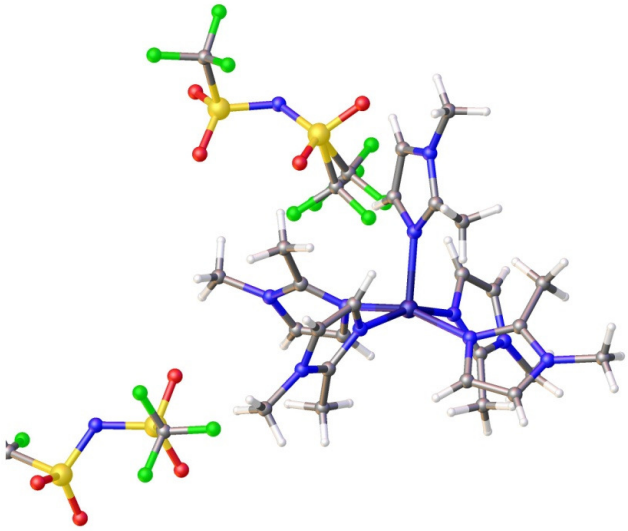

Figure 6.12: View of the structure of $[Ni(dmIm)_5][Tf_2N]_2$ (disorder on the anions omitted for clarity).

The geometry of the cation of **[Ni(dmIm)$_5$][Tf$_2$N]$_2$** lies in between the square-pyramidal and trigonal-bipyramidal. An ideal square-pyramid has angles of 90° between the neighboring equatorial ligands and 90° between any equatorial ligand and the axial ligand, whereas in trigonal bipyramid angles between the neighbouring equatorial ligands measure 120° and the angles between any equatorial ligand and any axial ligand measure 90°. Addison *at al.* systematized such distorted geometries by using a structural index parameter τ that defines the degree of trigonality in five coordinated systems on the basis of the angles present in the structure.[60] For an ideally trigonal structure τ = 1 and for a tetragonal structure τ = 0. In the case of **[Ni(dmIm)$_5$][Tf$_2$N]$_2$**, τ = 0.02 indicating that the geometry of the complex is a distorted square pyramid. The steric hindrance created by the methyl group in the 2-position of imidazole ligands prevents the ligands from lying in the same plane.

6.3. Conclusions

The polymer-IL blend membranes, incorporation metal-containing ILs with imidazole ligands were prepared and evaluated in CO_2/N_2 separation. Two different approaches were tested. In the first approach, Ni^{2+}, Zn^{2+} or Mn^{2+} ions served as scaffolds to accommodate six imidazole ligands in one mole of the IL. The influence of the metallic centre and the ligand functionalization were studied. The membranes prepared with nickel complexes exhibited the highest selectivities, while the nitrile functionalisation was the most beneficial. In the second approach, tetra- and pentacoordinate complexes were prepared. They were supposed to dissolve CO_2 on the basis of both physical and chemical absorption, nevertheless, they turned out to be less efficient, probably due to insufficient number of ligands and small influence of weak CO_2 binding on the performance.

A common problem associated with the use of highly functionalised ILs is the elaborate synthesis and difficult purification leading to low yields. The presented here metal-containing IL systems are a promising alternative to the SILMs and metal-free ILs, especially due to the ease of synthesis, purification and upscaling. The use of the metal ion as a scaffold enables compiling an IL from different ligands, tremendously increasing the tuneability factor.

6.4. Experimental

6.4.1. Materials and instruments

Hydrogen bis(trifluoromethylsulfonyl)imide (80 wt.%) was obtained from Iolitec (Heilbronn, Germany) and the remaining chemicals were purchased from Acros Organics (Geel, Belgium) or from Sigma-Aldrich (Diegem, Belgium). The Polysulfone (PSf) Udel P-1835 in powder form was obtained from Solvay (Belgium). All chemicals were used as received, without further purification. Differential scanning calorimetry (DSC) measurements were performed on a Mettler-Toledo DSC822e module, at a scan rate of 10 °C min^{-1} in a helium atmosphere. Elemental analyses (CHN) were carried out using a CE Instruments EA-1110 elemental analyser. The IR spectra were recorded in attenuated total reflectance mode on a Bruker Vertex70 FTIR spectrometer at a resolution of 4 cm^{-1}. Diffuse reflection measurements were obtained using an Agilent Cary 5000 spectrophotometer.

6.4.2. Syntheses

The starting metal salts, $[Ni(H_2O)_6][Tf_2N]_2 \cdot 2H_2O$, $[Zn(H_2O)_6][Tf_2N]_2 \cdot 2H_2O$, $[Mn(H_2O)_6][Tf_2N]_2 \cdot 2H_2O$ and the glycol- and nitrile-functionalised imidazoles were prepared according to literature procedures.[38,61] The syntheses of glycol- [41] and nitrile-functionalized imidazoles[49] were described earlier.

General method for the synthesis of the nickel(II) and zinc(II) complexes

The starting metal salt was dissolved in 10 to 20 mL of absolute ethanol with stirring. Six equivalents of the ligand, dissolved in 10 to 20 mL of ethanol, were added to this solution and the mixture was stirred for 10 min (the synthesis of the N-substituted imidazoles used for was described earlier [49]. Evaporation of the solvent and water gave liquid or solid product which was dried in vacuum at room temperature for at least 24 h. When two different ligands were used, they were first mixed together in 10 mL of ethanol and only then added to an ethanol solution of the metal salt.

$[Ni(C_3CNIm)_6][Tf_2N]_2$

1-(3-cyanopropyl)imidazole (2.0 g, 14.8 mmol) and $[Ni(H_2O)_6][Tf_2N]\cdot 2H_2O$ (1.88 g, 2.46 mmol) gave a dark blue viscous liquid in a quantitative yield. Melting point: 82°C. CHN [%] (calculated): C: 38.87 (38.64), H: 3.95 (3.81), N: 19.26 (19.59). IR (ATR, cm^{-1}): 3136, 2951, 2889, 2249, 1519, 1450, 1427, 1349, 1292, 1228, 1182, 1135, 1107, 1090, 1054, 966, 938, 832, 788, 739, 665, 614, 600, 570, 510, 406.

$[Ni(TEG)_3(C_3CNIm)_3][Tf_2N]_2$

1-(3-cyanopropyl)imidazole (1.33g, 9.83mmol) and 1-[2-[2-(2-methoxyethoxy)ethoxy]ethyl]imidazole (2.11g, 9.83mmol) and $[Ni(H_2O)_6][Tf_2N]\cdot 2H_2O$ (2.5g, 3.28mmol) gave a dark blue complex in a quantitative yield. Glass transition temperature: -37 °C. CHN [%] (calculated): C: 39.13 (39.96), H: 4.90 (4.94), N: 14.06 (13.56). IR (ATR, cm^{-1}): 3135, 2937, 2879, 2249, 1519, 1450, 1350, 1332, 1290, 1228, 1182, 1134, 1106, 1090, 1055, 938, 831, 788, 761, 740, 665, 614, 600, 570, 511, 406.

$[Ni(TEG)_6][Tf_2N]_2$

1-[2-[2-(2-methoxyethoxy)ethoxy]ethyl]-1*H*-Imidazole (1.94 g, 9.05 mmol) and $[Ni(H_2O)_6][Tf_2N]\cdot 2H_2O$ (1.15 g, 1.51 mmol) gave a dark blue complex in a quantitative yield. Glass transition temperature: -54 °C. CHN [%] (calculated): C: 39.93 (40.36), H: 6.03 (5.72), N: 10.07 (10.30). IR (ATR, cm^{-1}): 3132, 2875, 1517, 1450, 1351, 1333, 1288, 1229, 1184, 1133, 1105, 1066, 937, 830, 787, 760, 739, 665, 570, 512, 404.

$[Zn(C_3CNIm)_6][Tf_2N]_2$

1-(3-cyanopropyl)imidazole (1.39 g, 10.3 mmol) and $[Zn(H_2O)_6][Tf_2N]\cdot 2H_2O$ (1.32 g, 1.71 mmol) gave a slightly yellow, transparent crystalline product in a quantitative yield. Melting point: 44°C. CHN [%] (calculated): C: 38.20 (38.46), H: 4.12 (3.79), N: 19.18 (19.50). IR (ATR, cm^{-1}): 3138, 2949, 2888, 2250, 1513, 1451, 1423, 1343, 1285, 1288, 1229, 1184, 1138, 1107, 1087, 1053, 934, 827, 794, 747, 661, 610, 569, 513, 409.

$[Zn\ (TEG)_3(C_3CNIm)_3][Tf_2N]_2$

1-(3-cyanopropyl)imidazole (1.04g, 7.73mmol) and 1-[2-[2-(2-methoxy-ethoxy)ethoxy]ethyl]imidazole (1.66g, 7.73mmol) and $[Zn(H_2O)_6][Tf_2N]\cdot 2H_2O$ (1.98g, 2.58mmol) gave a transparent oil in a quantitative yield. Glass transition temperature: -49 °C. CHN [%] (calculated) M: C: 39.32(39.46), H: 4.37(4.88), N: 13.93(14.22). IR (ATR, cm^{-1}): 3131, 2878, 2249, 1527, 1451, 1350, 1288, 1185, 1135, 1098, 1056, 956, 843, 740, 657, 616, 570, 513.

$[Zn\ (TEG)_6][Tf_2N]_2$

1-[2-[2-(2-methoxyethoxy)ethoxy]ethyl]imidazole (1.71 g, 7.98 mmol) and $[Zn(H_2O)_6][Tf_2N]\cdot 2H_2O$ (1.02 g, 1.33 mmol) gave a transparent oil in a quantitative yield. Glass transition temperature: -56 °C. CHN [%] (calculated): C: 39.47 (40.22), H: 5.13 (5.70), N: 9.96 (10.26). IR (ATR,

cm^{-1}): 31282, 2876, 1623, 1525, 1450, 1351, 1288, 1185, 1134, 1098, 1057, 933, 846, 788, 760, 740, 656, 570, 513.

$[Mn(C_3CNIm)_6][Tf_2N]_2$

To 1-(3-cyanopropyl)imidazole (2.52g, 18.6 mmol) in 30mL acetone $[Mn(H_2O)_6][Tf_2N]_2$(2.25g, 3.11 mmol) in 20mL acetone was added. The mixture was stirred for ½ h. After evaporation of the solvent and water, a pale yellow, translucent solid was obtained in a quantitative yield. The yellow color results from the initial color of the imidazole derivative. Melting point: 74°C.

CHN [%] (calculated) [M·H_2O]: C: 38.25 (38.74), H: 3.91 (3.82), N: 19.40 (19.64). IR (ATR, cm^{-1}): 3133, 2954, 2250, 1515, 1449, 1353, 1324, 1285, 1228, 1195, 1185, 1137, 1110, 1086, 1048, 1035, 979, 932, 831, 792, 772, 741, 661, 608, 568, 513, 409.

$[Ni(dmIm)_4][Tf_2N]_2$

1,2-Dimethylimidazole (1.51g, 15.7 mmol) and $[Ni(H_2O)_6][Tf_2N]$ ·$2H_2O$ (3.00 g, 3.93 mmol) gave a dark green-yellow solution. Removal of the solvent and water and subsequent evacuation on the vacuum line gave orange crystals in a quantitative yield. Melting point: 120 °C. CHN [%] (calculated): C: 28.52 (28.72), H: 3.83 (3.21), N: 13.66 (13.96). IR (ATR, cm^{-1}): 3160, 2966, 1611, 1557, 1515, 1421, 1349, 1330, 1295, 1226, 1177, 1137, 1105, 951, 791, 732, 679, 607, 569, 512, 459, 409.

$[Ni(dmIm)_5][Tf_2N]_2$

1,2-Dimethylimidazole (1.89g, 19.7 mmol) and $[Ni(H_2O)_6][Tf_2N]$ ·$2H_2O$ (3.00 g, 3.93 mmol) gave a dark green crystalline product in a quantitative yield. Melting point: 89 °C. CHN [%] (calculated): C: 31.52 (31.68), H: 3.46 (3.67), N: 15.03 (15.29). IR (ATR, cm^{-1}): 3143, 2963, 1547, 1508, 1418, 1348, 1330, 1286, 1227, 1183, 1136, 1080, 1055, 1000, 789, 756, 740, 681, 649, 607, 569, 512, 459, 446.

6.4.3. Membrane preparation and measurements

0.9 g of PSf, dried overnight at 100 °C, 0.1 g of IL and 10 ml of DCM were mixed at about 50 °C until they appeared homogenous, then continued stirring without any heat treatment for overnight. The solutions were then cast on petri dishes and left on air for about 4 to 6 h. A custom-built high throughput gas separation (HTGS) setup (HTML, Belgium) was used to determine the binary gas selectivities (CO_2/N_2) of all membranes. The construction and operation of the set-up is described elsewhere.[62] The equipment can simultaneously measure gas permeability and selectivity of 16 membranes at variable operating conditions, e.g. feed composition, pressure and temperature. Before starting the measurement, the permeation cell is kept under vacuum overnight to remove gases present in the module and membrane permeate lines. The gas mixture (50% CO_2 : 50% N_2, vol %) is fed into the system through mass flow controllers, and the desired upstream pressure is maintained by adjusting the back pressure regulator on the purge line, which was always set at 7 bars in this study. The temperature of membrane module is set constant at 35 °C and controlled by an external regulator. The permeate composition is then analysed by a compact gas chromatograph (CGC) from Interscience (Louvain-la-Neuve, Belgium). Mixed-gas selectivity of gas A over gas B is calculated using Eq. 6.1:

$$\alpha_{\frac{A}{B}} = \frac{x_{perm,A}/x_{perm,B}}{x_{feed,A}/x_{feed,B}} \qquad 6.1$$

where $x_{\text{feed,A}}$ and $x_{\text{perm,A}}$ are the mole fractions of component A in the feed and permeate stream, respectively. $x_{\text{feed,B}}$ and $x_{\text{perm,B}}$ are the mole fractions of component B in the feed and permeate stream, respectively. Gas permeability was measured with a constant volume, variable pressure method, by allowing the permeate gas to expand in a constant volume auxiliary cylinder.[63] Overall permeability of gases, P, is

calculated from the rate of pressure (p_1) increase in a known downstream volume (V) at constant temperature (T) using the ideal gas law. When the steady state was achieved, the flow rate was acquired every 1 s for 5 min. For thin film composite membranes in this study, due to the difficulty in accurately measuring the selective layer thickness (l), permeance (P/l) is used to describe gas flux through the membranes and expressed in gas permeation units (GPU), where 1 GPU = 10^{-6} cm^3 (STP)/(cm^2 s cm Hg).[64] Given a nearly constant pressure difference (ΔP) across the membrane, permeance of the sample membrane can be written as Eq. 6.2:

$$\frac{P}{l} = \left(\frac{dp_1}{dt}\right)_{t\to\infty} \frac{V}{RTA\Delta P} \qquad 6.2$$

where A is the effective membrane area and R is the universal gas constant.[65]

Compatibility of the polymer-MIL blends

Compatibility of the polymer with the ILs was tested by the means of DSC, by comparing the glass transition temperature (T_g) of the polymer and the IL before and after blending. In the case of each membrane, the T_g of the IL and of the polymer after blending, lied in the range between the T_g of the pure IL and the pure polymer, suggesting uniform mixing but nevertheless, a presence of two phases and thus limited compatibility.

6.4.4. XRD measurements

Crystals of the ILs suitable for single crystal X-ray diffraction were mounted on a nylon loop attached to a copper pin and placed in a cold N_2 stream of Cryostreams cryocooler at 100(2), on an Agilent SuperNova diffractometer using Mo Kα radiation (λ= 0.71073 Å). The absorption corrections were applied using CrysAlisPro (Agilent Technologies). All structures were solved using direct methods and refined by the full-

matrix least-squares procedure in SHELXL.[66] All hydrogen atoms were placed in calculated positions and refined using a riding model. The program OLEX2 was also used in refinement and making pictures.[67] A summary of the crystallographic data can be found in Table 6.5 and 6.6.

Table 6.5: Crystal data and structure refinement for hexacoordinate ILs.

	$Ni(C_3CNIm)_6][Tf_2N]_2$	$Zn(C_3CNIm)_6][Tf_2N]_2$	$[Mn(C_3CNIm)_6][Tf_2N]_2$
Empirical formula	$C_{46}H_{54}F_{12}N_{20}O_8S_4Ni$	$C_{46}H_{54}F_{12}N_{20}O_8S_4Zn$	$C_{46}H_{54}F_{12}N_{20}O_8S_4Mn$
Formula weight	1430.04	1436.70	1426.27
T/K	100(2)	100(2)	100(2)
Colour	blue	colourless	colourless
Size/mm^3	0.20×0.20×0.04	0.40×0.20×0.16	0.3×0.2×0.1
Crystal system	Monoclinic	Monoclinic	Monoclinic
Space group	$P2_1/c$	$P2_1/c$	$P2_1/c$
a/Å	12.2979(4)	12.2725(4)	12.1620(5)
b/Å	8.1962(2)	8.2099(3)	8.4079(4)
c/Å	30.4591(16)	30.4922(10)	30.2054(13)
α (°)	90.00	90.00	90.00
β (°)	99.807(4)	99.858(3)	99.365(4)
γ (°)	90.00	90.00	90.00
Volume/$Å^3$	3025.3(2)	3026.90(18)	3047.5(2)
Z	2	2	2
ρ_{calc}/Mg m^{-3}	1.563	1.576	1.554
μ/mm^{-1}	0.564	0.649	0.458
Wavelength	0.71073	0.71073	0.71073
Reflections collected	14561	13911	15141
Independent reflexions	6906	6913	6987

R(int)	0.0274	0.0133	0.0146
$R_1[I \geq 2\sigma(I)]$	0.0786	0.0287	0.0278
wR_2 [all data]	0.1495	0.0706	0.0694
$\Delta\rho_{max,\ min}$/e Å^{-3}	0.84/-0.70	0.33/-0.35	0.42/-0.42

Table 6.6: Crystal data and structure refinement for tetra- and pentacoordinate ILs.

	$Ni(dmIm)_4][Tf_2N]_2$	$[Ni(dmIm)_5][Tf_2N]_2$
Empirical formula	$C_{24}H_{32}F_{12}N_{10}NiO_8S_4$	$C_{29}H_{40}F_{12}N_{12}NiO_8S_4$
Weight formula	1003.55	1099.68
T/K	100(2)	100(2)
Color	Orange	Dark green
Size/mm^3	0.25 x 0.16 x 0.12	0.22 x 0.18 x 0.12
Crystal system	Monoclinic	Orthorhombic
Space group	$P2_1/n$	$Pna2_1$
a/Å	9.6242(5)	14.2396(4)
b/Å	13.4108(7)	26.5281(7)
c/Å	15.8711(9)	12.0419(3)
α (°)	90.00	90.00
β (°)	104.601(6)	90.00
γ (°)	90.00	90.00
Volume/Å^3	1982.28(19)	4548.8(2)
Z	2	4
ρ_{calc}/M g m^{-3}	1.681	1.606
μ/mm^{-1}	0.814	0.718
Wavelength	0.71073	0.71073
Reflections collected	9605	15074
Independent reflexions	4559	8828

R(int)	0.0243	0.0227
$R_1[I \geq 2\sigma(I)]$	0.0502	0.0333
wR_2 [all data]	0.1381	0.0737
$\Delta\rho_{max,\ min}$/e Å^{-3}	0.92/-0.89	0.43/-0.33

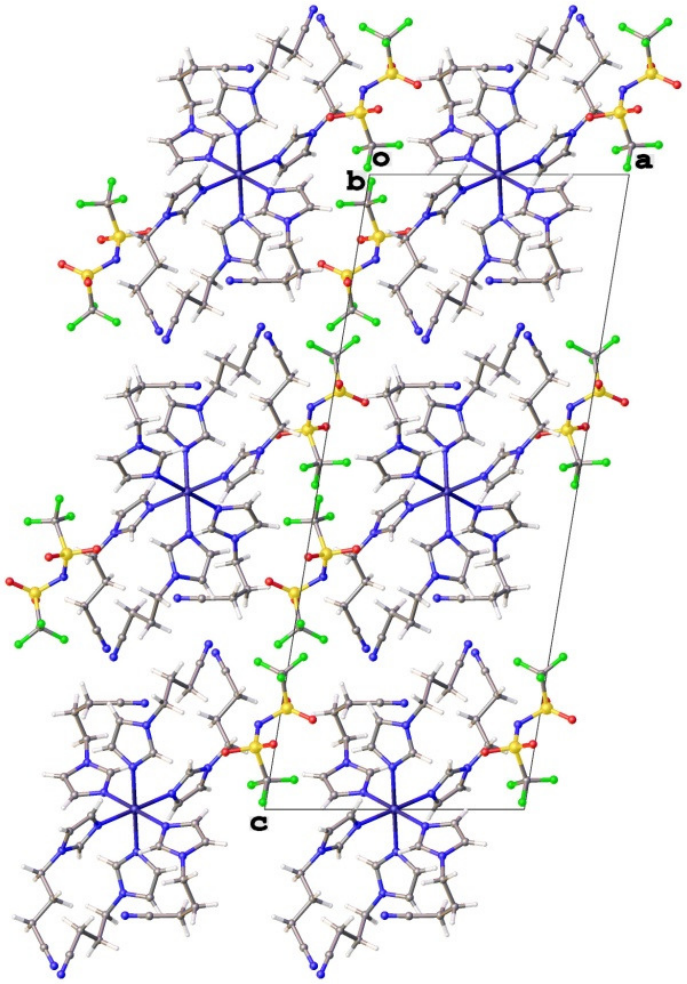

Figure 6.13: View of the packing in the crystal structure of $[Mn(C_3CNIm)_6][Tf_2N]_2$.

6.5. References

1. Hu, X.; Tang, J.; Blasig, A.; Shen, Y.; Radosz, M., CO_2 permeability, diffusivity and solubility in polyethylene glycol-grafted polyionic membranes and their CO_2 selectivity relative to methane and nitrogen. *J. Membr. Sci.* **2006,** *281*, 130-138.
2. Tang, J.; Tang, H.; Sun, W.; Radosz, M.; Shen, Y., Poly(ionic liquid)s as new materials for CO_2 absorption. *J. Polym. Sci. A Polym. Chem.* **2005,** *43*, 5477-5489.
3. Li, P.; Paul, D. R.; Chung, T.-S., High performance membranes based on ionic liquid polymers for CO_2 separation from the flue gas. *Green Chem.* **2012,** *14*, 1052-1063.
4. Bara, J. E.; Lessmann, S.; Gabriel, C. J.; Hatakeyama, E. S.; Noble, R. D.; Gin, D. L., Synthesis and Performance of Polymerizable Room-Temperature Ionic Liquids as Gas Separation Membranes. *Ind. Eng. Chem. Res.* **2007,** *46*, 5397-5404.
5. Li, P.; Pramoda, K.; Chung, T.-S., CO_2 separation from flue gas using polyvinyl-(room temperature ionic liquid)–room temperature ionic liquid composite membranes. *Ind. Eng. Chem. Res.* **2011,** *50*, 9344-9353.
6. Bara, J. E.; Hatakeyama, E. S.; Gabriel, C. J.; Zeng, X.; Lessmann, S.; Gin, D. L.; Noble, R. D., Synthesis and light gas separations in cross-linked gemini room temperature ionic liquid polymer membranes. *J. Membr. Sci.* **2008,** *316*, 186-191.
7. Jansen, J. C.; Friess, K.; Clarizia, G.; Schauer, J.; Izák, P., High Ionic Liquid Content Polymeric Gel Membranes: Preparation and Performance. *Macromolecules* **2010,** *44*, 39-45.
8. Uk Hong, S.; Park, D.; Ko, Y.; Baek, I., Polymer-ionic liquid gels for enhanced gas transport. *Chem. Comm.* **2009**, 7227-7229.
9. Uchytil, P.; Schauer, J.; Petrychkovych, R.; Setnickova, K.; Suen, S. Y., Ionic liquid membranes for carbon dioxide–methane separation. *J. Membr. Sci.* **2011,** *383*, 262-271.
10. Erdni-Goryaev, E. M.; Alent'ev, A. Y.; Belov, N. A.; Ponkratov, D. O.; Shaplov, A. S.; Lozinskaya, E. I.; Vygodskii, Y. S., Gas separation characteristics of new membrane materials based on poly(ethylene glycol)-crosslinked polymers and ionic liquids. *Pet. Chem.* **2012,** *52*, 494-498.
11. Chen, H. Z.; Li, P.; Chung, T.-S., PVDF/ionic liquid polymer blends with superior separation performance for removing CO_2 from hydrogen and flue gas. *Int. J. Hydrogen Energy* **2012,** *37*, 11796-11804.
12. Friess, K.; Jansen, J. C.; Bazzarelli, F.; Izák, P.; Jarmarová, V.; Kačírková, M.; Schauer, J.; Clarizia, G.; Bernardo, P., High ionic liquid content polymeric gel membranes: Correlation of membrane structure with gas and vapour transport properties. *J. Membr. Sci.* **2012,** *415–416*, 801-809.
13. Bernardo, P.; Jansen, J. C.; Bazzarelli, F.; Tasselli, F.; Fuoco, A.; Friess, K.; Izák, P.; Jarmarová, V.; Kačírková, M.; Clarizia, G., Gas

transport properties of Pebax®/room temperature ionic liquid gel membranes. *Sep. Purif. Technol.* **2012,** *97*, 73-82.
14. Jansen, J. C.; Clarizia, G.; Bernardo, P.; Bazzarelli, F.; Friess, K.; Randová, A.; Schauer, J.; Kubicka, D.; Kacirková, M.; Izak, P., Gas transport properties and pervaporation performance of fluoropolymer gel membranes based on pure and mixed ionic liquids. *Sep. Purif. Technol.* **2013,** *109*, 87-97.
15. Tomé, L. C.; Mecerreyes, D.; Freire, C. S. R.; Rebelo, L. P. N.; Marrucho, I. M., Pyrrolidinium-based polymeric ionic liquid materials: New perspectives for CO_2 separation membranes. *J. Membr. Sci.* **2013,** *428*, 260-266.
16. Kanehashi, S.; Kishida, M.; Kidesaki, T.; Shindo, R.; Sato, S.; Miyakoshi, T.; Nagai, K., CO_2 separation properties of a glassy aromatic polyimide composite membranes containing high-content 1-butyl-3-methylimidazolium bis(trifluoromethylsulfonyl)imide ionic liquid. *J. Membr. Sci.* **2013,** *430*, 211-222.
17. Liang, L.; Gan, Q.; Nancarrow, P., Composite ionic liquid and polymer membranes for gas separation at elevated temperatures. *J. Membr. Sci.* **2014,** *450*, 407-417.
18. Mahurin, S. M.; Hillesheim, P. C.; Yeary, J. S.; Jiang, D.; Dai, S., High CO_2 Solubility, Permeability and Selectivity in Ionic Liquids with Tetracyanoborate Anion. *RSC Advances* **2012,** *2*, 11813-11819.
19. Prabhu, C.; Valechha, A.; Wanjari, S.; Labhsetwar, N.; Kotwal, S.; Satyanarayanan, T.; Rayalu, S., Carbon composite beads for immobilization of carbonic anhydrase. *J. Mol. Catal. B: Enzym.* **2011,** *71*, 71-78.
20. Bond, G. M.; Stringer, J.; Brandvold, D. K.; Simsek, F. A.; Medina, M.-G.; Egeland, G., Development of integrated system for biomimetic CO_2 sequestration using the enzyme carbonic anhydrase. *Energy Fuels* **2001,** *15*, 309-316.
21. Gerdemann, S. J.; O'Connor, W. K.; Dahlin, D. C.; Penner, L. R.; Rush, H., Ex situ aqueous mineral carbonation. *Environ. Sci. Technol.* **2007,** *41*, 2587-2593.
22. Bhaduri, G. A.; Siller, L., Nickel nanoparticles catalyse reversible hydration of carbon dioxide for mineralization carbon capture and storage. *Catal. Sci. Tech.* **2013**.
23. Liu, H.; Huang, J.; Pendleton, P., Experimental and modelling study of CO_2 absorption in ionic liquids containing Zn (II) ions. *Energy Procedia* **2011,** *4*, 59-66.
24. Lin, I. J.; Vasam, C. S., Metal-containing ionic liquids and ionic liquid crystals based on imidazolium moiety. *J. Organomet. Chem.* **2005,** *690*, 3498-3512.
25. Estager, J.; Holbrey, J.; Swadźba-Kwaśny, M., Halometallate ionic liquids–revisited. *Chem. Soc. Rev.* **2014,** *43*, 847-886.
26. Del Sesto, R. E.; McCleskey, T. M.; Burrell, A. K.; Baker, G. A.; Thompson, J. D.; Scott, B. L.; Wilkes, J. S.; Williams, P., Structure and

magnetic behavior of transition metal based ionic liquids. *Chem. Comm.* **2008**, 447-449.
27. Funasako, Y.; Nosho, M.; Mochida, T., Ionic liquids from copper (II) complexes with alkylimidazole-containing tripodal ligands. *Dalton Trans.* **2013,** *42*, 10138-10143.
28. Pratt Iii, H. D.; Rose, A. J.; Staiger, C. L.; Ingersoll, D.; Anderson, T. M., Synthesis and characterization of ionic liquids containing copper, manganese, or zinc coordination cations. *Dalton Trans.* **2011,** *40*, 11396-11401.
29. Huang, J.-F.; Luo, H.; Dai, S., A new strategy for synthesis of novel classes of room-temperature ionic liquids based on complexation reaction of cations. *J. Electrochem. Soc.* **2006,** *153*, J9-J13.
30. Masui, H.; Murray, R. W., Room-temperature molten salts of ruthenium tris (bipyridine). *Inorg. Chem.* **1997,** *36*, 5118-5126.
31. Inagaki, T.; Mochida, T.; Takahashi, M.; Kanadani, C.; Saito, T.; Kuwahara, D., Ionic Liquids of Cationic Sandwich Complexes. *Chem. Eur. J.* **2012,** *18*, 6795-6804.
32. Nockemann, P.; Thijs, B.; Postelmans, N.; Van Hecke, K.; Van Meervelt, L.; Binnemans, K., Anionic rare-earth thiocyanate complexes as building blocks for low-melting metal-containing ionic liquids. *J. Am. Chem. Soc.* **2006,** *128*, 13658-13659.
33. Schaltin, S.; Brooks, N. R.; Stappers, L.; Van Hecke, K.; Van Meervelt, L.; Binnemans, K.; Fransaer, J., High current density electrodeposition from silver complex ionic liquids. *Phys. Chem. Chem. Phys.* **2012,** *14*, 1706-1715.
34. Brooks, N. R.; Schaltin, S.; Van Hecke, K.; Van Meervelt, L.; Binnemans, K.; Fransaer, J., Copper (I)- Containing Ionic Liquids for High-Rate Electrodeposition. *Chem. Eur. J.* **2011,** *17*, 5054-5059.
35. Schaltin, S.; Brooks, N. R.; Binnemans, K.; Fransaer, J., Electrodeposition from cationic cuprous organic complexes: ionic liquids for high current density electroplating. *J. Electrochem. Soc.* **2011,** *158*, D21-D27.
36. Lee, J. H.; Chae, I. S.; Song, D.; Kang, Y. S.; Kang, S. W., Metallic copper incorporated ionic liquids toward maximizing CO_2 separation properties. *Sep. Purif. Technol.* **2013,** *112*, 49-53.
37. Zarca, G.; Ortiz, I.; Urtiaga, A., Copper(I)-containing supported ionic liquid membranes for carbon monoxide/nitrogen separation. *J. Membr. Sci.* **2013,** *438*, 38-45.
38. Vander Hoogerstraete, T.; Brooks, N. R.; Norberg, B.; Wouters, J.; Van Hecke, K.; Van Meervelt, L.; Binnemans, K., Crystal structures of low-melting ionic transition-metal complexes with N-alkylimidazole ligands. *CrystEngComm* **2012,** *14*, 4902-4911.
39. Steichen, M.; Brooks, N. R.; Van Meervelt, L.; Fransaer, J.; Binnemans, K., Homoleptic and heteroleptic N-alkylimidazole zinc(ii)-containing ionic liquids for high current density electrodeposition. *Dalton Trans.* **2014,** *43*, 12329-12341.

40. Bara, J. E.; Carlisle, T. K.; Gabriel, C. J.; Camper, D.; Finotello, A.; Gin, D. L.; Noble, R. D., Guide to CO_2 Separations in Imidazolium-Based Room-Temperature Ionic Liquids. *Ind. Eng. Chem. Res.* **2009,** *48*, 2739-2751.
41. Bara, J. E.; Gabriel, C. J.; Lessmann, S.; Carlisle, T. K.; Finotello, A.; Gin, D. L.; Noble, R. D., Enhanced CO_2 Separation Selectivity in Oligo(ethylene glycol) Functionalized Room-Temperature Ionic Liquids. *Ind. Eng. Chem. Res.* **2007,** *46*, 5380-5386.
42. Cadena, C.; Anthony, J. L.; Shah, J. K.; Morrow, T. I.; Brennecke, J. F.; Maginn, E. J., Why Is CO_2 So Soluble in Imidazolium-Based Ionic Liquids? *J. Am. Chem. Soc.* **2004,** *126*, 5300-5308.
43. Santos, E.; Albo, J.; Irabien, A., Acetate based Supported Ionic Liquid Membranes (SILMs) for CO_2 separation: Influence of the temperature. *J. Membr. Sci.* **2014,** *452*, 277-283.
44. Scovazzo, P., Determination of the upper limits, benchmarks, and critical properties for gas separations using stabilized room temperature ionic liquid membranes (SILMs) for the purpose of guiding future research. *J. Membr. Sci.* **2009,** *343*, 199-211.
45. Shannon, M. S.; Bara, J. E., Properties of Alkylimidazoles as Solvents for CO_2 Capture and Comparisons to Imidazolium-Based Ionic Liquids. *Ind. Eng. Chem. Res.* **2011,** *50*, 8665-8677.
46. Shannon, M. S.; Tedstone, J. M.; Danielsen, S. P. O.; Bara, J. E., Evaluation of Alkylimidazoles as Physical Solvents for CO_2/CH_4 Separation. *Ind. Eng. Chem. Res.* **2011,** *51*, 515-522.
47. Hojniak, S. D.; Khan, A. L.; Holloczki, O.; Kirchner, B.; Vankelecom, I. F. J.; Dehaen, W.; Binnemans, K., Separation of Carbon Dioxide from Nitrogen or Methane by Supported Ionic Liquid Membranes (SILMs): Influence of the Cation Charge of the Ionic Liquid. *J. Chem. Phys. B* **2013,** *117*, 15131-15140.
48. Carlisle, T. K.; Bara, J. E.; Gabriel, C. J.; Noble, R. D.; Gin, D. L., Interpretation of CO_2 Solubility and Selectivity in Nitrile-Functionalized Room-Temperature Ionic Liquids Using a Group Contribution Approach. *Ind. Eng. Chem. Res.* **2008,** *47*, 7005-7012.
49. Hojniak, S. D.; Silverwood, I. P.; Khan, A. L.; Vankelecom, I. F. J.; Dehaen, W.; Kazarian, S. G.; Binnemans, K., Highly Selective Separation of Carbon Dioxide from Nitrogen and Methane by Nitrile/Glycol-Difunctionalized Ionic Liquids in Supported Ionic Liquid Membranes (SILMs). *J. Chem. Phys. B* **2014,** *118*, 7440-7449.
50. D'Alessandro, D. M.; Smit, B.; Long, J. R., Carbon Dioxide Capture: Prospects for New Materials. *Angew. Chem. Int. Ed.* **2010,** *49*, 6058-6082.
51. Powell, C. E.; Qiao, G. G., Polymeric CO2/N2 gas separation membranes for the capture of carbon dioxide from power plant flue gases. *J. Membr. Sci.* **2006,** *279*, 1-49.
52. http://www.epa.gov/iris/toxreviews/0426tr.pdf (accessed 30.04.2014).
53.http://www.epa.gov/teach/chem_summ/manganese_summary.pdf (accessed 30.04.2014).

54. Gibson, D. H., Carbon dioxide coordination chemistry: metal complexes and surface-bound species. What relationships? *Coord. Chem. Rev.* **1999,** *185–186*, 335-355.
55. Song, J.; Klein, E. L.; Neese, F.; Ye, S., The Mechanism of Homogeneous CO_2 Reduction by Ni(cyclam): Product Selectivity, Concerted Proton–Electron Transfer and C–O Bond Cleavage. *Inorg. Chem.* **2014,** *53*, 7500-7507.
56. Desrochers, P. J.; Telser, J.; Zvyagin, S. A.; Ozarowski, A.; Krzystek, J.; Vicic, D. A., Electronic Structure of Four-Coordinate C_{3v} Nickel(II) Scorpionate Complexes: Investigation by High-Frequency and -Field Electron Paramagnetic Resonance and Electronic Absorption Spectroscopies. *Inorg. Chem.* **2006,** *45*, 8930-8941.
57. Carvalho, P. J.; Álvarez, V. H.; Machado, J. J. B.; Pauly, J.; Daridon, J.-L.; Marrucho, I. M.; Aznar, M.; Coutinho, J. A. P., High pressure phase behavior of carbon dioxide in 1-alkyl-3-methylimidazolium bis(trifluoromethylsulfonyl)imide ionic liquids. *J. Supercrit.Fluid* **2009,** *48*, 99-107.
58. Sarkar, S.; Moon, D.; Lah, M. S.; Lee, H.-I., Structure and Heme-Independent Peroxidase Activity of a Fully-Coordinated Mononuclear Mn (II) Complex with a Schiff-Base Tripodal Ligand Containing Three Imidazole Groups. *Bull. Korean Chem. Soc.* **2010,** *31*, 3173-3179.
59. Shannon, R. D., Revised effective ionic radii and systematic studies of interatomic distances in halides and chalcogenides. *Acta Crystallogr. Sect. A: Crystal Physics, Diffraction, Theoretical and General Crystallography* **1976,** *32*, 751-767.
60. Addison, A. W.; Rao, T. N.; Reedijk, J.; van Rijn, J.; Verschoor, G. C., Synthesis, structure, and spectroscopic properties of copper(II) compounds containing nitrogen-sulphur donor ligands; the crystal and molecular structure of aqua[1,7-bis(N-methylbenzimidazol-2[prime or minute]-yl)-2,6-dithiaheptane]copper(II) perchlorate. *J. Chem. Soc., Dalton Trans.* **1984**, 1349-1356.
61. Steichen, M.; Brooks, N. R.; Van Meervelt, L.; Fransaer, J.; Binnemans, K., Homoleptic and heteroleptic N-alkylimidazole zinc(II)-containing ionic liquids for high current density electrodeposition. *Dalton Trans.* **2014**.
62. Khan, A. L.; Basu, S.; Cano-Odena, A.; Vankelecom, I. F. J., Novel high throughput equipment for membrane-based gas separations. *J. Membr. Sci.* **2010,** *354*, 32-39.
63. Sanders, D. F.; Smith, Z. P.; Ribeiro Jr, C. P.; Guo, R.; McGrath, J. E.; Paul, D. R.; Freeman, B. D., Gas permeability, diffusivity, and free volume of thermally rearranged polymers based on 3, 3′-dihydroxy-4, 4′-diamino-biphenyl (HAB) and 2, 2′-bis-(3, 4-dicarboxyphenyl) hexafluoropropane dianhydride (6FDA). *J. Membr. Sci.* **2012,** *409*, 232-241.
64. Lin, H.; Thompson, S. M.; Serbanescu-Martin, A.; Wijmans, J. G.; Amo, K. D.; Lokhandwala, K. A.; Merkel, T. C., Dehydration of natural gas

using membranes. Part I: Composite membranes. *J. Membr. Sci.* **2012,** *413*, 70-81.
65. Minelli, M.; Giacinti Baschetti, M.; Hallinan Jr, D. T.; Balsara, N. P., Study of gas permeabilities through polystyrene-*block*-poly (ethylene oxide) copolymers. *J. Membr. Sci.* **2013,** *432*, 83-89.
66. Sheldrick, G. M., A short history of SHELX. *Acta Crystallographica Section A* **2008,** *64*, 112-122.
67. Dolomanov, O. V.; Bourhis, L. J.; Gildea, R. J.; Howard, J. A. K.; Puschmann, H., OLEX2: a complete structure solution, refinement and analysis program. *J. Appl. Crystallogr.* **2009,** *42*, 339-341.

General Conclusions and Future Perspectives

Until recently, IL cations were considered less important than anions in the design of ILs used for CO_2 separation, and most of the studied ILs contained the imidazolium cation. Moreover, the structure-performance relationships for ILs used in gas separation were not yet fully understood.

The aim of this PhD thesis was to design and synthesize ILs for the separation of CO_2 from N_2 and CH_4 on membranes, and to deepen our understanding of the molecular basis of CO_2 separation, *i.a.*, by the use of infrared spectroscopy.

In the first part of this dissertation, the influence of the cationic core type and charge on the performance of SILMs was investigated by preparing membranes with ILs composed of various cationic cores (imidazolium, pyrrolidinium, piperi-dinium, and morpholinium) with appended tri(ethylene glycol) chains. It has been proven that the choice of the cationic core significantly influenced the selectivity. The monocationic ILs performed in the following order of increasing selectivity: pyrrolidinium > piperidinium > imidazolium > morpholinium.

In the next step, the performance of SILMs containing analogous dicationic ILs was investigated. The selectivities exhibited by the dicationic ILs were up to two times higher than the selectivities of the corresponding monocationic ILs. The permeances of N_2 and CH_4 through the IL layer were observed to decrease in dicationic ILs, presumably due to the less favourable interactions of these gases with ILs. Quantum chemical calculations helped elucidating one more reason for the increased gas separation selectivity of the dicationic ILs: the increase of

the number of cationic moieties in dicationic ILs provided more interaction sites for CO_2. This work has shown that there are still simple, unexplored solutions that can be applied in membrane gas separation (here: ILs with a double charge).

In the second part of this thesis, imidazolium and pyrrolidinium ILs containing two CO_2-philic moieties, a tri(ethylene glycol) and a nitrile group, were incorporated into SILMs. These difunctionalised ILs exhibited *ca.* 2.3 times higher CO_2/N_2 and CO_2/CH_4 gas separation selectivities than analogous ILs functionalised only with a glycol chain. The high selectivity of the difunctionalised ILs was found to be caused by the considerably reduced permeances of N_2 and CH_4, most likely due to the ability of the –CN group to reject the non-polar contaminant gases by reducing the free volume of the resulting ILs.

Interpretation of these results was supported by *in situ* FTIR-ATR measurements of the IL-CO_2 systems in pressurised gas cells. Apart from the CO_2 solubility, IL-CO_2 interactions and IL swelling were studied. Different strengths of the IL-CO_2 interactions were found to be the major difference between the two classes of ILs: the difunctionalised ILs interacted stronger with CO_2 than the glycol-functionalised ILs. Double or multiple functionalisation, although demanding, can be very rewarding when it comes to the performance of membranes containing such ILs. This part has shown that even more important than finding new CO_2-philic is combining the already known groups in a logical manner.

In the third part of this PhD, an industrially relevant approach has been tested by preparing polymer-IL blend membranes instead of SILMs. To overcome the problems of elaborate synthesis and difficult purification, typical in ILs synthesis, a new approach to CO_2 separation was suggested, namely, to use ILs with metal-containing complex cations. These ILs were obtained by mixing functionalised imidazolium

ligands with a metal salt hydrate containing the desired anion, bis(trifluoromethylsulfonyl)imide.

Two different approaches were applied. In the first approach, the metal ion, Ni^{2+}, Zn^{2+} or Mn^{2+}, served as a scaffold to accommodate six imidazole ligands functionalised with a 3-cyanopropyl or a tri(ethylene glycol) group. Gas separation was in this case based on the physical interactions between the ligands and the anions with CO_2. These hexacoordinate ILs achieved moderate selectivities, with the nickel(II)-containing ILs providing the highest selectivities.

In the second approach, tetra- and pentacoordinate complex nickel(II) cations were employed, that is, cations possessing a coordination vacancy and the potential of chemically binding CO_2 molecules. The IL–CO_2 interactions were studied with UV-Vis-NIR spectroscopy as well as with ^{1}H and ^{13}C NMR spectroscopy, but no binding was observed. These ILs achieved slightly lower selectivities than the hexa-coordinate ILs, indicating the importance of the IL functionalisation over the potential CO_2-metal ion interactions.

Future perspectives

Currently, ILs are not yet employed in the industrial membrane gas separation, and the price, low membrane performance, as well as elaborate syntheses of the ILs, have been the limiting factors. The solubility of CO_2 in ILs at ambient conditions and ideal solubility selectivity for CO_2/N_2 and CO_2/CH_4 separations, are comparable to the values offered by the common organic solvents.[1] Nevertheless, while there are approximately 600 classical molecular solvents, there are billions of possible ILs. Taking into consideration that annually, 35 billion tones of CO_2 are generated worldwide, it is not too daring to say that even a small improvement could have an enormous impact on the global scale.[2] Eventually, the price should be less of a concern because only a small amount of IL is needed to prepare a membrane. For

example, to produce a SLM with 50% porosity, only 10 cm^3 of a solvent is required to impregnate 1m^2 of a 20 µm thick support.[3]

Despite significant progress in the understanding of gas dissolution in ILs, the functional groups used in the design of these compounds are still randomly selected. A much higher performance of the ILs could be achieved when a conscious choice of the functionalisation is made, not necessarily by the synthesis of new functional groups but also by the combination of known moieties in a way to achieve a synergistic effect. Much more emphasis should be placed on the fact that different properties on the nano-scale should be aimed at in the case of bulk absorption and gas separation. In the cases where the multi-functionalisation is too difficult or the yields are low, mixtures of ILs can be used.

Therefore, the priority should be given to deepening our understanding of the gas dissolution mechanism in ILs and polymers. Since the polymeric membranes are the future of gas separations, it is very important to know how the polymer–IL–CO_2 systems perform on the molecular level. So far *in-situ* FTIR-ATR and FT-Raman spectroscopy have proved extremely useful in elucidating the CO_2–IL interactions and these accessible methods should be further employed.[4-5] Also computer simulation techniques, such as molecular dynamics, DFT calculations, as well as spectroscopic experiments with fluorescent probes molecules can help determining the size and characteristics of the polar domains in ILs.[6]

Despite rather mediocre performance of the metal-containing ILs presented in this thesis, the novel approach to CO_2 separation by using complex metal cations is still very promising. When optimised and combined with a suitable polymer, IL-polymer blends can be an answer to some long-standing industrial problems. Their special advantage is the extremely high tuneability: not only the cationic core type (e.g. imidazole, triazole) and functionalisation can be adjusted, but the

central metal ion and the anion are also tuneable. Although anions are usually more difficult to modify, metal-containing, complex anions leave a lot of possibilities for functionalisation.[7]

Certain NMR-based techniques could be proposed to elucidate the behaviour of CO_2 in metal-containing ILs with a coordination vacancy. For example, the using the Paramagnetic Relaxation Enhancement NMR technique, similarly to the NOE technique, information about the relative positions of the nuclei can be obtained.[8] This technique involves the use of a paramagnetic probe (in this case the IL) that can bind to the diamagnetic CO_2 molecule. Should there be a bond formation, the distances between the ^{13}C atom of CO_2 and ^{13}C atoms the IL could be obtained. Also the diffusion NMR methods could be very useful, as they would allow observation of the viscosity changes on gas introduction that could be indicative of gas binding.[9]

Additionally, the influence of common impurities on the membrane performance of ILs should be studied. For the time being, only ideal pure systems have been tested. As BF_4 and PF_6 ILs were found to decompose with generation of HF, similar problems can occur when the membranes will be confronted with real industrial conditions.
Finally, simplification of the IL design should be always kept in mind. After all, the popularity of this class of compounds is largely based on the simplicity of their design.

1. Bara, J. E.; Carlisle, T. K.; Gabriel, C. J.; Camper, D.; Finotello, A.; Gin, D. L.; Noble, R. D., Guide to CO_2 Separations in Imidazolium-Based Room-Temperature Ionic Liquids. *Ind. Eng. Chem. Res.* **2009,** *48*, 2739-2751.
2. http://www.pbl.nl/ (accessed 05.05.2014).
3. Noble, R. D.; Stern, S. A., *Membrane Separations Technology—Principles and Applications*. Elsevier Science B. V. P.: The Netherlands, 1995.
4. Kazarian, S. G.; Briscoe, B. J.; Welton, T., Combining ionic liquids and supercritical fluids: ATR-IR study of CO_2 dissolved in two ionic liquids at high pressures. *Chem. Commun.* **2000**, 2047-2048.

5. Romanos, G. E.; Zubeir, L. F.; Likodimos, V.; Falaras, P.; Kroon, M. C.; Iliev, B.; Adamova, G.; Schubert, T. J. S., Enhanced CO_2 Capture in Binary Mixtures of 1-alkyl-3-methylimidazolium Tricyanomethanide Ionic Liquids with Water. *J. Chem. Phys. B* **2013,** *117*, 12234-12251.
6. Hu, Y.-F.; Liu, Z.-C.; Xu, C.-M.; Zhang, X.-M., The molecular characteristics dominating the solubility of gases in ionic liquids. *Chem. Soc. Rev.* **2011,** *40*, 3802-3823.
7. Albo, J.; Santos, E.; Neves, L. A.; Simeonov, S. P.; Afonso, C. A. M.; Crespo, J. G.; Irabien, A., Separation performance of CO_2 through Supported Magnetic Ionic Liquid Membranes (SMILMs). *Sep. Purif. Technol.* **2012,** *97*, 26-33.
8. Clore, G. M.; Iwahara, J., Theory, practice, and applications of paramagnetic relaxation enhancement for the characterization of transient low-population states of biological macromolecules and their complexes. *Chem. Rev.* **2009,** *109*, 4108-4139.
9. Li, W.; Kagan, G.; Hopson, R.; Williard, P. G., Measurement of Solution Viscosity via Diffusion-Ordered NMR Spectroscopy (DOSY). *J. Chem. Educ.* **2011,** *88*, 1331-1335.

Health, Safety and Environment Aspects

All experimental work performed during the 4 years of this PhD was executed in compliance with the Code of Practice for Safety in the Lab[1] and the Departmental Safety Regulations (Introductory Safety Guidelines).[2]

Before handling a chemical product the KU Leuven Hazardous Substances Database in KU LOKET was consulted for safety measures and potential incompatible products. Risk Analyses were filled in for the new types of reactions and procedures or existing risk assessments were checked and necessary precautions were taken.[3]

When handling chemicals, lab coat, safety goggles and nitrile gloves were worn. Additional safety precautions were used when working with silica gel (disposable dust mask) and when a high pressure-gas cell was handled (safety screen).

Particular caution was taken when working with compounds classified as E4 and E4+, such as common but harmful solvents (e.g.: methanol: neurotoxic; dichloromethane: carcinogenic). Nickel(II) oxide used as a precursor of nickel(II) salts is highly toxic and can cause cancer by inhalation (H372, H350i). Similarly, the resulting nickel(II) salts are also highly toxic when brought into contact with the skin.

One has to be particularly careful when handling ionic liquids, as most of the compounds from this class has not been fully tested yet. It was therefore always assumed that the compounds pose a significant risk. Although due to the low volatility of ionic liquids there is no risk of poisoning by inhalation, they can be very harmful when in contact with skin. Ionic liquids with long alkyl chains are more toxic (as tested on

aquatic life) than those with shorter chains.[5] Long glycol chains used frequently in this thesis pose a smaller risk than alkyl chains.[5] Aquatic life toxicity of imidazolium ionic liquids with various anions (e.g. Cl^-, Br^-, $[PF_6]^-$, $[BF_4]^-$) can be compared to that of methanol.[4]

[1] Code of Practice for Safety in the Lab, http://chem.kuleuven.be/en/hse/procedures/liab1.htm

[2] Departmental Safety Brochure, http://chem.kuleuven.be/veiligheid/documenten/safety-brochure.pdf

[3] Risk Assessment depository website for the Department of Chemistry: https://www.groupware.kuleuven.be/sites/depchemrisico/Risk%20Assessments/Forms/Per%20division.aspx

[4] Wells, A. S.; Coombe, V. T., "On the Freshwater Ecotoxicity and Biodegradation Properties of Some Common Ionic Liquids." *Org. Proc. Res. & Dev.* **2006**, *10* (4), 794-798.

[5] Pretti, C.; Chiappe, C.; Baldetti, I.; Brunini, S.; Monni, G.; Intorre, L., "Acute toxicity of ionic liquids for three freshwater organisms: Pseudokirchneriella subcapitata, Daphnia magna and Danio rerio." *Ecotox. Environm. Safety* **2009,** *72* (4), 1170-1176.

Publications

[2] Sandra D. Hojniak, Ian P. Silverwood, Asim Laeeq Khan, Ivo F. J. Vankelecom, Wim Dehaen, Sergei G. Kazarian, and Koen Binnemans, "Highly Selective Separation of Carbon Dioxide from Nitrogen and Methane by Nitrile/Glycol-Difunctionalized Ionic Liquids in Supported Ionic Liquid Membranes (SILMs)", *The Journal of Physical Chemistry B*, **2014** 118 (26), 7440-7449.

[1] Sandra D. Hojniak, Asim Laeeq Khan, Oldamur Hollóczki, Barbara Kirchner, Ivo F. J. Vankelecom, Wim Dehaen, and Koen Binnemans, "Separation of Carbon Dioxide from Nitrogen or Methane by Supported Ionic Liquid Membranes (SILMs): Influence of the Cation Charge of the Ionic Liquid", *The Journal of Physical Chemistry B*, **2013** 117 (48), 15131-15140.

Attended Conferences

[2] **CCS 2013**, *European Conference on Carbon Capture and Storage*, Antwerp, 27–29 May 2013.

Title of the poster: “Design and Synthesis of Ionic Liquids for Separation of Carbon Dioxide from Nitrogen and Methane.”

[1] **EUCHEM 2012**, *Conference on Molten Salts and Ionic Liquids*, Celtic Manor Resort, Wales (UK), 5–10 August 2012.

Title of the poster: “Design and Synthesis of Ionic Liquids for Separation of Carbon Dioxide from Nitrogen and Methane.”